



**Tiago Gil da Silva Paiva**

Licenciado em Química Aplicada – Perfil de Química Orgânica

**Synthesis and characterization of  
C<sub>3</sub>-symmetric 1,3,5 -  
Benzenetricarboxamide  
derived supramolecular systems**

Dissertação para obtenção do Grau de Mestre em  
Química Bioorganica

Orientador: Marta Cristina Parracho Cançado Corvo,  
Investigador Pós-Doc, FCT-UNL  
Co-orientador: Eurico José da Silva Cabrita, Professor  
Auxiliar, FCT-UNL

Júri:

Presidente: Prof. Doutora Paula Cristina de Sérgio Branco  
Arguente: Doutora Maria Manuel Martinho Sequeira Barata Marques  
Vogal: Doutora Marta Cristina Parracho Cançado Corvo



FACULDADE DE  
CIÊNCIAS E TECNOLOGIA  
UNIVERSIDADE NOVA DE LISBOA

**Setembro 2015**

## **Synthesis and characterization of C<sub>3</sub>-symmetric 1,3,5 – Benzenetricarboxamide derived supramolecular systems**

**Copyright** © Tiago Gil da Silva Paiva, Faculdade de Ciências e Tecnologia da Universidade Nova de Lisboa.

A Faculdade de Ciências e Tecnologia e a Universidade Nova de Lisboa têm o direito, perpétuo e sem limites geográficos, de arquivar e publicar esta dissertação através de exemplares impressos reproduzidos em papel ou de forma digital, ou por qualquer outro meio conhecido ou que venha a ser inventado, e de a divulgar através de repositórios científicos e de admitir a sua cópia e distribuição com objectivos educacionais ou de investigação, não comerciais, desde que seja dado crédito ao autor e editor.

# Agradecimentos

Gostaria de agradecer ao professor Dr. Eurico Cabrita e à Dra. Marta Corvo pela sua orientação e pela oportunidade que me deram de desenvolver a tese no seu grupo num ambiente de aprendizagem constante.

Gostaria também de agradecer aos meus colegas de laboratório Ricardo Martinho, Micael Silva, Inês Rosete, Ana Diniz e Wagner Silva que me acompanharam ao longo deste ano e pelas proveitosas discussões durante esse período.

# Resumo

O objetivo deste trabalho foi estudar o processo de *self-assembly* de moléculas C<sub>3</sub>-simétricas. Para atingir este objectivo derivados de 1,3,5 - benzenotricarboxamidas (BTA) foram preparados. Cinco moléculas C<sub>3</sub>-simétricas foram sintetizados com rendimentos de moderados a bons (39-72%) usando azo-benzeno, anilina, benzilamina, triptofano e tirosina. O comportamento de agregação dos derivados de BTA foi estudado por espectroscopia de <sup>1</sup>H-NMR, <sup>1</sup>H-<sup>1</sup>H 2D Nuclear Overhauser Effect Espectroscopia (NOESY) e Diffusion Ordered Spectroscopy (DOSY). Estas experiências permitiram estudar a influência de grupos que estabelecem ligações de hidrogénio, anéis aromáticos, ligações insaturadas e a geometria global de *self-assembly* molecular associado com os diferentes padrões estruturais presentes em tais moléculas.

O empilhamento e comportamento de grande molécula é observado em BTA **1**, derivado de anilina, BTA **4**, derivado tirosina ou BTA **5**, derivado do triptofano, com vários desses grupos funcionais discutidos tais como ligações insaturadas e grupos que estabelecem pontes de hidrogénio.

BTA **5** foi usada em alguns estudos preliminares de interação com glucose e cloreto de amónio que mostra a interação com o ião amónio.



# Abstract

The aim of this work was to study the self-assembly process of  $C_3$ -symmetric molecules. To accomplish this objective 1,3,5 – benzentricarboxamides (BTA) derivatives were obtained. Five  $C_3$ -symmetric molecules were synthesized in moderate to good yields (39-72%) using azo-benzene, aniline, benzylamine, tryptophan and tyrosine. The aggregation behavior of the BTA derivatives was probed with  $^1\text{H}$ -NMR spectroscopy,  $^1\text{H}$ - $^1\text{H}$  2D Nuclear Overhauser Effect Spectroscopy (NOESY) and Diffusion Ordered Spectroscopy (DOSY). These experiments allowed to study the influence of H-bonding groups, aromatic rings, unsaturated bonds and the overall geometry in the molecular self-assembly associated with the different structural patterns present on these molecules.

The stacking and large molecule behavior were observed in BTA **1**, aniline derivative, BTA **4**, tyrosine derivative or BTA **5**, tryptophan derivative, with several of those discussed functional groups such as unsaturated bonds and H-bonding groups.

BTA **5** was used in a few preliminary interaction studies with glucose and ammonium chloride showing interaction with the ammonium ion.

# Keywords

---

**AK** Attenuated equilibrium constant model

**ar** Aromatic

**BBO** Broadband Observe

**Br** Broad

**BTA** Benzenetricarboxamide

**BTC** Benzenetricarbonyl

**COSY** Correlation Spectroscopy

**δ**

**IR** Deformation vibration

**NMR** Chemical shift

**d** Doublet

**DCM** Dicloromethane

**dd** Doublet of doublets

**ddd** Doublet of doublets of doublets

**DMF** Dimethylformamide

**DMSO** Dimethylsulfoxide

**DOSY** Diffusion Ordered Spectroscopy

**EK** Equal equilibrium constant model

**HF** Hartree-Fock

**HMBC** Heteronuclear Multiple-bond Correlation Spectroscopy

**HSQC** Heteronuclear Single Quantum Coherence Spectroscopy

**K** Equilibrium constant

**Ip** In-plane

**m** Multiplet

**NOE** Nuclear Overhauser Effect

**NOESY** Nuclear Overhauser Effect Spectroscopy

**STO** Slater Type Orbitals

**mp** Melting point

**ppm** Parts per million

**q** Quartet

**RT** Room temperature

**s****IR** Strong**NMR** Singlet**Sh** Sharp**st** Stretch**sy** symmetric**t** Triplet**TEA** Triethylamine**THF** Tetrahydrofuran**TLC** Thin layer chromatography**TMS** Tetramethylsilane**w** Weak**UV/Vis** Ultraviolet visible

---

# Table of contents

<b>Agradecimientos</b>	<b>ii</b>
<b>Resumo</b>	<b>iv</b>
<b>Abstract</b>	<b>v</b>
<b>Keywords</b>	<b>vi</b>
<b>Table of contents</b>	<b>1</b>
<b>Index of figures</b>	<b>2</b>
<b>1. Introduction</b>	<b>6</b>
<b>2. Objectives</b>	<b>13</b>
<b>3. Experimental</b>	<b>14</b>
3.1 <i>Synthesis</i>	15
3.2 <i>Self-assembly studies</i>	25
3.3 <i>Preliminary interaction studies</i>	27
<b>4. Results and discussion</b>	<b>28</b>
4.1 <i>Synthesis</i>	28
4.2 <i>Self-assembly studies</i>	33
4.3 <i>Preliminary interaction studies</i>	49
<b>5. Conclusions and future perspectives</b>	<b>54</b>
<b>Annexe</b>	<b>56</b>
<b>References</b>	<b>95</b>

# Index of figures

Figure 1 - Example of several non-covalent forces in supramolecular chemistry	7
Figure 2 - Structure of acylhydrazone derivatives capable of assembly into spherical aggregates	7
Figure 3 - Chemical equilibrium in a growing stack <sup>14</sup> (image adapted from ref 14)	7
Figure 4 - Structure of 5,10,15,20-Tetra(4-pyridyl)-21H,23H-porphine opposed to an overview of the condition/morphologies that can be obtained with this compound	8
Figure 5 - Model of a 3:3 complex between CD40 and CD40L opposed to CD40 mimetic compounds (taken from ref <sup>37</sup> )	9
Figure 6 - C <sub>3</sub> symmetric basket type receptor for organophosphates (adapted from ref <sup>47</sup> )	10
Figure 7 - Inclusion complex of ammonium ion in an oxazoline-based receptor	10
Figure 8 - Structure of compound 1 opposed to hollow spheres in 1:1 THF-H <sub>2</sub> O and fibers in 1:1 DMSO-H <sub>2</sub> O	11
Figure 9 - Scheme for the Curtius synthesis of BTA derivative	11
Figure 10 - Scheme for Rohm and Haas patented BTA derivative synthesis	11
Figure 11 - Scheme for common synthesis of BTA derivatives	12
Figure 12 - Scheme of the reaction of the synthesis of BTA derivative 1	15
Figure 13 - Scheme of the reaction of synthesis of BTA derivative 2	16
Figure 14 - Scheme of the reaction of synthesis of BTA derivative 3	17
Figure 15 - Scheme of the reaction of synthesis of Tyrosine Methyl Ester Hydrochloride	18
Figure 16 - Scheme of the reaction of synthesis of BTA derivative 4	19
Figure 17 - Scheme of the reaction of synthesis of BTA derivative 4	19
Figure 18 - Scheme of the reaction of synthesis of BTA derivative 4	20
Figure 19 - Scheme of the reaction of synthesis of BTA derivative 4	20
Figure 20 - Scheme of the reaction of synthesis of BTA derivative 4	21
Figure 21 - Scheme of the reaction of synthesis of BTA derivative 4	21
Figure 22 - Scheme of the reaction of synthesis of Tryptophan Methyl Ester Hydrochloride	22
Figure 23 - Scheme of the reaction of synthesis of BTA derivative 5	23
Figure 24 - General scheme for the synthesis of BTA 1-5.	28
Figure 25 - Correlation of the amide proton and vicinal proton in the COSY spectrum of BTA 5 in DMSO- <i>d</i> <sub>6</sub>	30
Figure 26 - Correlation of the amide and BTC core with the amide carbonyl in the HMBC spectrum of BTC 5 in DMSO- <i>d</i> <sub>6</sub>	31
Figure 27 - <sup>1</sup> H- <sup>1</sup> H NOESY correlation between the amide proton and the BTC core in the BTA 5	31
Figure 28 - Comparison of dispersion of aggregates size in a cooperative and isodesmic mechanism	34

Figure 29 - Comparison of BTA 1 spherical aggregates obtained in THF-H <sub>2</sub> O a) 60:40 b) 80:20 c) 100:0	34
Figure 30 - Stacked spectra of dilution experiment of BTA 1 in THF	35
Figure 31 - Zoom in the aromatic region of BTA 1 in the water titration experiment in THF- <i>d</i> 8:THF (1:9)	36
Figure 32 - Overview of the signals shift in BTA 1 <sup>1</sup> H-NMR water titration experiment	36
Figure 33 - Plot of $\Delta\delta$ against concentration of BTA 1	38
Figure 34 - Aromatic region of <sup>1</sup> H-NMR concentration dependent spectra of compound 1 in DMSO- <i>d</i> 6	39
Figure 35 - Overview of the $\Delta\delta$ in the BTA 1 concentration dependent <sup>1</sup> H-NMR experiments	40
Figure 36 - Origin fits to eq. 4 for BTA 2 a) amide proton, b) BTC core proton and c) H6, H6'	41
Figure 37 - Plot of $\Delta\delta$ against concentration of BTA 4	42
Figure 38 - Overview of the $\Delta\delta$ in the BTA 4 concentration dependent <sup>1</sup> H-NMR experiments	42
Figure 39 - Plot of $\Delta\delta$ against concentration of BTA 5	43
Figure 40 - Overview of the $\Delta\delta$ in the BTA 5 concentration dependent <sup>1</sup> H-NMR experiments	43
Figure 41 - HF/STO-3G results of the geometry optimizations of a. BTA 1, b. BTA 2, c. BTA 3, d. BTA 4 and e. BTA 5	44
Figure 42 - Proposed assembly for a reported molecular basket (image adapted form ref. 74)	44
Figure 43 - NOESY spectrum of BTA 1 at 12.7 mM in DMSO- <i>d</i> 6	45
Figure 44 - NOESY spectrum of BTA 1 at 2.68 mM in DMSO- <i>d</i> 6	46
Figure 45 - NOESY spectrum of BTA 2 at 20mM in DMSO- <i>d</i> 6	47
Figure 46 - Aromatic region of BTA 5 in the titration experiment with glucose	49
Figure 47 - Zoom in the aromatic region of BTA 5 stacked <sup>1</sup> H-NMR spectra in the titration experiment with ammonium chloride at 25 °C. Guest/host ratio is displayed on the spectra starting from a condition (*) with only host present at 6.23 mM	50
Figure 48 - Zoom in the aromatic region of BTA 5 stacked <sup>1</sup> H-NMR spectra in the titration experiment with ammonium chloride at 35 °C. Guest/host ratio is displayed on the spectra starting from a condition (*) with only host present at 6.84 mM	50
Figure 49 - Overview of the $\Delta\delta$ in the BTA 5 ammonium chloride titration experiments	51
Figure 50 - Proposed ammonium-BTA 5 interaction	51
Figure 51 - $\Delta\delta$ against guest/host proportion in the BTA 5 ammonium chloride titration experiment at 25 °C	52
Figure 52 - $\Delta\delta$ against guest/host proportion in the BTA 5 ammonium chloride titration experiment at 35 °C	52
Figure 53 - Possible BTA derived compound with 4-styrylaniline as a substituent	55
Figure 54 - Melamine core	55
Figure 55 - <sup>1</sup> H NMR spectrum of BTA 1 in DMSO- <i>d</i> 6	67
Figure 56 - <sup>13</sup> C NMR spectrum of BTA 1 in DMSO- <i>d</i> 6	67
Figure 57 - COSY spectrum of BTA 1 in DMSO- <i>d</i> 6	68
Figure 58 - HSQC spectrum of BTA 1 in DMSO- <i>d</i> 6	68

Figure 59 - HMBC spectrum of BTA 1 in DMSO- <i>d</i> <sub>6</sub>	69
Figure 60 - <sup>1</sup> H NMR spectrum of BTA 2 in DMSO- <i>d</i> <sub>6</sub>	69
Figure 61 - <sup>13</sup> C NMR spectrum of BTA 2 in DMSO- <i>d</i> <sub>6</sub>	70
Figure 62 - COSY spectrum of BTA 2 in DMSO- <i>d</i> <sub>6</sub>	70
Figure 63 - HSQC spectrum of BTA 2 in DMSO- <i>d</i> <sub>6</sub>	71
Figure 64 - HMBC spectrum of BTA 2 in DMSO- <i>d</i> <sub>6</sub>	71
Figure 65 - <sup>1</sup> H NMR spectrum of BTA 3 in DMSO- <i>d</i> <sub>6</sub>	72
Figure 66 - <sup>13</sup> C NMR spectrum of BTA 3 in DMSO- <i>d</i> <sub>6</sub>	72
Figure 67 - COSY spectrum of BTA 3 in DMSO- <i>d</i> <sub>6</sub>	73
Figure 68 - HSQC spectrum of BTA 3 in DMSO- <i>d</i> <sub>6</sub>	73
Figure 69 - HMBC spectrum of BTA 3 in DMSO- <i>d</i> <sub>6</sub>	74
Figure 70 - Water suppressed <sup>1</sup> H NMR spectrum of tyrosine methyl ester hydrochloride in D <sub>2</sub> O	74
Figure 71 - <sup>13</sup> C NMR spectrum of tyrosine methyl ester hydrochloride in D <sub>2</sub> O	75
Figure 72 - COSY spectrum of tyrosine methyl ester hydrochloride in D <sub>2</sub> O	75
Figure 73 - HSQC spectrum of tyrosine methyl ester hydrochloride in D <sub>2</sub> O	76
Figure 74 - HMBC spectrum of tyrosine methyl ester hydrochloride in D <sub>2</sub> O	76
Figure 75 - <sup>1</sup> H NMR spectrum of BTA 4 in DMSO- <i>d</i> <sub>6</sub>	77
Figure 76 - <sup>13</sup> C NMR spectrum of BTA 4 in DMSO- <i>d</i> <sub>6</sub>	77
Figure 77 - COSY spectrum of BTA 4 in DMSO- <i>d</i> <sub>6</sub>	78
Figure 78 - HSQC spectrum of BTA 4 in DMSO- <i>d</i> <sub>6</sub>	78
Figure 79 - HMBC spectrum of BTA 4 in DMSO- <i>d</i> <sub>6</sub>	79
Figure 80 - Water suppressed <sup>1</sup> H NMR spectrum of tryptophan methyl ester hydrochloride in D <sub>2</sub> O	79
Figure 81 - <sup>13</sup> C NMR spectrum of tryptophan methyl ester hydrochloride in D <sub>2</sub> O	80
Figure 82 - COSY spectrum of tryptophan methyl ester hydrochloride in D <sub>2</sub> O	80
Figure 83 - HSQC spectrum of tryptophan methyl ester hydrochloride in D <sub>2</sub> O	81
Figure 84 - HMBC spectrum of tryptophan methyl ester hydrochloride in D <sub>2</sub> O	81
Figure 85 - <sup>1</sup> H NMR spectrum of BTA 5 in DMSO- <i>d</i> <sub>6</sub>	82
Figure 86 - <sup>13</sup> C NMR spectrum of BTA 5 in DMSO- <i>d</i> <sub>6</sub>	82
Figure 87 - COSY spectrum of BTA 5 in DMSO- <i>d</i> <sub>6</sub>	83
Figure 88 - HSQC spectrum of BTA 5 in DMSO- <i>d</i> <sub>6</sub>	83
Figure 89 - HMBC spectrum of BTA 5 in DMSO- <i>d</i> <sub>6</sub>	84
Figure 90 - NOESY spectrum of BTA 2 at 20.90 mM in DMSO- <i>d</i> <sub>6</sub>	84
Figure 91 - NOESY spectrum of BTA 3 at 20.94 mM in DMSO- <i>d</i> <sub>6</sub>	85
Figure 92 - NOESY spectrum of BTA 3 at 0.84 mM in DMSO- <i>d</i> <sub>6</sub>	85
Figure 93 - NOESY spectrum of BTA 4 at 9.80 mM in DMSO- <i>d</i> <sub>6</sub>	86
Figure 94 - NOESY spectrum of BTA 4 at 0.98 mM in DMSO- <i>d</i> <sub>6</sub>	86
Figure 95 - NOESY spectrum of BTA 5 at 20.97 mM in DMSO- <i>d</i> <sub>6</sub>	87
Figure 96 - Full stack of BTA 1 concentration dependent spectra from 0.74 mM to 12.37 mM	87

Figure 97 - Aromatic region of BTA 1 concentration dependent spectra from 0.74 mM to 12.37 mM	88
Figure 98 - Full stack of BTA 2 concentration dependent spectra from 0.84 mM to 20.90 mM	88
Figure 99 - Aromatic region of BTA 2 concentration dependent spectra from 0.84 mM to 20.90 mM	89
Figure 100 - Full stack of BTA 3 concentration dependent spectra from 0.84 mM to 20.94 mM	89
Figure 101 - Aromatic region of BTA 3 concentration dependent spectra from 0.84 mM to 20.94 mM	90
Figure 102 - Full stack of BTA 4 concentration dependent spectra from 0.98 mM to 9.80 mM	90
Figure 103 - Aromatic region of BTA 4 concentration dependent spectra from 0.98 mM to 9.80 mM	91
Figure 104 - Full stack of BTA 5 concentration dependent spectra from 0.86 mM to 21.58 mM	91
Figure 105 - Aromatic region of BTA 5 concentration dependent spectra from 0.86 mM to 21.58 mM	92
Figure 106 - Full stack of $^1\text{H}$ -NMR spectra in the water titration experiments of BTA 1 in THF from 2.0% of added $\text{H}_2\text{O}$ to 15.3%	92
Figure 107 - Full stack of $^1\text{H}$ -NMR experiments in the glucose titration	93
Figure 108 - Full stack of $^1\text{H}$ -NMR experiments in the ammonium chloride titration at 25 $^\circ\text{C}$ starting with only host present until a guest/host ratio of 1.45	93
Figure 109 - Full stack of $^1\text{H}$ -NMR experiments in the ammonium chloride titration at 35 $^\circ\text{C}$ starting with only host present until a guest/host ratio of 1.32	94



# 1. Introduction

Supramolecular chemistry as stated by Lehn<sup>1</sup> is the “chemistry beyond the molecule”, structures that by intermolecular or intramolecular non-covalent interactions give rise to higher complexity and ordered architectures.

Traditionally, chemistry relies upon the covalent bond in step by step reactions until the formation of the desired compound, that fact makes it quite hard to build very large and complex systems.<sup>2</sup> By synthesizing a molecule that can assemble in solution into the desired final structure one can overcome that problem, so the interest in going beyond the covalent bond is in the building of large and complex molecules in an easier way.

The term supramolecule (or supermolecule as it was first named) is first employed by Wolf<sup>3</sup> in his paper about hydrogen bonding in acetic acid dimers. Since then is a general description for a wide range of different types of assemblies such as dendrimers<sup>4,5</sup>, micelles<sup>6</sup>, vesicles<sup>7</sup> or liquid crystals<sup>8</sup>. With the exception of dendrimers that are covalently bonded, non-covalent forces usually form these assemblies.


The process that forms these types of molecules is called self-assembly which is the spontaneous and reversible self-organization of molecules in solution<sup>9</sup>.

It is found in nature many examples of biological self-assembled structures such as protein-based complexes, hemoglobin<sup>10</sup> or nucleic acid derivatives such as DNA double chain.<sup>11</sup>

Self-assembly and organization typically occurs between at least two molecules, one exception to that are proteins in which the tertiary structure, and quaternary if existent, assemble from one molecule intramolecular interactions only.

For its characteristics such as reversibility self-assembled structures are common study subjects for host-guest interactions, such as in sensing application and coordination chemistry<sup>12</sup> in the development of ligands.

Figure 1 is an example of several forces involved in the assembly of a reported acylhydrazone derivative (Figure 2).<sup>13</sup>



Monomer

Dimer

Polymer

**Figure 3 - Chemical equilibrium in a growing stack<sup>14</sup> (image adapted from ref 14)**

An organisation of molecules in solution results in the loss of degrees of freedom that has an entropic penalty in the thermodynamics of the assembly process. In order to overcome the loss in entropy of the system, the enthalpic contribution of each interaction as to make the final structure thermodynamically favoured and that makes the binding interactions a crucial point of the assembly process.

Overall the type of assembly achieved depends on the structure of the monomers and how they interact in order to assemble into a higher ordered structure. That can result in different morphologies and shapes of aggregates such as fibers<sup>15</sup>, rods<sup>16</sup> or spherical aggregates.<sup>17</sup>

For the controllability of this type of structures, one has to understand how their assembly occurs and how the chemical equilibrium is established in solution. Qiu *et al* in their 2010 paper discovered that by controlling the surface tension and the nano particle aging time could obtain different final morphologies like bulk spheres, hollow spheres and nanotubes<sup>18</sup>.

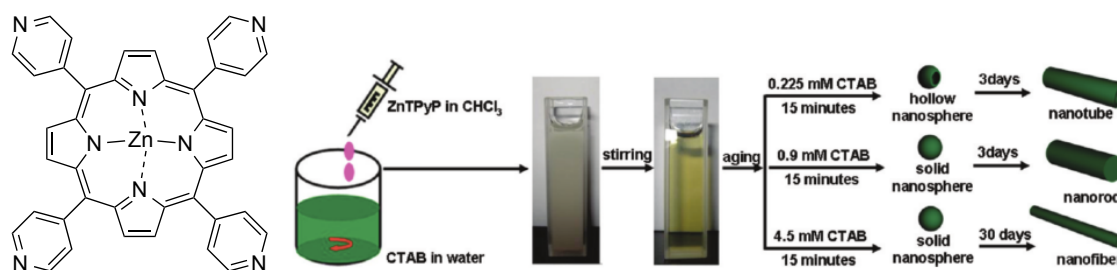


**Figure 4 - Structure of 5,10,15,20-Tetra(4-pyridyl)-21H,23H-porphine opposed to an overview of the condition/morphologies that can be obtained with this compound**

The control of the morphology of the aggregate is important in the development of smart responsive materials<sup>19,20,21</sup> that can be used for biomedical applications, environmental sciences or information technologies.<sup>22</sup> A possible medical application is the development of drug delivery methods. Those can be made to encapsulate a drug and deliver it by the application of an external stimulus that disrupts the structure and delivers the drug on the intended target.

Because of biocompatibility macromolecules such as peptides,<sup>23,24</sup> lipids,<sup>25–27</sup> sugars<sup>28,29</sup> or nuclei acids<sup>30–32</sup> are usually employed.

There are other types of structures and compounds that can be used and are under different stages of development, for instance metallic nanoparticles<sup>33–35</sup> are one used for drug delivery and imaging agents,<sup>36</sup> others being non-lipidic polymeric materials, but they lack the controllability factor that one can achieve using small responsive organic compounds.

$C_3$ -Symmetry is a known ordering motif found in nature.<sup>37,38</sup> In 2005 Fournel<sup>39</sup> *et al* developed a low molecular weight CD40L receptor based on CD40 a natural receptor that by binding its ligand contributes to regulation of B cell proliferation, immunoglobulin production, immunoglobulin class switching, germinal center formation and development of B cell memory.

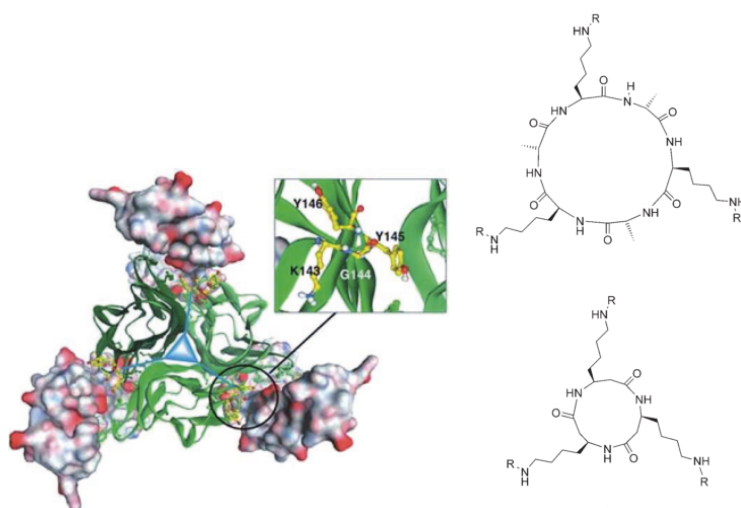


**Figure 5 - Model of a 3:3 complex between CD40 and CD40L opposed to CD40 mimetic compounds (taken from ref. 37)**

$C_3$ -Symmetric compounds have been studied for several applications, such as the development of catalysts in the area of asymmetric catalysis,<sup>40,41</sup> and in the area of chiral separation. These compounds have also been employed in the development of chiroptical devices<sup>42</sup> since chiral helical gels become non-random coiled, if some monomer molecules are chiral or in the presence of a small quantity a second optical active compound enclosed in the stack. That principle of a few molecules that governs the bulk assembly process is called the “sergeants-and-soldiers” principle<sup>43,44</sup> and has been fairly reported in literature.

The field of molecular recognition for the development of sensors which has always been a part of the study of supramolecules in host-guest interactions and sensing applications.<sup>45</sup>

Several  $C_3$ -symmetric compounds are reported to act as molecular receptors<sup>39</sup> for sensing applications,<sup>46</sup> for instance in the recognition of organophosphates,<sup>47,48</sup> which is a class of compounds that comprise several nerve agents.

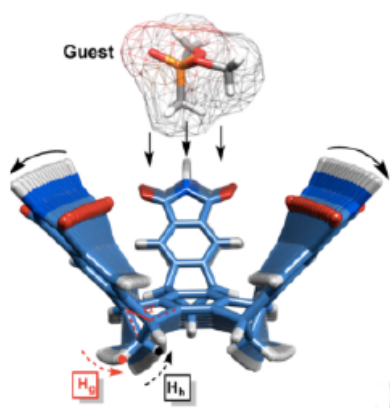


Figure 6 –  $C_3$  symmetric basket type receptor for organophosphates (adapted from ref. 47)

A  $C_3$ -symmetric compound bearing oxazoline groups has been reported to bind ammonium ions<sup>49</sup> there are also several studies that report that amino acid aromatic side-chains interact with cation by cation- $\pi$  interactions.<sup>50,51</sup> In Figure 7 is presented a complex made by the recognition of a ammonium ion by a oxazoline based receptor.<sup>52</sup>



Figure 7 - Inclusion complex of ammonium ion in an oxazoline-based receptor

The assembly process of a 1,3,5 -  $C_3$ -symmetric benzenetricarboxamide (BTA) was earlier described in literature.<sup>53</sup> This particular compound, BTA **1**, exhibits a stimuli responsive behaviour towards solvent effects and light irradiation. The structure of the BTA **1** is presented in Figure 8 opposed to some morphologies obtained in different solvent compositions.

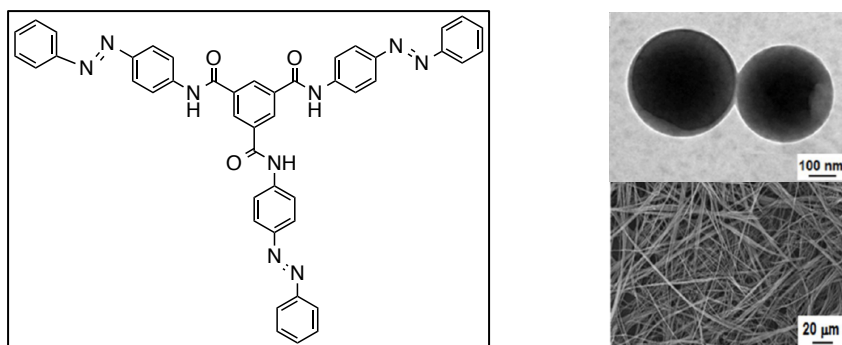


**Figure 8 - Structure of compound 1 opposed to SEM images of hollow spheres in 1:1 THF-H<sub>2</sub>O and fibers in 1:1 DMSO-H<sub>2</sub>O**

On the synthesis of these kind of molecules, the first BTA molecule was reported in 1915 by Curtius<sup>54</sup> the reaction involved the use of benzene-1,3,5-tricarboxylic acid as the starting material obtaining the triacyl triazide via the triester. The triacyl triazide was then treated with aniline resulting in the formation of a triphenyl substituted BTA. The highly explosive triacyl triazide, however, does not allow large-scale preparation of BTAs.

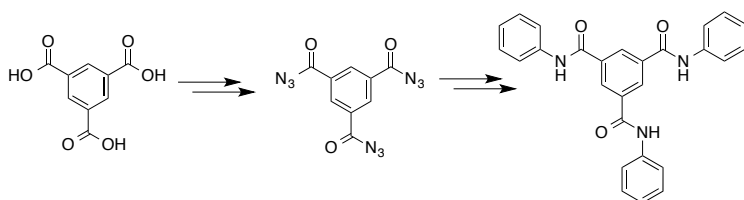


**Figure 9 - Scheme for the Curtius synthesis of BTA derivative**

In 1954 Rohm and Haas patented<sup>55</sup> the preparation of the tris(vinyloxyethyl) BTA analogue, starting from trimethyl benzene-1,3,5-tricarboxylate and 2-vinyloxyethylamine. This amidation reaction required high reaction temperatures and long reaction times.

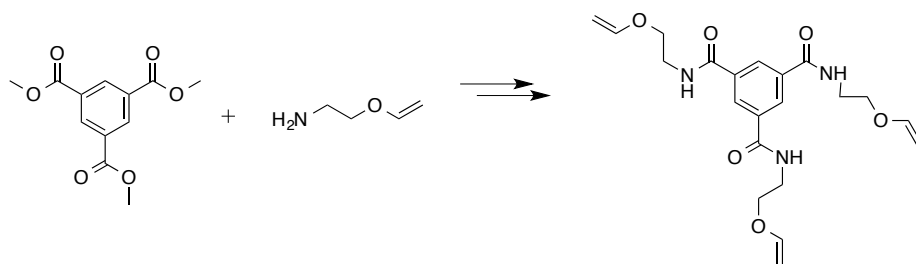


**Figure 10 – Scheme for Rohm and Haas patented BTA derivative synthesis**

In 1959, the tris(ortho-nitrophenyl) analogue was obtained<sup>56</sup> by first reacting benzene-1,3,5-tricarboxylic acid with thionyl chloride, the acid chloride formed then reacted with an amine at room temperature. This synthetic procedure significantly reduced the reaction time, as a result of the reactive acid chloride intermediate.

The most common<sup>57</sup> synthetic strategy to prepare C=O-centred BTAs today is the reaction of benzene-1,3,5-tricarbonyl trichloride with the appropriate amine in the presence of base, although direct functionalization of benzene-1,3,5-tricarboxylic acid with the appropriate amine by using coupling agents is also frequently applied.

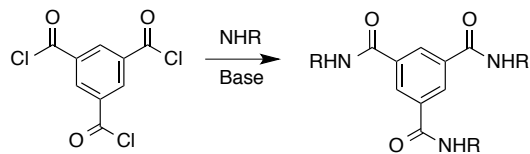


**Figure 11 - Scheme for common synthesis of BTA derivatives**

## 2. Objectives

It is imperative to gain a molecular detailed knowledge of the self-assembly process to be able to tune it for specific applications. As was mentioned before the assembly process of 1,3,5 - C<sub>3</sub>-symmetric benzenetricarboxamide (BTA) was earlier described in literature.<sup>53</sup> One problem with this kind of molecules is that they are usually insoluble in water and this narrows its possible applications (medical applications for instance), so it is also important to tune their solubility properties by introducing structural modifications.

NMR spectroscopy can be a valuable tool to gain structural insight into the self-assembly process since it can be used to probe local effects such as chemical shift differences, relaxation times, intramolecular or intermolecular interactions and diffusion measurements that correlates with molecular size.

Based on the already reported C<sub>3</sub>-symmetric 1,3,5 BTA compounds that stack into supramolecular helical gel and fibbers, the approach employed in this work was to introduce structural modification in the 1,3,5 – C<sub>3</sub>-symmetric BTA. This can be achieved by synthesizing several derivatives with different substituents that will induce changes in conformation of the molecule, H-bonding capability and how the extent of the aromatic system relate with  $\pi$ -  $\pi$  stacking in order to relate these structural features with the stacking (self-assembly) process itself. This knowledge of how to fine tune the aggregation process on a molecular level is imperative in the development of smart materials.

To study the aggregation and self-assembly process NMR spectroscopy was explored as the main tool. Since C<sub>3</sub>-symmetric compounds have been reported to bind ions and small molecules the synthesized molecules were also probed for uses in sensing of small molecules.



### 3. Experimental

#### Materials and methods

FTIR absorption spectra were recorded using 16 scans on a Perkin Elmer Spectrum BX spectrometer using KBr as support, the most intense and/or characteristic vibrations are presented stating their intensity and shape with the following abbreviations: br, broad; sh, sharp; s, strong; m, medium; w, weak; ar aromatic; st stretch; sy symmetric; ip in plane vibration;  $\delta$  deformation vibration.

NMR experiments were acquired in a Bruker Avance III 400 spectrometer operating at 400.15 MHz for hydrogen, 100.61 MHz for carbon using 5mm tubes and a gas flow of 400 l/h either in a Bruker High Resolution BBO probe or TXI probe. Spectra description is presented stating the deuterated solvent used and for each signal, chemical shift value, multiplicity, integration and atom assignment. The following abbreviations were used to indicate signal multiplicity: s, singlet; d, doublet; t, triplet; q, quartet; m, multiplet.

Analytical grade solvents and commercially available reagents were used without further purification, except where noted.

Reactions were monitored by TLC using silica coated aluminium plates by Merck and revealed by UV/Vis Light and/or staining solution such as ninhydrin, bromophenol blue or potassium permanganate.

### 3.1 Synthesis

#### Synthesis of $N^1, N^3, N^5$ -tris(4-((*E*)-phenyldiazenyl)phenyl)benzene-1,3,5-tricarboxamide (BTA 1)

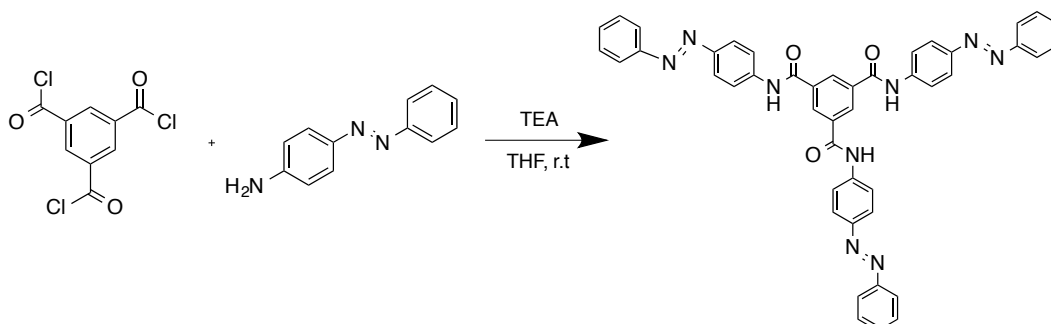


Figure 12 - Scheme of the reaction of the synthesis of BTA derivative 1

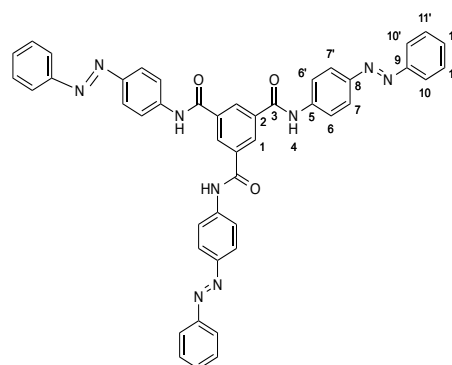
To a solution containing 4-phenylazoaniline (766.5 mg, 3.89 mmol) and distilled triethylamine (1 mL, 7.53 mmol) in THF (5 mL) was added dropwise a THF solution (10 mL) of 1,3,5-benzenetricarbonyl trichloride<sup>53</sup> (149  $\mu$ L, 0.75 mmol). The resulting mixture was stirred at room temperature for 24 h and filtered. The filtrate was concentrated in vacuum and MeOH was added to the residue. The resulting mixture was filtered under vacuum and the solid precipitate, (400 mg, 71% yield) washed with methanol until discoloration<sup>53</sup>.

Mp ( $^{\circ}$ C) >250

IR (KBr/ $\text{cm}^{-1}$ ) 1664 (m, sh, C=O st), 1654 (m, sh, C=O st), 1597 (m, sh, ar C-C st), 1534 (s, sh, N-C=O st sy), 1442 (w, sh, N=N st) 1406 (m, sh, ar C-C st), 1325, 1254 (m, sh, C-N st), 1154 (w, sh, NH  $\delta$  ip), 846, 768, 729, 686, 448.

$^1\text{H}$  NMR (400 MHz, DMSO)  $\delta$  10.99 (s, 3H, H4), 8.83 (s, 3H, H1), 8.12 (d,  $J$  = 8.8 Hz, 6H, H7, H7'), 8.00 (d,  $J$  = 8.7 Hz, 6H, H6, H6'), 7.90 (d,  $J$  = 7.2 Hz, 6H, H10, H10'), 7.72 – 7.45 (m, 9H, H11, H11', H12).

$^{13}\text{C}$  NMR (101 MHz, DMSO)  $\delta$  165.25 (C3), 152.56 (C9), 148.56 (C8), 142.56 (C5), 135.71



(C2), 131.64 (C1), 130.79 (C11), 129.92 (C12), 124.05 (C6, C6'), 122.86 (C10, C10'), 121.10 (C7, C7').

### Synthesis of $N^1, N^3, N^5$ -triphenylbenzene-1,3,5-tricarboxamide (BTA 2)

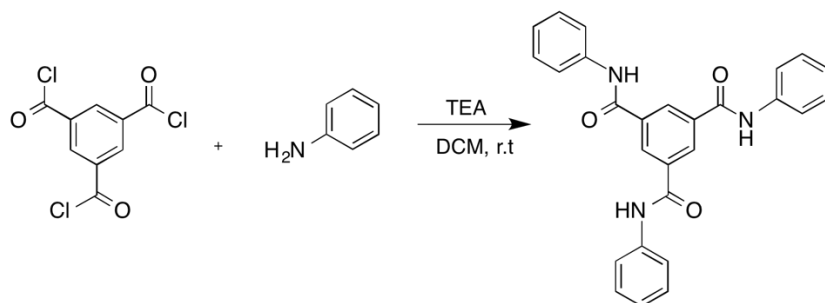


Figure 13 - Scheme of the reaction of synthesis of BTA derivative 2

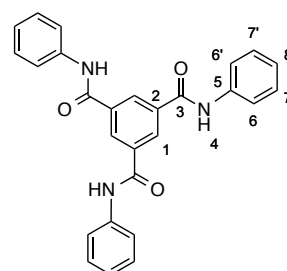
To a solution containing freshly distilled aniline (110  $\mu$ l 1.21 mmol) and distilled triethylamine (263  $\mu$ l, 1.88 mmol) in dichloromethane (5 mL) was added dropwise a dichloromethane solution (10 mL) of 1,3,5-benzenetricarbonyl trichloride<sup>58</sup> (74  $\mu$ l, 376  $\mu$ mol). The resulting mixture was stirred at room temperature for 24 h and concentrated in vacuum. The resulting solid was dissolved in cold THF and filtered in silica to obtain the product as a white solid (109.1 mg, 67 % yield).

Mp ( $^{\circ}$ C) >250

IR (KBr/ $\text{cm}^{-1}$ ) 3458 (br, m, ), 3292 (br, m ), 1664 (m, sh, C=O st), 1648 (s, sh, C=O st), 1602 (m, sh, ar C-C st), 1548 (m, sh, N-C=O st sy), 1520 (m, sh, ar C-C st), 1496, 1444, 1322, 1258 (m, sh, C-N st), 908, 752, 718, 688, 586, 506, 492.

$^1\text{H}$  NMR (400 MHz, DMSO)  $\delta$  10.60 (s, 3H, H4), 8.72 (s, 3H, H1), 7.84 (d,  $J$  = 7.6 Hz, 6H, H6, H6'), 7.41 (t,  $J$  = 7.9 Hz, 6H, H7, H7'), 7.16 (t,  $J$  = 7.4 Hz, 3H, H8).

$^{13}\text{C}$  NMR (101 MHz, DMSO)  $\delta$  165.02 (C3), 139.40 (C5, C5'), 135.99 (C2), 130.23 (C1), 129.21 (C6, C6'), 124.48 (C7), 120.91 (C5).



### Synthesis of $N^1,N^3,N^5$ -tribenzylbenzene-1,3,5-tricarboxamide (BTA 3)

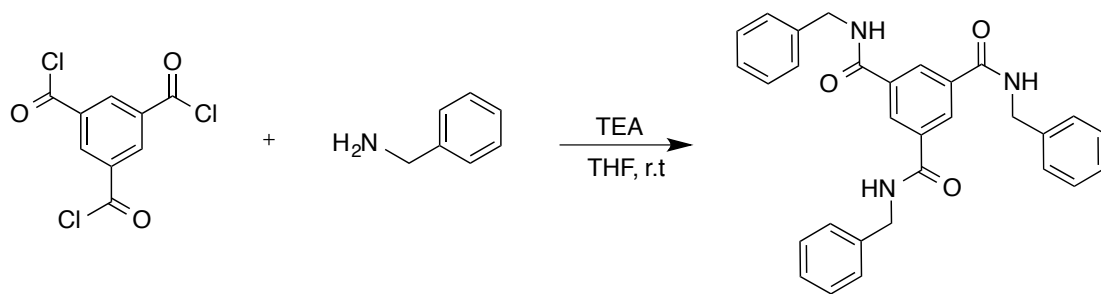


Figure 14 - Scheme of the reaction of synthesis of BTA derivative 3

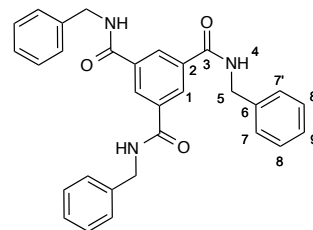
To a solution containing benzylamine (263  $\mu$ l, 2.41 mmol) and distilled triethylamine (336  $\mu$ l, 2.41 mmol) in THF (5mL) was added dropwise a THF solution (10mL) of 1,3,5-benzenetricarbonyl trichloride (149  $\mu$ l, 0.75 mmol). The resulting mixture was stirred at room temperature for 24 h and filtered. The filtrate was concentrated in vacuum. The solid was washed with sodium carbonate and ammonia chloride solution to obtain the desired product as a white solid (240 mg, 67 % yield).

Mp ( $^{\circ}$ C) 230-232

IR (KBr/ $\text{cm}^{-1}$ ) 3233, 3066, 2935, 1645(s, sh, C=O st), 1635 (s, sh, C=O st), 1556 (s, sh, N-C=O st sy), 1456, 1292 (s, sh, C-N st), 1080, 1027, 906, 696, 607, 486.

$^1\text{H}$  NMR (400 MHz, DMSO)  $\delta$  9.27 (t,  $J$  = 5.7 Hz, 3H, H4), 8.51 (s, 3H, H1), 7.45 – 7.14 (m, 15H, H7, H7', H8, H8', H9), 4.51 (d,  $J$  = 5.8 Hz, 6H, H5).

$^{13}\text{C}$  NMR (101 MHz, DMSO)  $\delta$  165.94 (C3), 139.86 (C6), 135.39 (C2), 129.22 (C1), 128.76 (C8), 127.85 (C7), 127.29 (9), 43.32 (C5).



## Tyrosine Methyl Ester Hydrochloride

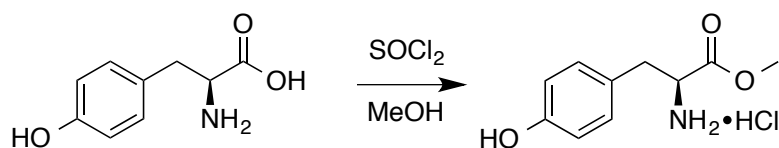


Figure 15 - Scheme of the reaction of synthesis of Tyrosine Methyl Ester Hydrochloride

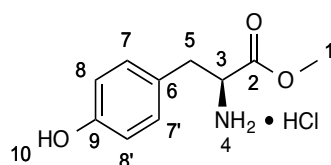
Thionyl Chloride (0.8 ml, 7.34 mmol) was added dropwise to a suspension of L-Tyrosine (1.81 g, 9.99 mmol) in 25 ml of dry methanol.<sup>59</sup> The mixture was refluxed for 18 h and concentrated in vacuum. The resulting crude product was triturated with hexane resulting in tyrosine methyl hydrochloride ester as a cream coloured solid (2.26 g, 98 % yield).

Mp (°C) 188-190

IR (KBr/ $\text{cm}^{-1}$ ) 3384 (s, br, N-H st), 3348 (s, br, N-H st), 3012(s, sh, ar C-H st), 2904 (s, br, C-H st), 1744 (s, sh, C=O st), 1616 (m, sh, ar C-C st), 1592 (m, sh, ar C-C st), 1516 (s, sh, ar C-C st), 1450, 1434, 1396, 1348, 1276 (m, sh, C-N st), 1250 (s, sh, C-O st), 1224 (s, sh, C-O st), 1108, 1056, 990, 934, 866, 840, 734, 618, 600, 514.

$^1\text{H}$  NMR (400 MHz,  $\text{D}_2\text{O}$ )  $\delta$  7.09 (d,  $J = 8.0$  Hz, 2H, H7, H7'), 6.83 (d,  $J = 8.0$  Hz, 2H, H8, H8'), 4.31 (t,  $J = 6.3$  Hz, 1H, H3), 3.77 (s, 3H, H1), 3.14 (ddd,  $J = 21.9, 14.6, 6.5$  Hz, 2H, H5).

$^{13}\text{C}$  NMR (101 MHz,  $\text{D}_2\text{O}$ )  $\delta$  170.13 (C2), 155.29 (C9), 130.88 (C7), 125.46 (C6), 116.04 (C8), 54.25 (C3), 53.60 (C1), 34.66 (C5).



**Synthesis of trimethyl 2,2',2''-(((benzene-1,3,5-tricarbonyl)tris(azanediy)))(2*S*,2'*S*,2''*S*)-tris(3-(4-hydroxyphenyl)propanoate) (BTA 4)**

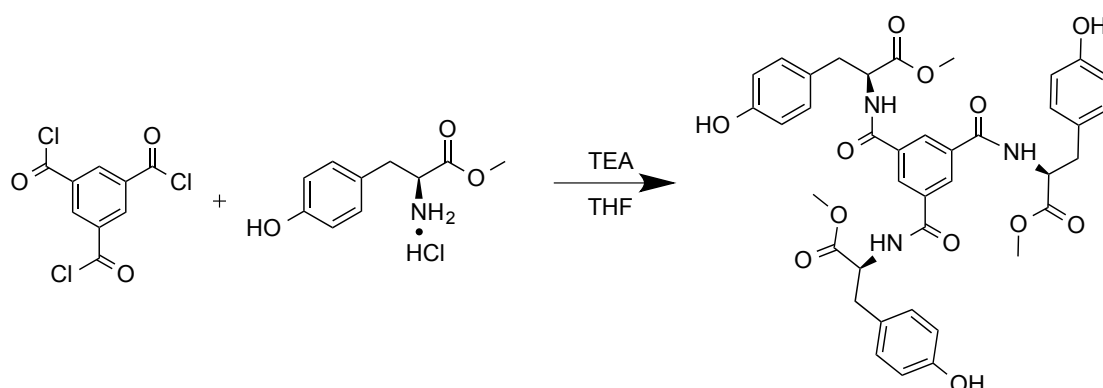


**Figure 16 - Scheme of the reaction of synthesis of BTA derivative 4**

To a solution containing tyrosine methyl ester hydrochloride (279.2 mg, 1.21 mmol) and distilled triethylamine (336  $\mu$ L, 1.29 mmol) in THF (5 mL) was added dropwise a THF solution (10 mL) of 1,3,5-benzenetricarbonyl trichloride (74  $\mu$ L, 376  $\mu$ mol). The resulting mixture was stirred at room temperature for 6 h and filtered. The reaction didn't proceed to completion as revealed by NMR spectroscopy and the product wasn't isolated.

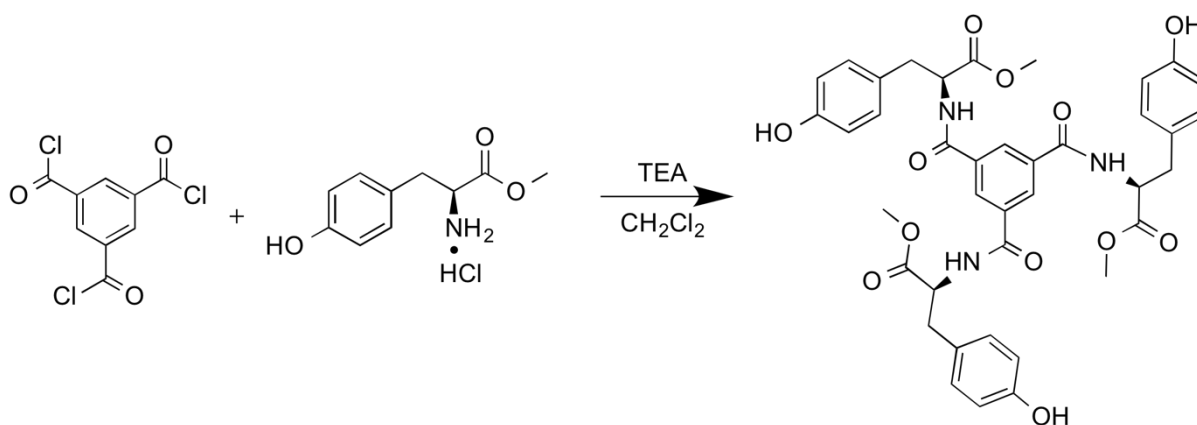


**Figure 17 - Scheme of the reaction of synthesis of BTA derivative 4**

To a solution containing tyrosine methyl ester hydrochloride (261.9 mg, 1.13 mmol) and distilled triethylamine (308  $\mu$ L, 2.21 mmol) in  $\text{CH}_2\text{Cl}_2$  (5 mL) was added dropwise a  $\text{CH}_2\text{Cl}_2$  solution (10 mL) of 1,3,5-benzenetricarbonyl trichloride (74  $\mu$ L, 376  $\mu$ mol). The resulting mixture was stirred at room temperature for 18 h and filtered. The reaction didn't proceed to completion as revealed by NMR spectroscopy and the product wasn't isolated.

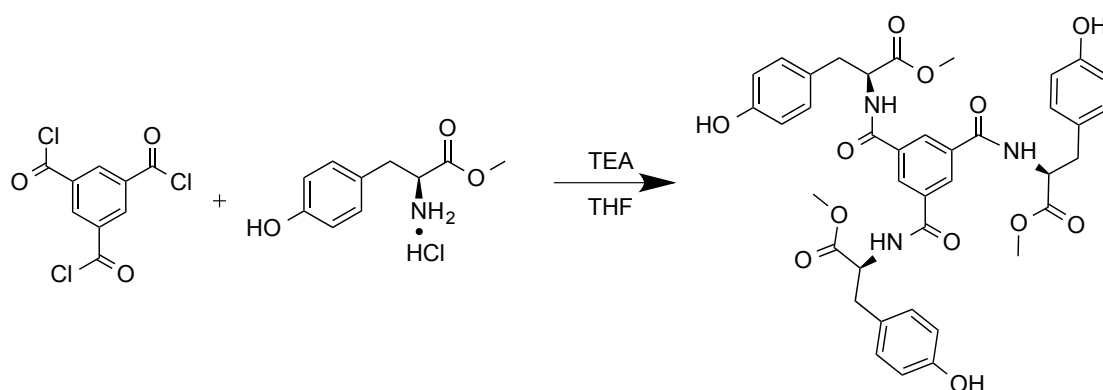


Figure 18 - Scheme of the reaction of synthesis of BTA derivative 4

To a solution containing tyrosine methyl ester hydrochloride (215.4 mg, 929.8  $\mu\text{mol}$ ) and distilled triethylamine (325  $\mu\text{L}$ , 2.33 mmol) in THF (5mL) was added dropwise a THF solution (10mL) of 1,3,5-benzenetricarbonyl trichloride (74  $\mu\text{L}$ , 376  $\mu\text{mol}$ ). The resulting mixture was stirred at room temperature for 26 h and filtered. The reaction didn't proceed to completion as revealed by NMR spectroscopy and the product wasn't isolated.

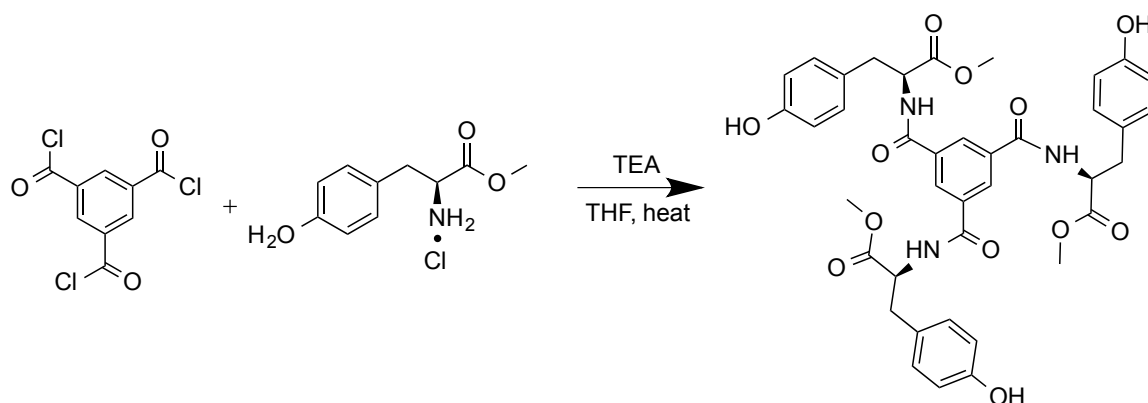
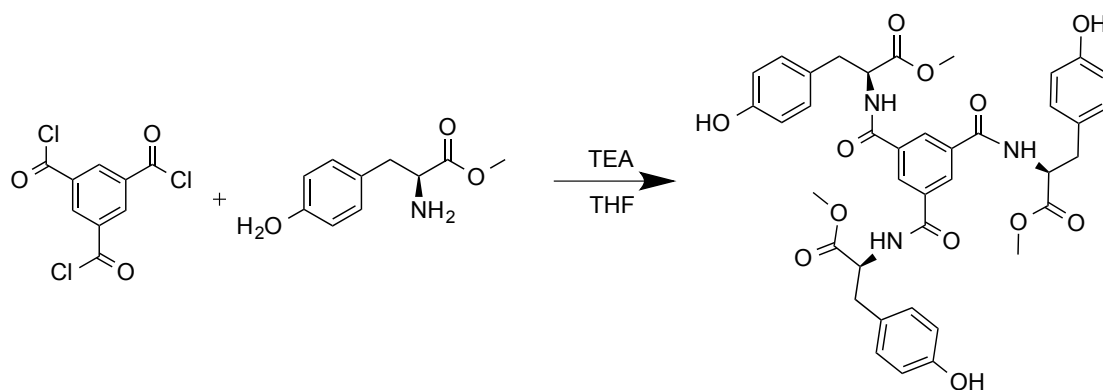


Figure 19 - Scheme of the reaction of synthesis of BTA derivative 4

To a solution containing tyrosine methyl ester hydrochloride (285.0 mg, 1.23 mmol) and distilled triethylamine (336  $\mu\text{L}$ , 2.41 mmol) in THF (5mL) was added dropwise a THF solution (10mL) of 1,3,5-benzenetricarbonyl trichloride (74  $\mu\text{L}$ , 376  $\mu\text{mol}$ ). The resulting mixture was stirred at room temperature for 24 h and filtered. The reaction didn't proceed to completion as revealed by NMR spectroscopy and the product wasn't isolated.



**Figure 20 - Scheme of the reaction of synthesis of BTA derivative 4**

Tyrosine methyl ester hydrochloride (302.4, 1.55 mmol) was taken in ethyl acetate and washed with 1 mM HCl solution and a sodium bicarbonate saturated solution. The organic phase was dried with anhydrous magnesium sulphate and evaporated.

The resulting solid was dissolved in THF (5 ml), added distilled triethylamine (336  $\mu$ l, 2.41 mmol) and stirred.

A THF solution (10 mL) of 1,3,5-benzenetricarbonyl trichloride (74  $\mu$ l, 376  $\mu$ mol) was then added dropwise<sup>60</sup>. The resulting mixture was stirred at room temperature for 24 h and filtered. The reaction didn't proceed to completion as revealed by NMR spectroscopy and the product wasn't isolated.

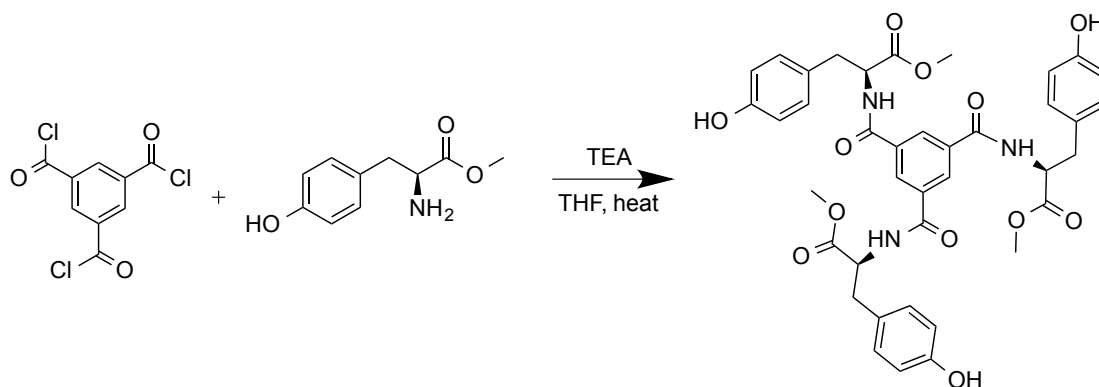


**Figure 21 - Scheme of the reaction of synthesis of BTA derivative 4**

Tyrosine methyl ester hydrochloride (300.0 mg, 1.29 mmol) was taken in ethyl acetate and washed with 1 mM HCl solution and a sodium bicarbonate saturated solution. The organic phase was dried with anhydrous magnesium sulphate and evaporated.

The resulting solid was dissolved in THF (5 ml), added distilled triethylamine (336  $\mu$ l, 2.41 mmol) and stirred.



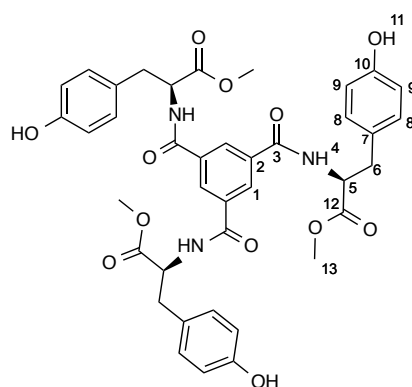
A THF solution (10 mL) of 1,3,5-benzenetricarbonyl trichloride (74  $\mu$ l, 376  $\mu$ mol) was then added dropwise<sup>60</sup>. The resulting mixture was stirred at room temperature for 24 h and filtered. The obtained solid was taken in ethyl acetate and washed with 1 mM HCl solution and a sodium bicarbonate saturated solution. The organic phase was dried with anhydrous magnesium sulphate and evaporated resulting in a yellow coloured solid (108 mg, 39% yield).

Mp ( $^{\circ}$ C) 120-130

IR (KBr/ $\text{cm}^{-1}$ ) 3366 (s, br, O-H st) 2956 (w, sh, C-H st), 1736 (m, sh, ester C=O st), 1652 (m, sh, amide C=O st), 1516 (m, sh, N-C=O st sy), 1438 (w, sh, ar C-C st), 1354, 1226 (s, sh, C-N st), 1108, 830.

$^1\text{H}$  NMR (400 MHz, DMSO)  $\delta$  9.22 (s, 3H, H11), 9.12 (d,  $J$  = 7.5 Hz, 3H, H4), 8.39 (s, 3H, H1), 7.08 (d,  $J$  = 8.2 Hz, 6H, H9 H9'), 6.67 (d,  $J$  = 8.2 Hz, 6H, H8 H8'), 4.60 (dd,  $J$  = 14.6, 7.7 Hz, 3H, H5), 3.64 (s, 9H, H13), 3.03 (t,  $J$  = 7.0 Hz, 6H, H6).

$^{13}\text{C}$  NMR (101 MHz, DMSO)  $\delta$  172.61 (C12), 166.10 (C3), 156.41 (C10), 134.69 (C2), 130.43 (C8), 129.78 (C1), 128.02 (C7), 115.58 (C9), 55.40 (C5), 52.40 (C13), 35.98 (C6).



### Triptophan Methyl Ester Hydrochloride

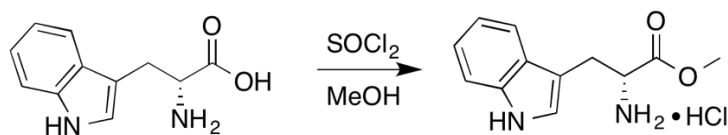


Figure 22 - Scheme of the reaction of synthesis of Triptophan Methyl Ester Hydrochloride

Thionyl Chloride (0.6 ml, 8.22 mmol) was added dropwise to a suspension of L-Tryptophan (1.50 g, 7.34 mmol) in 25 ml of dry methanol.<sup>59</sup> The mixture was refluxed for 18 h and concentrated in vacuum. The obtained white solid was recrystallized at 0  $^{\circ}$ C with

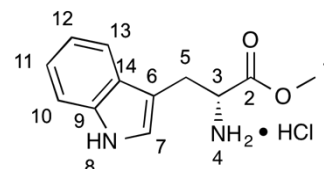
methanol/diethyl ether to obtain the tryptophan methyl ester hydrochloride as a cream coloured solid (1.40 g, 75 % yield).

Mp (°C) 220-224

IR (KBr/cm<sup>-1</sup>) 3424 (m, br, N-H st), 3294(s, br, N-H st), 3268 (s, br, N-H st), 3002 (s, br, ar C-H st), 2954(s, br, C-H st), 2022 (CO<sub>2</sub>), 1750 (s, sh, C=O st), 1620 (w, sh, ar C-C st), 1580(s, sh, ar C-C st), 1504(s, sh, ar C-C st), 1438, 1352, 1286, 1230 (s, sh, C-N st), 1212 (s, sh, C-N st), 1110, 732.

<sup>1</sup>H NMR (400 MHz, D<sub>2</sub>O) δ 7.53 (d, *J* = 7.9 Hz, 1H, H10), 7.47 (d, *J* = 8.2 Hz, 1H, H13), 7.26 – 7.17 (m, 2H, H7, H11), 7.13 (t, *J* = 7.5 Hz, 1H, H12), 4.37 (t, *J* = 6.2 Hz, 1H, H3), 3.73 (s, 3H, H1), 3.46 – 3.31 (m, 2H, H5).

<sup>13</sup>C NMR (101 MHz, D<sub>2</sub>O) δ 170.49 (C2), 136.36 (C9), 126.48 (C14), 125.45 (C7), 122.31 (C11), 119.67 (C12), 118.12 (C13), 112.14 (C10), 106.09 (C6), 53.65 (C1), 53.41 (C3), 25.73 (C5).



**Synthesis of trimethyl 2,2',2''-((benzene-1,3,5-tricarboxyl)tris(azanediyl)) (2*S*,2'*S*,2''*S*)-tris(3-(1*H*-indol-3-yl)propanoate) (BTA 5)**

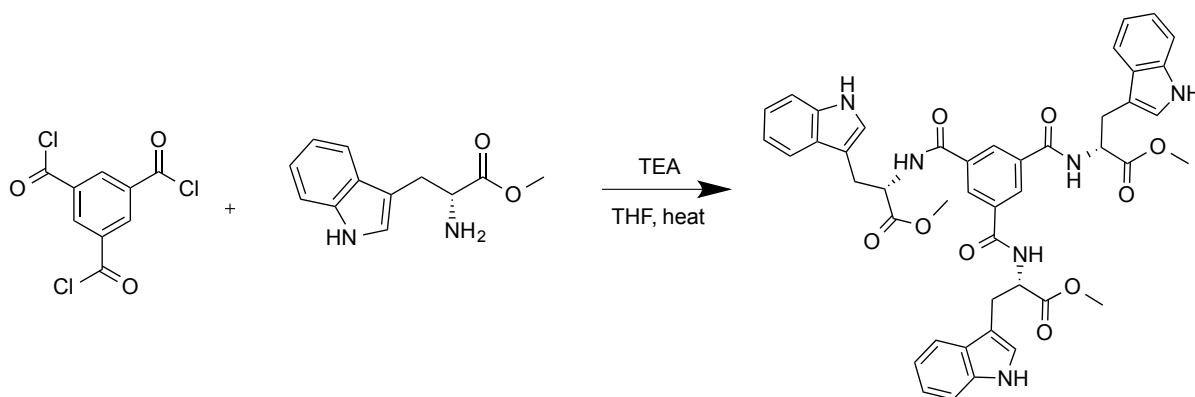


**Figure 23 - Scheme of the reaction of synthesis of BTA derivative 5**

Tryptophan methyl ester hydrochloride (400.0 mg 1.57 mmol) was taken in ethyl acetate and washed with 1 mM HCl solution and a sodium bicarbonate saturated solution. The organic phase was dried with anhydrous magnesium sulphate and evaporated.

The resulting solid was then taken in THF (5 ml) and added distilled triethylamine (336 µl, 2.41 mmol) and stirred.

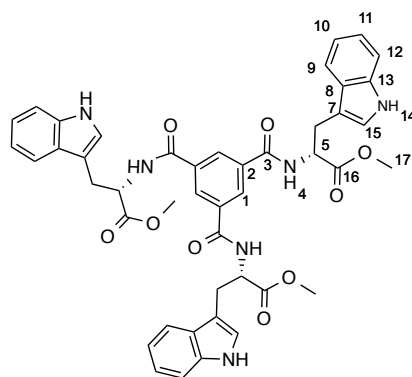
Then a THF solution (10 mL) of 1,3,5-benzenetricarbonyl trichloride (74  $\mu$ L, 376  $\mu$ mol) was added dropwise. The resulting mixture was stirred at room temperature for 24 h filtered and washed with cold THF. BTA **5** was obtained as a yellow coloured solid (219 mg, 72 % yield).

Mp ( $^{\circ}$ C) 120-135

IR (KBr/ $\text{cm}^{-1}$ ) 3408 (s, br, ), 3058(w, sh, ar C-H st), 2954 (w, sh, C-H st), 1736 (m, sh, ester C=O st), 1656 (m, sh, amide C=O st), 1528 (s sh, N-C=O st sy), 1438, 1342, 1220 (s, sh, C-N st), 1102, 742.

$^1\text{H}$  NMR (400 MHz, DMSO)  $\delta$  10.84 (s, 3H, H14), 9.17 (d,  $J$  = 7.4 Hz, 3H, H4), 8.46 (s, 3H, H1), 7.57 (d,  $J$  = 7.8 Hz, 3H, H12), 7.33 (d,  $J$  = 8.0 Hz, 3H, H9), 7.20 (s, 3H, H15), 7.07 (t,  $J$  = 7.5 Hz, 3H, H11), 6.99 (t,  $J$  = 7.4 Hz, 3H, H10), 4.81 – 4.59 (m, 3H, H5), 3.64 (s, 9H, H17), 3.31 – 3.21 (m, 6H, H6).

$^{13}\text{C}$  NMR (101 MHz, DMSO)  $\delta$  172.83 (C16), 166.67 (C3), 136.58 (C13), 134.63 (C2), 129.84 (C1), 127.48 (C8), 124.56 (C15), 121.47 (C11), 118.93 (C10), 118.45 (C12), 112.51 (C9), 110.31 (C7), 54.48 (C5), 52.43 (C17), 27.08 (C6)



## 3.2 Self-assembly studies

### NMR Spectroscopy

NMR experiments were acquired in a Bruker Avance III 400 spectrometer equipped with a temperature control unit and a pulsed field gradient unit capable of producing magnetic pulsed field gradients in the z-direction of 56.0 G/cm, operating at 400.15 MHz for hydrogen, 100.61 MHz for carbon using 5mm tubes and a gas flow of 400 l/h either in a Bruker High Resolution BBO probe or TXI probe.

DOSY experiments were acquired using the Oneshot<sup>61</sup> sequence or Bruker pulse sequence (ledbpgp2) with a LED (longitudinal eddy delay) using bipolar gradient pulses for diffusion. Each experiment consisted in acquiring 32 spectra of 64k data points. The pulse gradients (g) were incremented from 5 to 95 % of the maximum gradient strength in a linear ramp.

Concentration dependent spectra were obtained by acquiring <sup>1</sup>H-NMR spectra of the compounds at different concentrations, samples were prepared by diluting a concentrated solution of each compound in DMSO-*d*<sub>6</sub> or a mixture of THF: THF-*d*<sub>8</sub> (9:1) inside the NMR tubes.

The water titration experiment of BTA **1** was done by acquiring <sup>1</sup>H-NMR spectra at each step of addition of D<sub>2</sub>O from 0% to 18% of added water.

Concentration dependent spectra with an added percentage of water were made by acquiring <sup>1</sup>H-NMR spectra of solutions of the studied compound at different concentrations prepared by de dilution of a concentrated solution of the compound with an organic solvent-water mixture inside the NMR tubes.

Variable Temperature NMR experiments were obtained by varying the temperature of the samples used in the concentration dependent chemical shift measurement inside the NMR spectrometer.

2D COSY, HSQC, NOESY Spectra were acquired by using Bruker standard pulse programs.

Chemical shifts were referenced to the chemical shift of TMS, used as a internal reference or to the solvent residual peak where noted.

1D  $^1\text{H}$ ,  $^{13}\text{C}$  and 2D COSY, HSQC, NOESY Spectra were processed using Bruker Topspin 3.5 software and MestreLab Metrenova 6.0.2. DOSY spectra were processed using the DOSY Toolbox<sup>62</sup>.

### 3.3 Preliminary interaction studies

$^1\text{H}$ -NMR and Oneshot DOSY<sup>61</sup> were employed in order to probe for interaction between glucose and ammonium chloride with BTA **5**.

Chemical shifts were measured in  $^1\text{H}$ -NMR experiments by titrating a DMSO-*d*<sub>6</sub> solution of compound **5** in a NMR tube with the guest compound. Titration was made by adding 40  $\mu\text{l}$  of guest compound in 10  $\mu\text{l}$  steps. Each experiment started by acquiring a  $^1\text{H}$ -NMR spectrum of **5** without any guest added.

TMS was used as chemical shift reference and as a non-interacting reference in diffusion measurements to take solution effects into account, such as viscosity, pH or ionic strength.

# 4. Results and discussion

## 4.1 Synthesis

In order to understand how the structural variations in 1,3,5 – BTA compounds would influence their assembly process, several BTA derivatives were synthesized according to figure 24 and Table 1. C<sub>3</sub>-symmetric BTA derivatives were obtained in moderate to good yields from the reaction of 1,3,5-BTC chloride with aromatic amines in the presence of a base, triethylamine, to deprotonate the aromatic amines increasing its nucleophilicity. The stoichiometry of the reaction for the synthesis of compound **1-5** involves the addition of three molecules into one. Because of that it was necessary to use a small excess of the substituent in order to obtain the fully substituted core with three molecules.

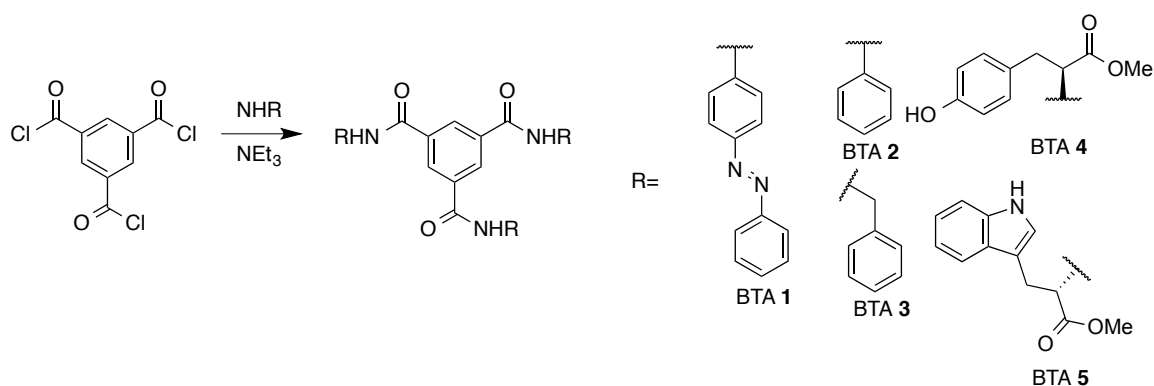
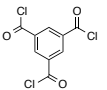
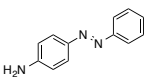
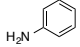
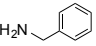
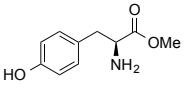
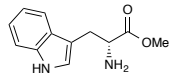


Figure 24 - General scheme for the synthesis of BTA 1-5.

Table 1 – Results of the synthesis of BTA 1-5

Core	Substituent	Solvent	Conditions	Yield (%)
		THF	r.t. 24 h	71
<b>2</b>		CH <sub>2</sub> Cl <sub>2</sub>	r.t. 18h	67
<b>3</b>		THF	r.t. 18 h	67
<b>4</b>		THF	Reflux, 24 h	39
<b>5</b>		THF	Reflux, 20 h	72

To evaluate the influence of the aromatic rings and molecular size in the aggregation process aniline and benzylamine derivatives were obtained (BTA **2** and **3**, respectively). These compounds would also allow to check how the structure rigidity would influence the assembly.

BTA derivatives are known to be only soluble in organic solvents such as THF, DMSO or DMF. In order to improve solubility in water and also biocompatibility, substitution with amino acids was pursued, in the reaction of BTC with aromatic amino acids - tyrosine for BTA **4** and tryptophan for BTA **5**. With these two latter compounds it was possible to add more unsaturated bonds to the final structure thus increasing its ability to establish  $\pi$ - $\pi$  interactions.

The amino acids addition to 1,3,5-BTC chloride was preceded by the introduction of a protecting group. The carboxamide formation requires the use of a base, however for tyrosine and tryptophan the presence of the carboxylic acid moiety, a group with a lower pKa than the amine would not allow a clean reaction. The esterification of the amino acids using methanol and thionyl chloride was the selected protecting strategy. The methyl group wouldn't bring much bulk to the final molecule, a factor that could affect the assembly capabilities because of steric hindrance. Deprotection was a possibility that was desired to keep, hydrolysis of the methyl ester would yield the BTA derivatives with the carboxylic acid group. While harder to deprotect than a silane ester or a tert-butyl group, requiring a concentrated strong base, the methyl ester was the compromise between steric bulk, and ease to protect/deprotect the carboxylic acid while doing its function in the reaction for the preparation of BTA **4** and **5**.

BTA **1**, **2**, **3** and **5** were obtained in good yield, for the synthesis of **4** it was necessary to optimize the reaction.

The phenol group in the tyrosine side-chain might affect the completion of the reaction in the desired path because its pKa is similar with the amine, 10 for the phenol and 9 for the amine, it is a potential reaction centre in the action of the triethylamine and result in several addition products in benzene tricarbonyl trichloride in several side-reactions, lowering the yield of the reaction on the BTC core.

In the synthesis of **4** it was also needed to deprotonate the hydrochloride salt in the tyrosine methyl ester, which was formed during the esterification reaction.

The hydrochloride was unreactive even under 6 equivalents of triethylamine that based on the stoichiometry of the reaction could be enough to break the hydrochloride salt and deprotonate the amine. The strategy employed was then a two step synthesis, first deprotonating the hydrochloride by dissolving it in ethyl acetate and washing with 1mM HCl



and saturated sodium bicarbonate solution and then to react the resulting product with the free amine with benzene-1,3,5-tricarbonyl trichloride. It was necessary to heat the reaction mixture to reflux in order to drive the reaction to completion, which can be justified because of the steric bulk of the tyrosine methyl ester.

After the optimization of the reaction conditions the same methodology was employed in the synthesis of **5**.

The measured melting points for **4** and **5** have a large temperature interval and might suggest several changes in possible conformations.

Regarding the analysis of the NMR spectra there were some similarities between the synthesized BTA that could be used to simplify the characterization procedure and ensure that the desired product was formed.

The molecular symmetry of compounds,  $C_3$  point symmetry group, made the analysis of the  $^1\text{H}$ -NMR easy to check if the desired product was obtained. The pattern of the chemical shifts for the amide and the aromatic core could be used as a probe the degree of substitution. Only complete substitution of the core leads to a  $C_3$ -symmetric molecule, where the magnetic and chemical equivalence of the protons give rise to single proton signals for each. On the COSY spectra it was possible to observe for BTA **3-5** the coupling of the amide proton with the vicinal proton, the COSY correlation is depicted in Figure 25.

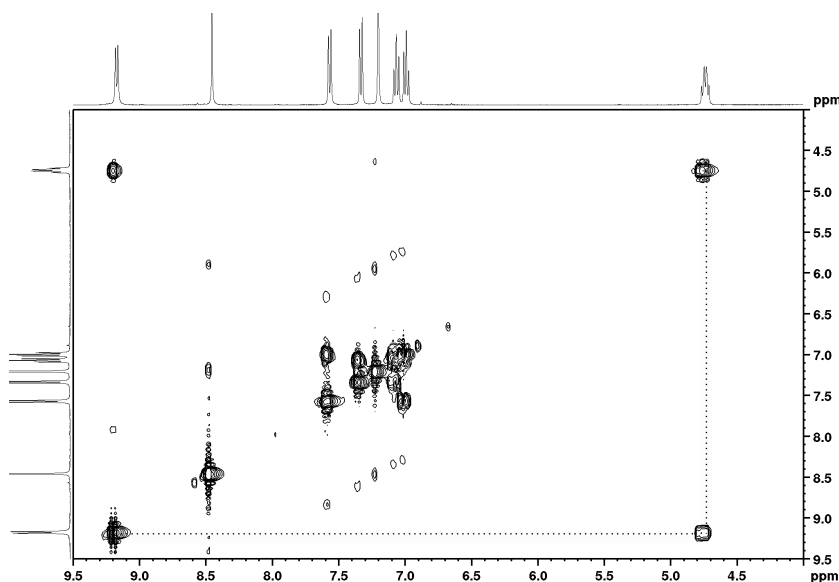
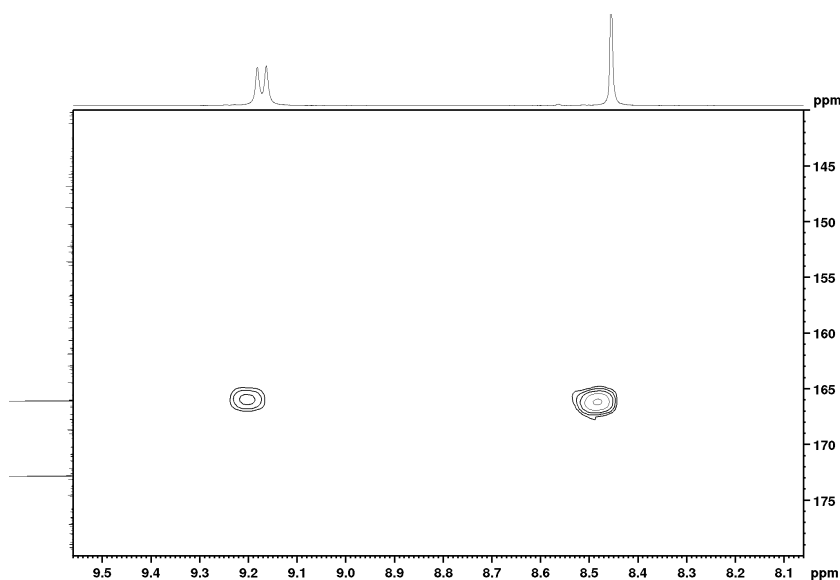


Figure 25 – Correlation of the amide proton and vicinal proton in the COSY spectrum of BTA **5** in  $\text{DMSO-}d_6$

That information combined with the integration in the  $^1\text{H}$ -NMR spectra and the change in the multiplicity, shape and chemical shift compared to the more easily exchangeable amine signal on the free substituent is a proof that the amide was formed. The formation of the amide bond could be later confirmed by the multiple bond correlation in the HMBC spectra as depicted in Figure 26 where is shown the amide correlation with carbonyl on the BTC core. Spatial correlation in the NOESY spectra between the BTC core proton and the amide proton was also observed and it is shown in Figure 27.

For BTA **1** and **2** all of those analyses were applicable, except the COSY correlation since in those compounds the amide doesn't have a vicinal proton.



**Figure 26 – Correlation of the amide and BTC core with the amide carbonyl in the HMBC spectrum of BTC 5 in DMSO- $d_6$**

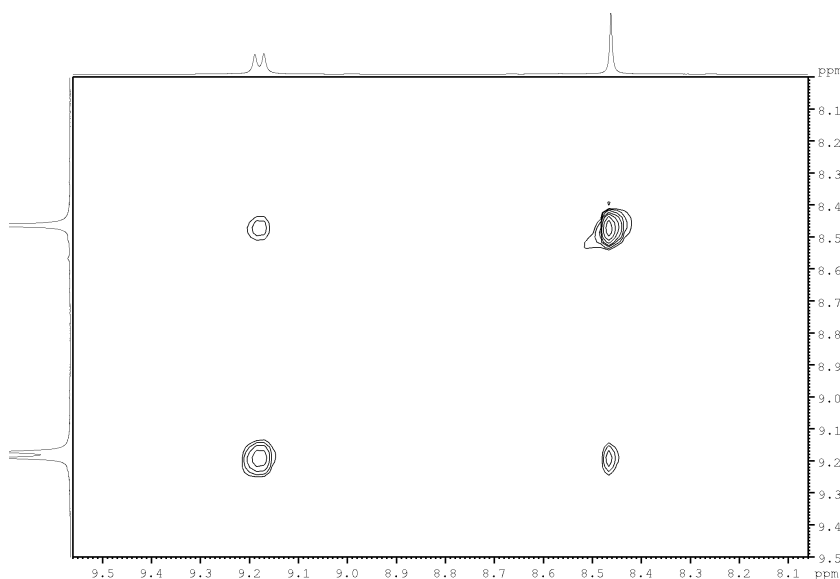


**Figure 27 -  $^1\text{H}$ - $^1\text{H}$  NOESY correlation between the amide proton and the BTC core in the BTA 5**

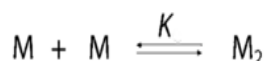
**Table 2 – Overview of the condition for the synthesis of BTA 4**

Triethylamine equivalents	Methyl ester hydrochloride salt	Solvent	Conditions	Yield (%)
3.4	yes	THF	r.t. 6 h	n.d
5.9	yes	CH <sub>2</sub> Cl <sub>2</sub>	r.t. 18h	n.d
6.2	yes	THF	r.t. 26 h	n.d.
6.4	yes	THF	Reflux, 16 h	n.d.
6.4	no	THF	r.t. 24h	n.d.
6.4	no	THF	Reflux, 24 h	39

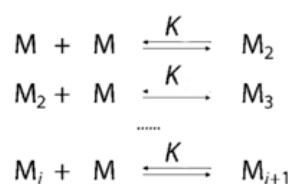
## 4.2 Self-assembly studies

Dimerization is the simplest case of assembly where the process is governed by a global equilibrium constant, that can have one, two or several different chemical equilibrium steps governed by different equilibrium constants.

Equation 1 - Equilibrium constant in a dimerization process



Equation 2 - Equilibrium constant in several aggregation steps



From the reported models in literature the most employed for the description of a growing molecular stack to form a supramolecular gel or fibres are the Equal K (EK) model or the Attenuated K (AK) model. The first model works for the case in which each equilibrium step is equal, meaning there is only one K governing each monomer addition to the growing stack, for that reason it is also called isodesmic mechanism. In that case there is a wide range of aggregate sizes in solution.

In the case of a higher aggregate after the dimerization process, each following K is different than the latter, being smaller at each addition because each following monomer addition to the stack will have a lower probability. From the data handling point of view it would be very difficult to employ this methodology to experimental data.

What is found in literature is a simplification of this model, called cooperative<sup>63</sup> mechanism, that assumes there are two equilibrium constants<sup>64</sup>. A nucleation step followed by the stack elongation<sup>65</sup> happens as a first non-favoured dimerization step is followed by several additions that would have the same K. A globally thermodynamic favoured process takes place because of the balance between the sum of the entropy loss in the organization of the molecules and the gain in enthalpy by a growing number of stabilizing interactions. The entropy penalty of two molecules losing degrees of freedom has to be substantial in order to the dimerization process to be less favoured than the elongation process of the stack. This results in terms of size distribution in solution, in the existence of a pool of free monomer and

a number of different size aggregates that would be less disperse regarding size comparing to the EK model.

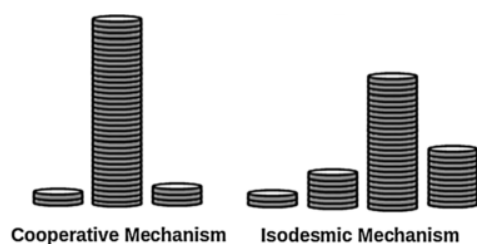


Figure 28 - Comparison of dispersion of aggregates size in a cooperative and isodesmic mechanism

There are two different cases in an aggregation study by a spectrometric technique, if the process happens in a timescale that is observable by the technique one can observe at least two different states in solution like monomer, dimer or higher aggregate or aggregates if existent. The other option, which is fairly reported in literature<sup>66,67</sup> and is the case of the present work, one can observe a property that is an average of every state of the studied compound in solution, which changes with the concentration of the species. As for the spectrometric technique employed it can be NMR<sup>67,68</sup> or UV/Vis absorption.<sup>69,70</sup>

Regarding NMR spectroscopy, a measurable propriety that correlates with molecular size can be a diffusion coefficient, as a larger aggregate moves slower in solution, relaxation (T1 or T2) or a chemical shift, since the chemical environment is changed by the aggregation process that results in changes in relaxation times and in the shielding of the observed nucleus. The chemical shift deviation was one of the chosen techniques to study the assembly process of the BTA derivatives. The first approach however was starting from macroscopic information by optical microscopy of BTA **1** before moving to NMR the results are presented below. BTA **1** solutions at different THF-H<sub>2</sub>O ratio were observed under the optical microscope the results are shown below (Figure 29).

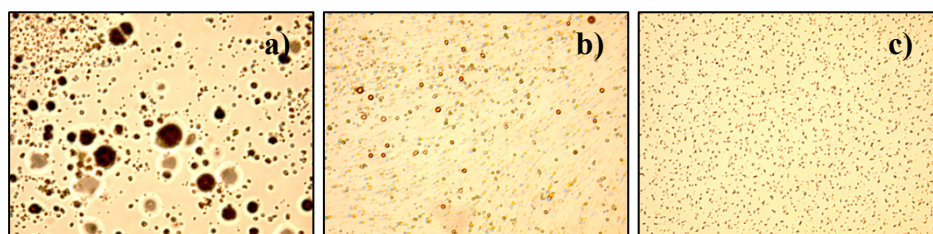
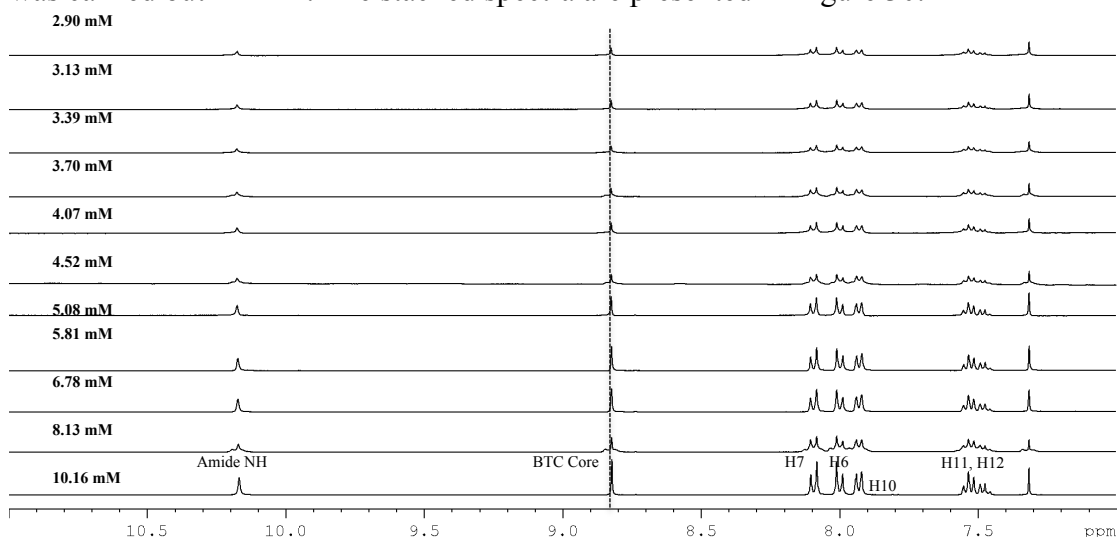


Figure 29 - Comparison of BTA **1** spherical aggregates obtained in THF-H<sub>2</sub>O a) 60:40 b) 80:20 c) 100:0

The size of the aggregates decreases at higher THF-H<sub>2</sub>O ratios and when there is only the trace water on THF (Figure 29c) the aggregates have a very small size. It is clear that water is needed for the aggregation process.

To fully understand the aggregation process, a more suitable technique that provides information at the molecular level is needed.

So using NMR to check for a critical aggregation concentration a dilution experiment was carried out in THF. The stacked spectra are presented in Figure 30.



**Figure 30 – Stacked spectra of dilution experiment of BTCA 1 in THF**

**Note:** For the sake of clarity H7', H6', H10' and H11' labels were omitted

At the working concentration range, from 10.16 mM to 2.90 mM, working in a non-deuterated solvent and without a internal chemical shift reference it wasn't possible to observe a trend in chemical shift difference by referring the shifts to the 1.78 ppm signal of THF and in the dilution experiment. The observation of the formation of other species in solution by aggregation and a critical concentration point in aggregation was also not possible with these experiments.

Since it was known from literature that water was necessary in the solvent used in order have the formation of the supramolecular assembly. To gain further insight in the effect of water in the assembly process a water titration experiment was done. The stacked spectra are presented in Figure 31.

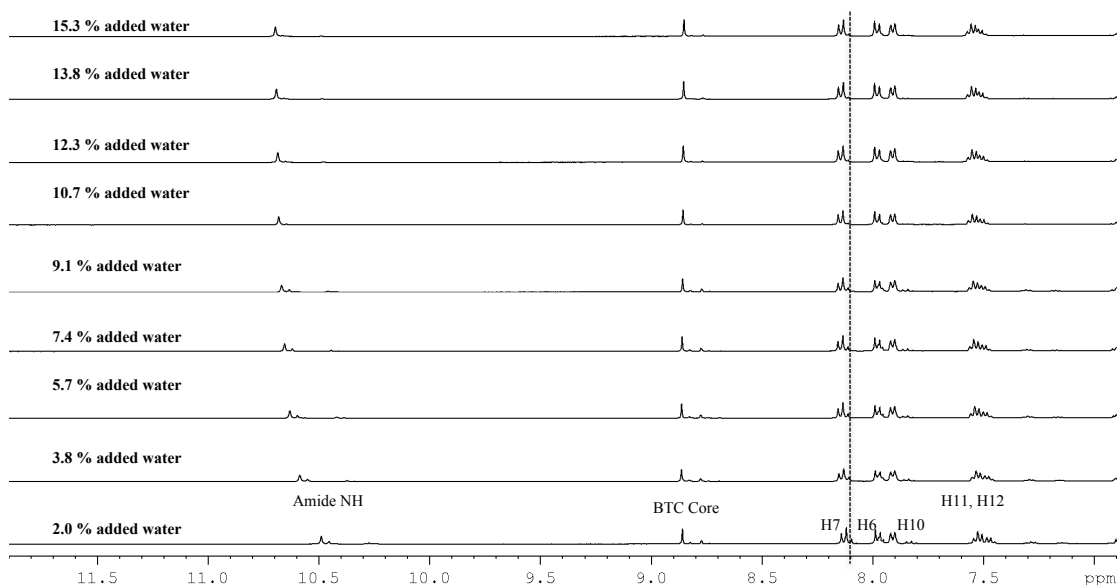


**Figure 31 - Zoom in the aromatic region of BTA 1 in the water titration experiment in THF-*d*8:THF (1:9)**

**Note:** For the sake of clarity H7', H6', H10' and H11' labels were omitted

From the spectra, a shift of the amide group, H6; H6' doublets and H11; H11' and H12 multiplet to lower field is observable with the increase in the percentage of water in THF while the BTC core protons, the H7; H7' doublet shift to higher field as shown in Figure 32.

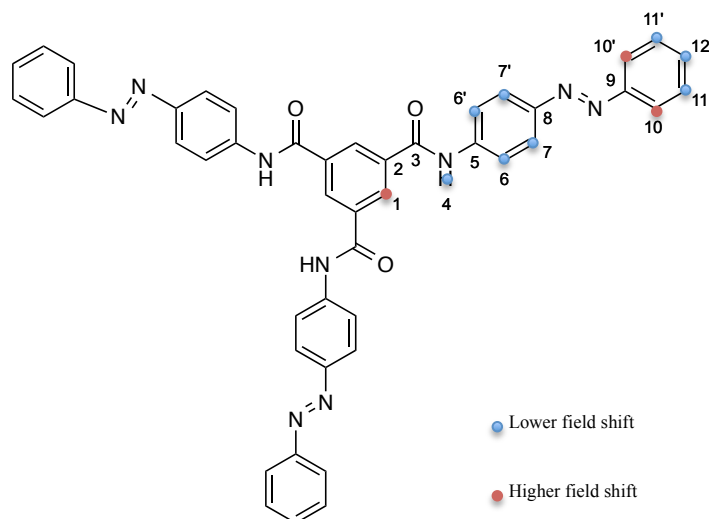


**Figure 32 – Overview of the signals shift in BTA 1 <sup>1</sup>H-NMR water titration experiment**

These signals show a larger variation in chemical shift upon the increase in concentration, this can be interpreted as being an indication of their higher involvement in the assembly process. In the Langmuir article<sup>53</sup> it is discussed that the BTA 1 hollow spheres are THF rich based on a solvatochromism experiment with fluorescein so the compound could be

adopting a supramolecular spherical arrangement in order to show less surface to the water in solution changing the chemical environment and shielding of some of the signals.

Since water is also needed for the assembly it is not unexpected to find that it interferes with the measured chemical shifts. The amide for its H-bonding capabilities would be fairly expected to change, but it could be also a consequence of proton exchange with water that results in that shift. In sum, the aromatic protons are being affected by the addition of water, getting more shielded as the structure could be packing more tightly in order to avoid contact with water.

For the concentration dependent  $^1\text{H}$ -NMR experiments some changes were made in the methodology. At the ratios of water:organic solvents described in literature for macroscopic observation of BTA **1** the compound aggregates resulting in a heterogeneous phase that caused broadening in the NMR spectra. At this point it was clear that the trace water in the organic solvents was enough to observe the aggregation process. BTA **1** was reported to form hollow spheres in THF, a 3D complex structure. The study of the variation in the chemical shifts was then pursued in DMSO, a solvent in which the compound displays stacking into fibres.

So several concentration dependent  $^1\text{H}$ -NMR spectra were acquired of BTA **1-5** and the results for one of the experiments of compound **1** in DMSO-*d*<sub>6</sub> are shown below. The results are presented as a chemical shift difference ( $\Delta\delta$ ) regarding the first and higher concentration (Table 3) the protons that showed a trend with the concentration change are presented in Figure 33. The original chemical shift tables of compound **1-5** are shown in annexe.



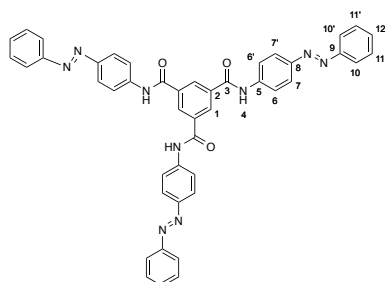


**Table 3 -  $^1\text{H}$ -NMR concentration dependent  $\Delta\delta$  of BTA 1**

C (mM)	N-H	BTC Core	H7, H7'	H6, H6'	H10,H10'
12.37	0.000	0.000	0.000	0.000	0.000
10.39	-0.012	0.006	0.004	0.001	0.001
7.92	0.009	0.008	0.007	0.000	0.001
6.19	0.016	0.004	0.005	0.000	0.001
3.96	0.020	0.009	0.008	0.000	0.001
1.98	0.042	0.008	0.010	-0.001	0.002
0.74	0.068	0.011	0.014	-0.051	-0.047

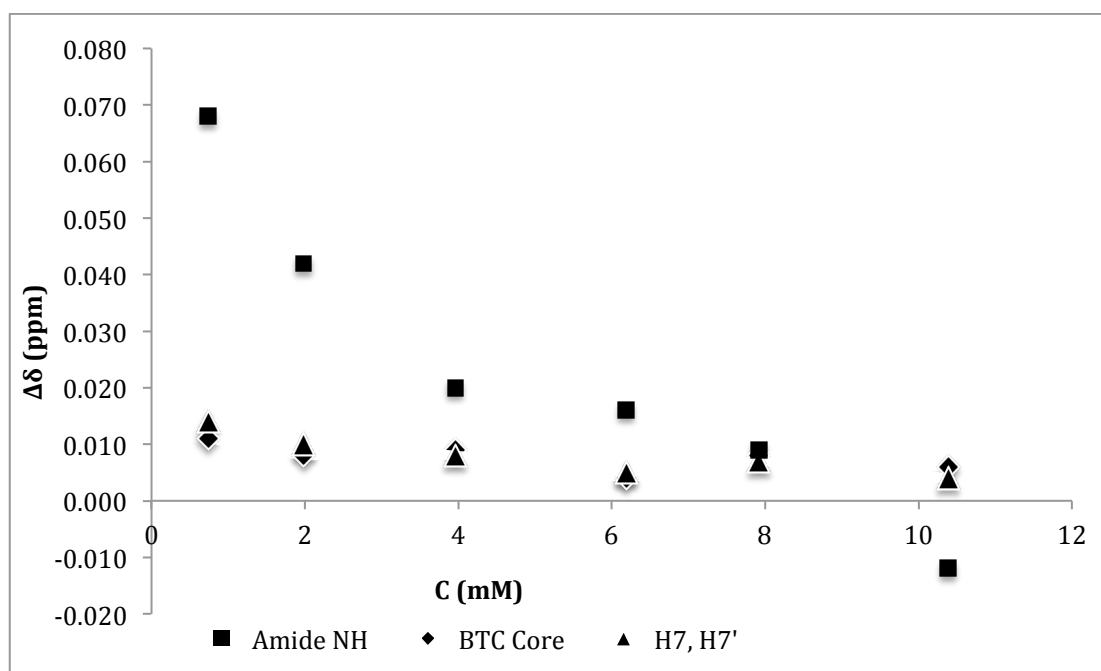


**Figure 33 - Plot of  $\Delta\delta$  against concentration of BTA 1**

With the change in concentration some of the signals as presented in Figure 33 show a trend with the change in concentration. The amide proton being the one that has the greatest shift having the same trend as the BTC core proton and H7, H7' also shown in Figure 35. Those nuclei could be getting a change in their local chemical environment to which

chemical shift is sensible by being more involved in the stacking process and since BTA **1** has a helical conformation the torsion involved in the chemical bonds some interactions could be more difficult to observe like in H10-H12 where the values of the measured concentration dependent chemical shifts are scattered. The packing of these helical monomers into the supramolecular fibre assembly could also influence the chemical environment and since different groups are involved in different kind of interactions like the amide NH in H-bonding with the carbonyl of an adjacent molecule or the aromatic groups  $\pi$ - $\pi$  stacking depending on the torsion of the chemical bonds the anisotropy of effects based on the chemical centres can be justified.

A zoom in the aromatic region of the BTA **1** concentration dependent  $^1\text{H}$ -NMR spectra is shown in Figure 34.

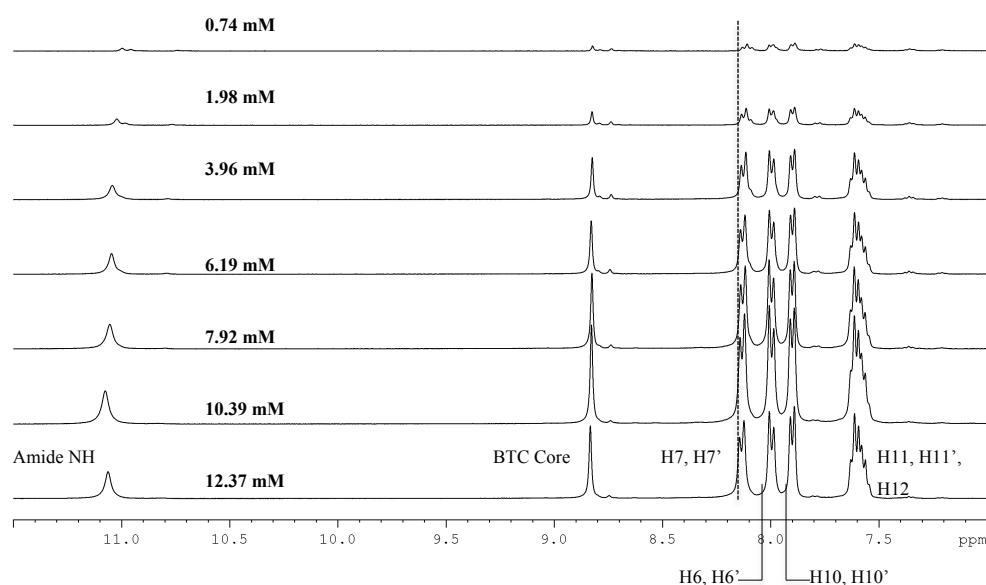


**Figure 34 – Aromatic region of  $^1\text{H}$ -NMR concentration dependent spectra of compound **1** in  $\text{DMSO-}d_6$**

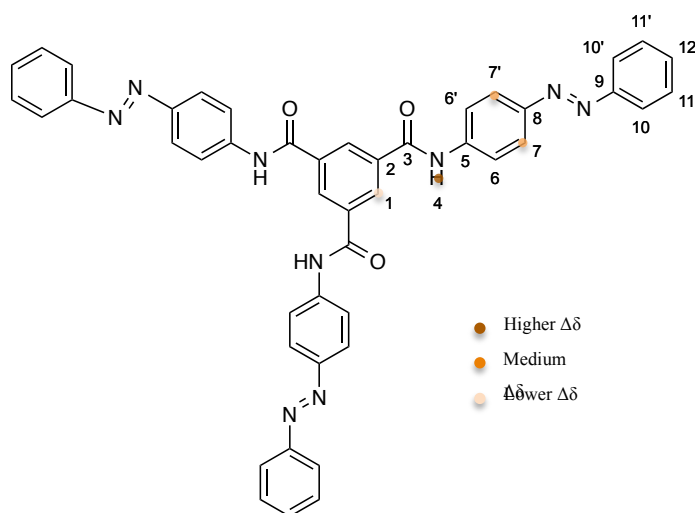


**Figure 35 – Overview of the  $\Delta\delta$  in the BTAA 1 concentration dependent  $^1\text{H}$ -NMR experiments**

From this data it is possible then to find out of the chemical shift value of the monomer and one of the aggregate and also the equilibrium constant or constants of the process.

The mathematical basis for that is well known from literature<sup>71</sup> and it is done by fitting the chemical shift data using an appropriate software to the following equations.

**Equation 3**

$$\delta_{obs} = \delta_m + (\delta_{ag} - \delta_m) \left( 1 + \frac{(1 - \sqrt{8Kt + 1})}{4Kt} \right)$$

**Equation 4**

$$\delta_{obs} = \delta_m + (\delta_{ag} - \delta_m) \left( 1 + \frac{(1 - \sqrt{4Kt + 1})}{2Kt} \right)$$

Equation 3 and Equation 4 are suitable for the fitting in the isodesmic case in order to obtain the equilibrium constant of the process. Equation 3 is suited for the dimerization process and Equation 4 for the larger stacking. It has to be noted for the same system both equation would give the same fitting quality despite the process since they are very similar simply the equilibrium constant calculated by Equation 3 would be the double of Equation 4. Because of that for the discrimination of a dimerization from a bigger stacking other strategies should be taken into account.

It was noted that those equations had a great dependence on the experimental data errors so in order to have more statistical relevant data the measurements were made in triplicate for each concentration range.

The chemical shift data was fitted to Equation 4, using Origin software by OriginLab and the results for two of the experiment arrays are presented below in Table 4.

**Table 4 - Results of the isodesmic model fit for BTA 2 and 3**

<b>BTA 2</b>		<b>BTA 3</b>	
K (mM)	Standard error	K (mM)	Standard error
0.046	0.027	0.019	0.010
0.046	0.010	0.017	0.013

Only the BTA 2 and BTA 3 could be fitted. In Figure 36 is shown one of the BTA 2 fittings for the signals of the amide NH, the BTC core and H6, H6'.

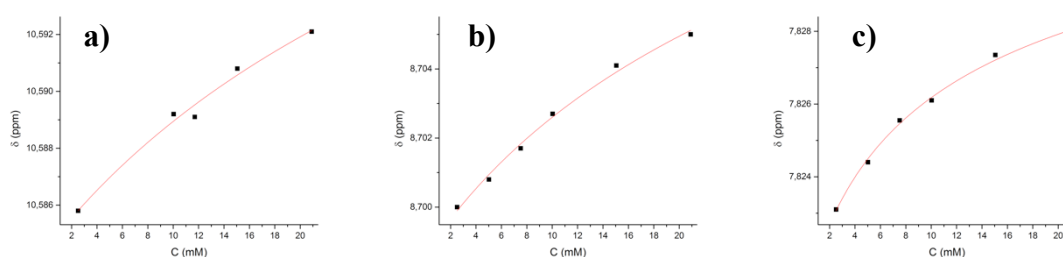


**Figure 36 - Origin fits to eq. 4 for BTA 2 a) amide proton, b) BTC core proton and c) H6, H6'**

From the fitting results to the isodesmic model several aspects should be taken in account, only the nuclei that displayed a trend with the change in concentration could be fitted. It has to be noted that the BTA 4 and 5, bigger compounds with more unsaturated bonds showed that linear behaviour in every proton, shown in Figure 37 and Figure 39 for BTA 4 and 5 respectively. The fitting however showed a large standard error what indicates that the model is not correct to describe the assembly of those molecules, the same fitting issues happen with BTA 1 for the amide, BTC core and H7; H7'. So with this approach, only the BTA 2 and BTA 3 could be fitted according to the isodesmic model, in spite of that with the added structural mobility introduced in BTA 3 because of the CH<sub>2</sub> bonded to the amide only the amide proton and the BTC core could be used for the fit. The equilibrium constant determined from the fitting for BTA 3 is half of the one determined for BTA 2, so there is less molecules in the aggregate compared to the free monomer in BTA 3 as opposed to BTA 2, that correlates with the fact that the structural flexibility given by the rotation of the single

NH-CH<sub>2</sub> bond can increase the difficulty for the molecules of BTA **3** to stack as opposed to the more rigid and planar system in BTA **2**.

It is not unexpected that the isodesmic model could only be used to describe BTA **2** and **3** since it is reported in literature has an assembly theory to model the growth of 1D stacks by planar molecules.<sup>72</sup> However, the model fails to predict the process in bigger helical systems such as BTA **1**<sup>73</sup> and in more complex systems like BTA **4** and **5** with more functional groups and more conformational freedom.

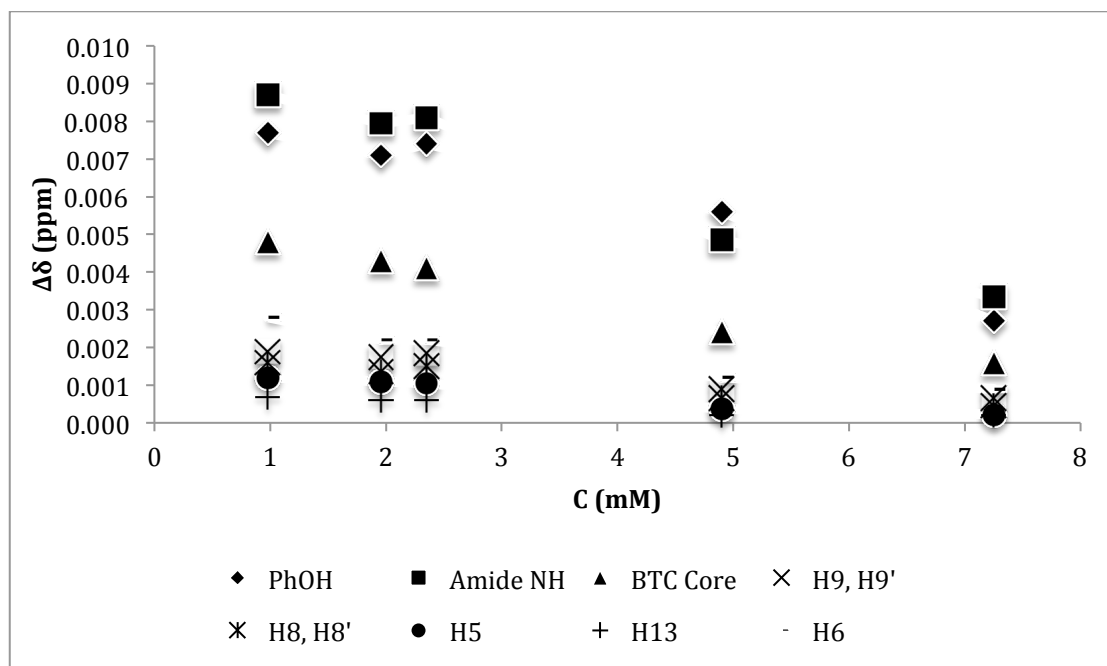


Figure 37 - Plot of  $\Delta\delta$  against concentration of BTA **4**

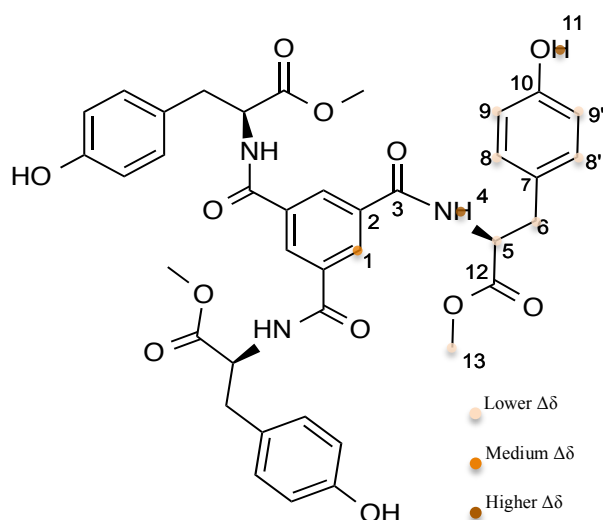


Figure 38 - Overview of the  $\Delta\delta$  in the BTA **4** concentration dependent <sup>1</sup>H-NMR experiments

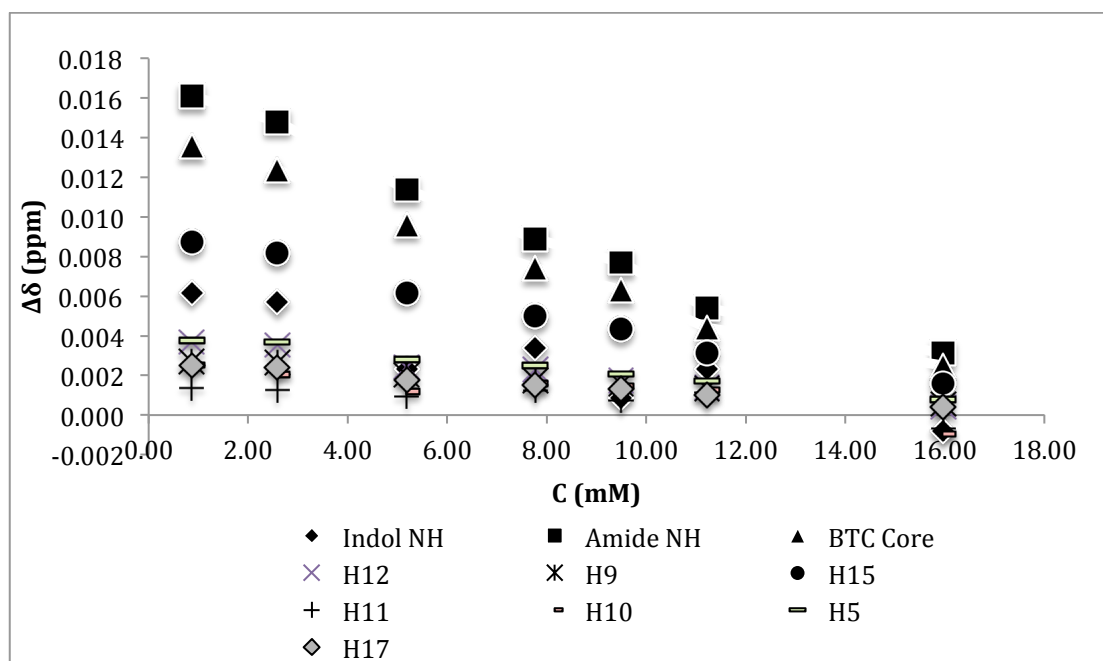


Figure 39 - Plot of  $\Delta\delta$  against concentration of BTA 5

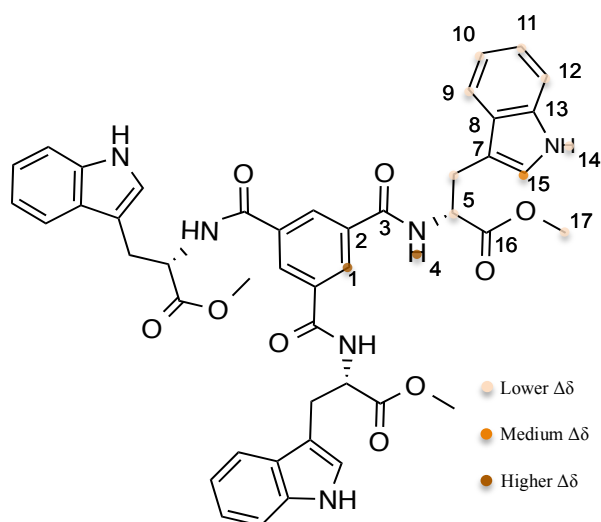


Figure 40 - Overview of the  $\Delta\delta$  in the BTA 5 concentration dependent  $^1\text{H}$ -NMR experiments

In order to relate molecular geometry to the observed chemical shift variation BTA **1-5** geometries were minimized using the Hartree-Fock level of theory and a minimal basis set, STO-3G, in Gaussian 09<sup>74</sup>. The HF/STO-3G optimized structures are shown below in Figure 41.

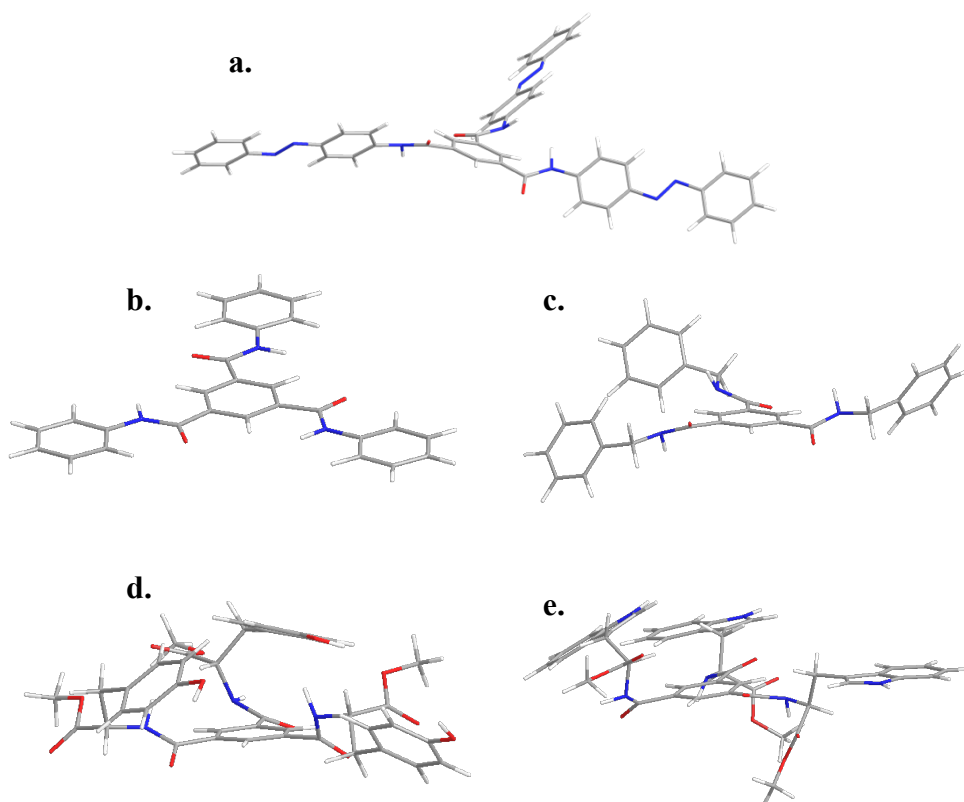


Figure 41 – HF/STO-3G results of the geometry optimizations of a. BTA 1, b. BTA 2, c. BTA 3, d. BTA 4 and e. BTA 5

The theoretical calculations show the helical conformation of BTA **1**, the planarity of BTA **2** and the torsion induced by the NH-CH<sub>2</sub>-Aromatic simple bonds in BTA **3** as stated before. BTA **4** and **5** resulted in a different three-dimensional arrangement that is similar to what is found in some C<sub>3</sub>-symmetric compounds entitled molecular baskets.<sup>48,75</sup> On these compounds the stacking could be happening as reported for the baskets in which two molecules associate back-to-back creating a layer.

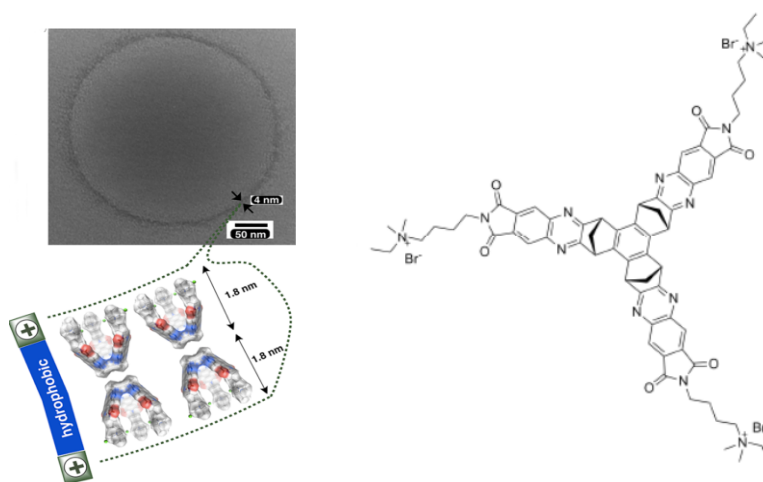


Figure 42 - Proposed assembly for a reported molecular basket (image adapted form ref. <sup>75</sup>)

That would explain the fact the substituent aromatics have a lower difference in chemical shift compared to the structure core as the concentration of the compound changes.

Other NMR techniques employed to further study the process were  $^1\text{H}$ - $^1\text{H}$  2D NOESY and diffusion NMR. NOESY spectra were acquired to check for intermolecular contacts.

Since two different aggregation states were unobservable the strategy taken was to do NOESY spectra of the higher and lower concentrated solutions used for the measurements of chemical shift to see if there are differences at two very different concentrations.

NOESY spectra acquired at 12.7 mM and 2.68 mM are shown in Figure 43 and Figure 44.

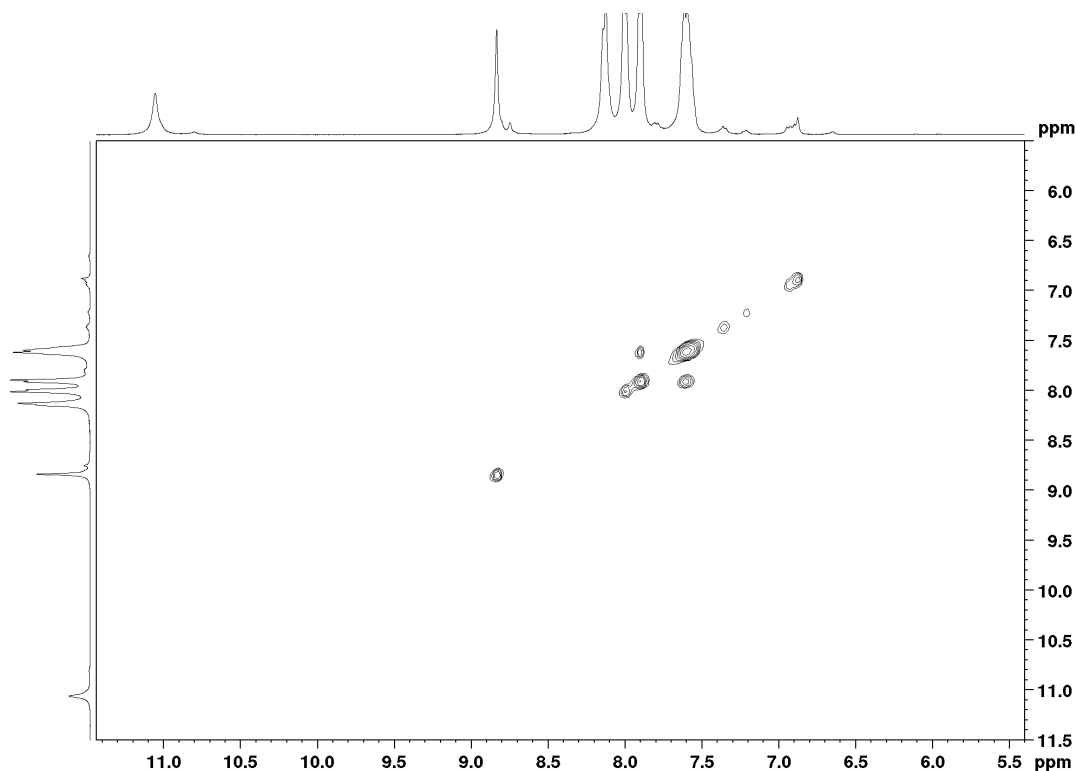


Figure 43 - NOESY spectrum of BTA 1 at 12.7 mM in DMSO- $d_6$



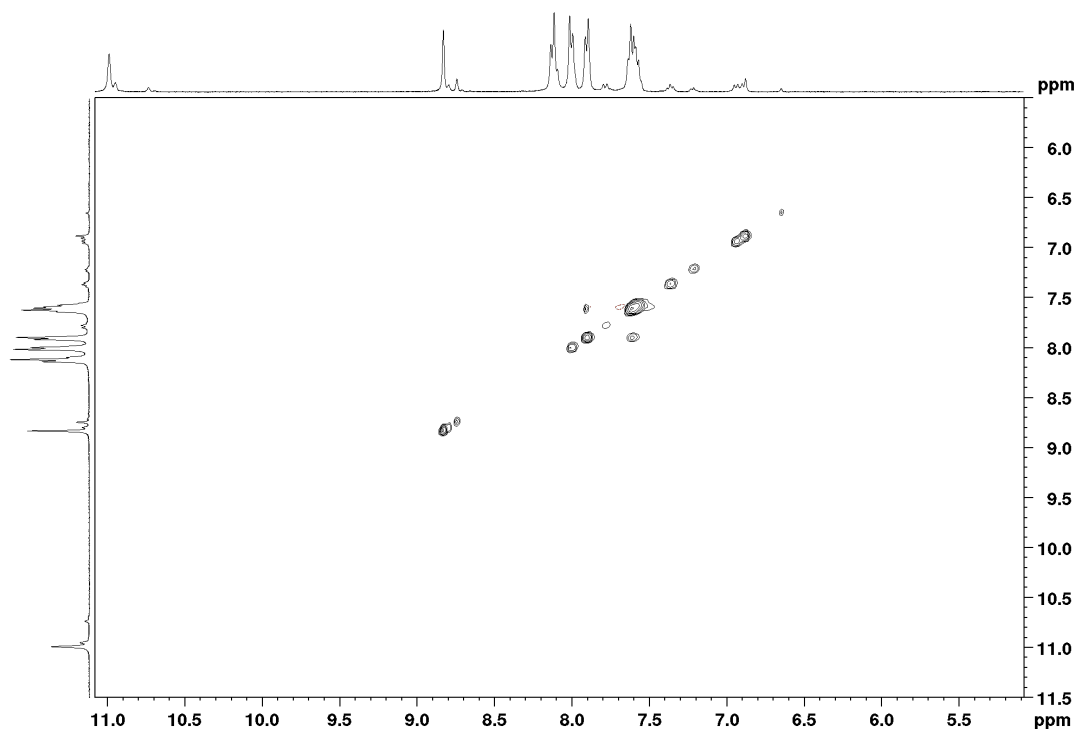
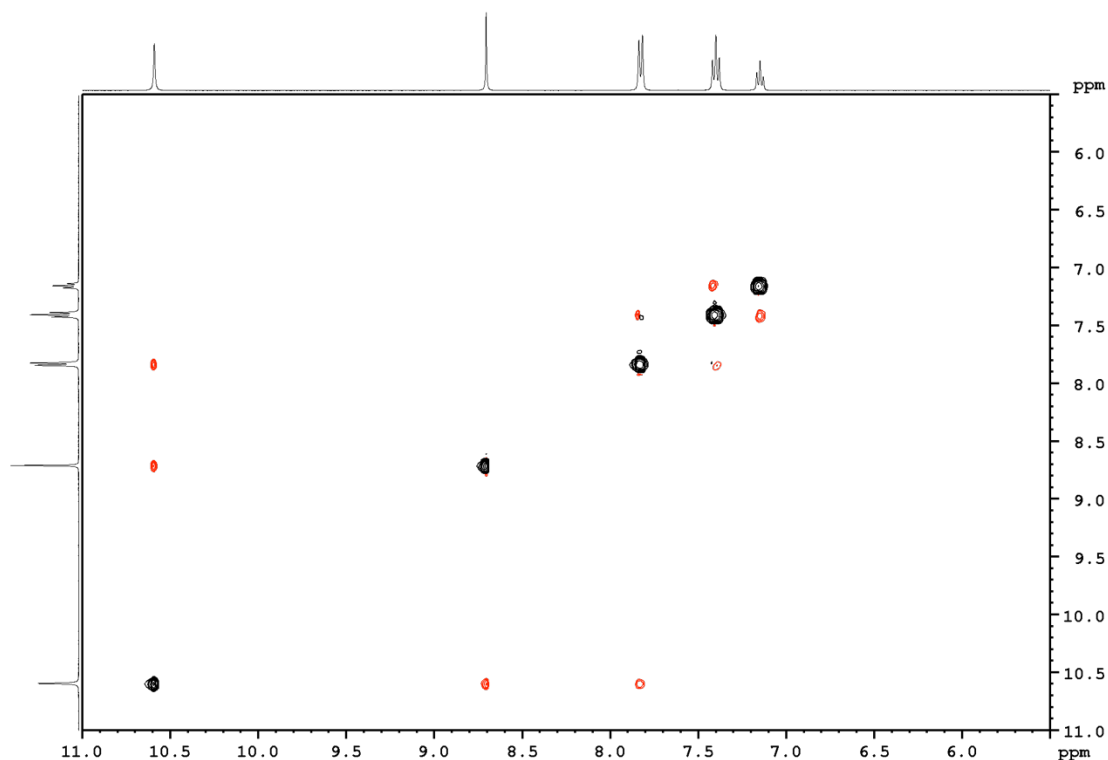


Figure 44 - NOESY spectrum of BTA 1 at 2.68 mM in DMSO-*d*<sub>6</sub>

It shows cross peaks with the same side of the diagonal revealing large molecule behaviour. If in fact the contacts observed are due to aggregation, it shows that is unaffected by dilution in the concentration range studied since both spectra at higher and lower concentration show the same behaviour. It was expected to observe these kinds of results from a molecule that is described to aggregate on solution. For a much smaller molecule like BTA **2** or **3**, the hypothesis was that it couldn't aggregate to a big stack and display large molecule behaviour. That was precisely what was observed in its NOESY spectra with the results shown on Figure 45, only showing crosspeaks with the typical small molecule behaviour, with the sign opposed to the diagonal of the spectrum and with the involved signal be close in the molecular structure it could be intramolecular contacts of free monomer. NOESY spectra of the other BTA are presented in annexe.



**Figure 45 - NOESY spectrum of BTA 2 at 20mM in DMSO-*d*<sub>6</sub>**

Diffusion measurements were carried out to look for different diffusing species in solution. As with NOESY spectra only a higher and lower concentration spectra were acquired to look for differences in the average measurement of all solution states of the studied compound, since it was expected that at higher concentrations the diffusion coefficients would get smaller due to the contribution of higher molecular weight aggregates of the compound. TMS diffusion was used to correct for solution viscosity effects<sup>76</sup> since changes in  $D/D_{\text{TMS}}$  reflects the changes in the size of the diffusing species. The results are shown below in Table 5 for BTA 1. The diffusion measurements for BTA 2-4 are in the annexe.

**Table 5 – BTA 1 DOSY corrected diffusion coefficients**

<b>BTA 1 0.74 mM</b>	<b><math>D/D_{\text{TMS}}</math></b>	<b>BTA 1 12.37 mM</b>	<b><math>D/D_{\text{TMS}}</math></b>
H10, H10'	0.25	H10, H10'	0.25
H6, H6'	0.25	H6, H6'	0.24
H7, H7'	0.23	H7, H7'	0.25
BTC core	0.21	BTC core	0.25

As can be seen in the table there aren't considerable changes in the diffusion with the change in concentration for the same nucleus. That could be explained by the fact that a

higher molecular weight aggregate exists in low concentration, but that needs verification by others techniques.

BTA **5** diffusion spectra were acquired with the OneShot sequence for all the concentrations used in the chemical shift measurements, the time needed to acquire that data is a lot shorter and so it was possible to measure all the concentration range to look for a trend in diffusion with the change in concentration. That wasn't possible to obtain and the results are shown in the annexe.

### 4.3 Preliminary interaction studies

Some preliminary interaction studies were carried out to check if there was recognition of glucose and ammonium ions by compound **5** since its non-planar conformation could be used as a molecular host.

It wasn't observable any recognition of glucose as shown in Figure 46 by titration of a 6 mM solution of BTA **5** in DMSO-*d*<sub>6</sub> with glucose solution. The measured chemical shifts were equal at each step of the titration.

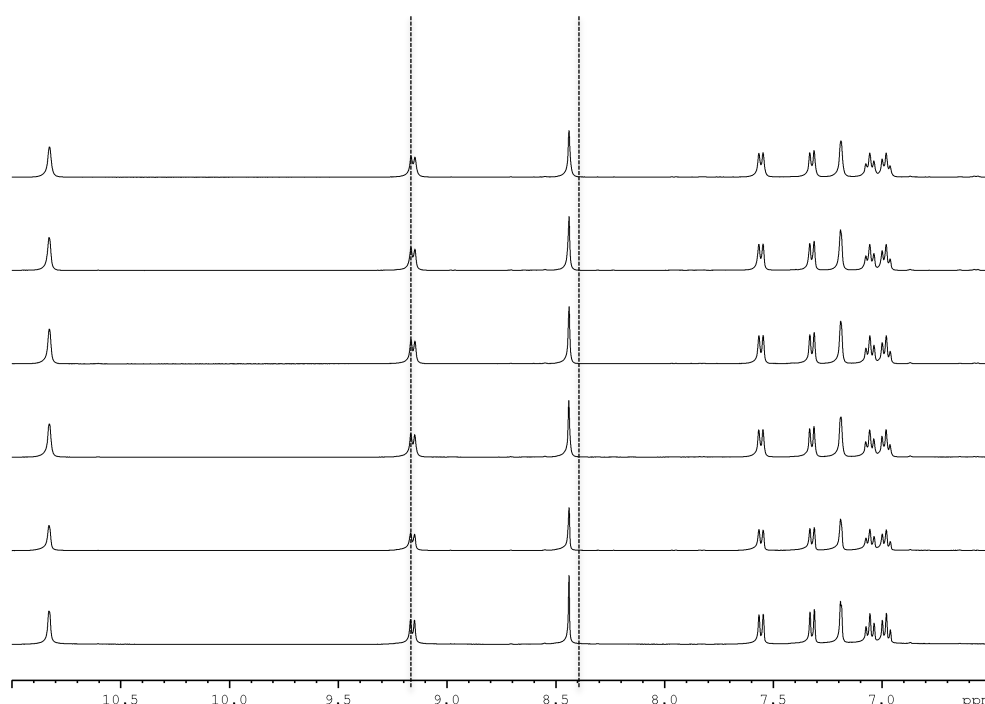


**Figure 46 - Aromatic region of BTA 5 in the titration experiment with glucose**

In a similar experiment with ammonium chloride changes could be observed in the measured chemical shifts. The experiments were carried out at two different temperatures to look for differences. In Figure 47 it is shown the titration experiment done at 25 °C and in Figure 48 at 35 °C.

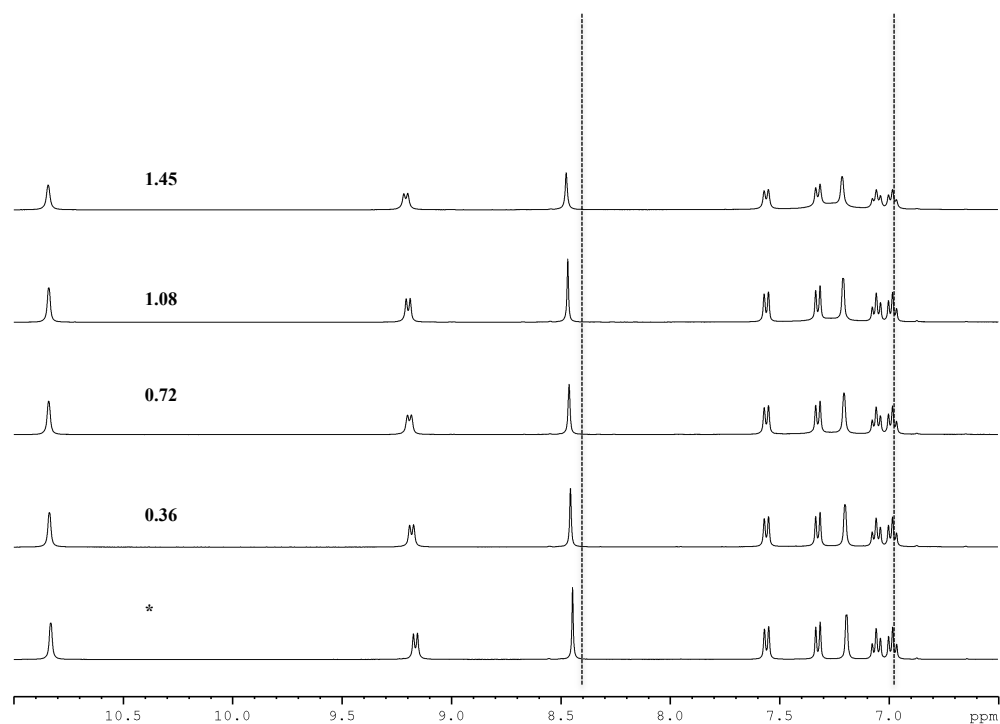


**Figure 47 - Zoom in the aromatic region of BTA 5 stacked  $^1\text{H}$ -NMR spectra in the titration experiment with ammonium chloride at 25 °C. Guest/host ratio is displayed on the spectra starting from a condition (\*) with only host present at 6.23 mM**

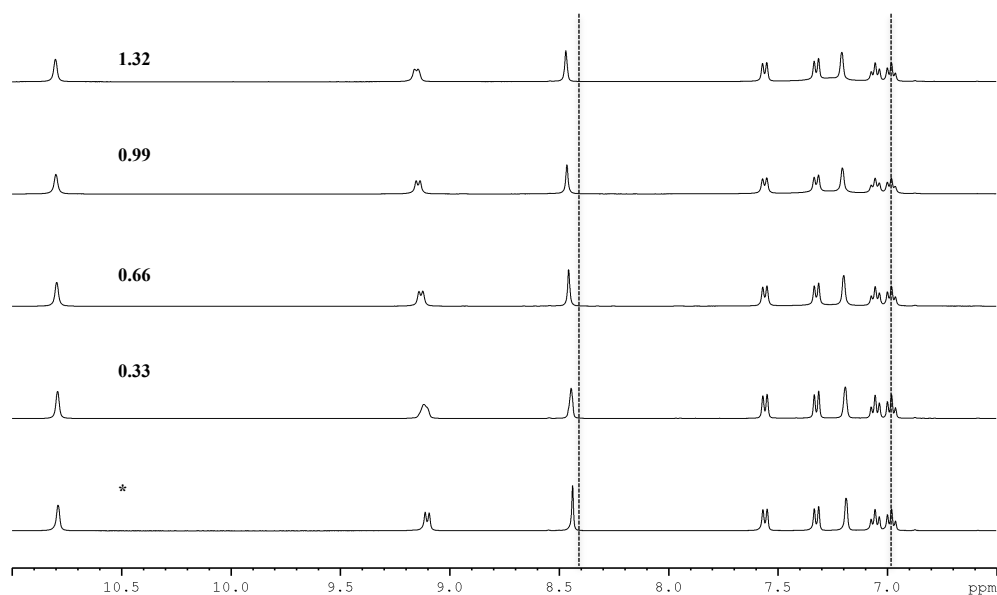


**Figure 48 - Zoom in the aromatic region of BTA 5 stacked  $^1\text{H}$ -NMR spectra in the titration experiment with ammonium chloride at 35 °C. Guest/host ratio is displayed on the spectra starting from a condition (\*) with only host present at 6.84 mM**

It is observed that with the addition of ammonium chloride the indole N-H, the amide and the BTC core proton are shifting to lower field. While most aromatic protons in the indole ring are shifting to lower field, H11 shifts to higher field as shown in Figure 49. There are many possibilities for the interaction between BTA 5 and ammonium ion, since BTA 5

monomers should interact with each other to form a supramolecular assembly either a stack like is reported for other BTA derived compounds or a molecular basket-like assembly, in either of the cases the interaction with the ammonium ion would displace the chemical equilibrium from the BTA **5** aggregate form to the monomeric form. Based on the measured chemical shift difference the ammonium ion should interact with the inner core of the BTA **5** as the H1, Amide H4, Indole H14 and H15 have the greatest chemical shift difference as the ammonium concentration increases a proposed ammonium ion-BTA **5** is presented in Figure 50.

The same behaviour and chemical shift difference magnitude is similar for the two different temperatures. The chemical shift difference is made in comparison to a first measurement with only host present, an overview of the measured chemical shift difference is shown in Figure 49 and the results are presented in Figure 51 and Figure 52 and in Table 6 and Table 7. The original measured chemical shifts are presented in the annexe.

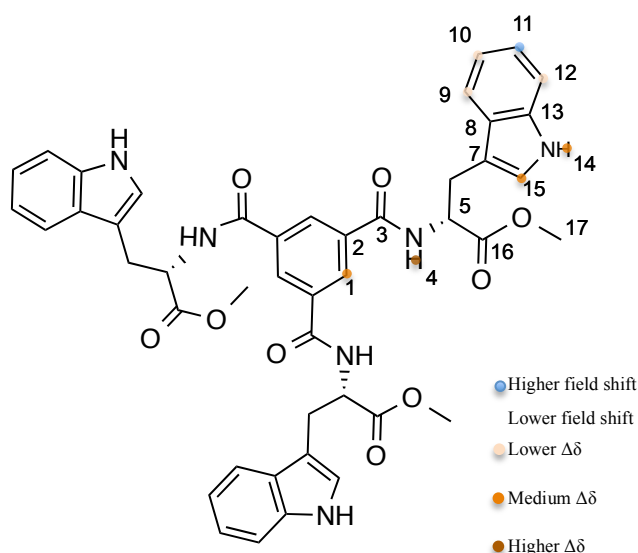


**Figure 49 - Overview of the  $\Delta\delta$  in the BTA **5** ammonium chloride titration experiments**

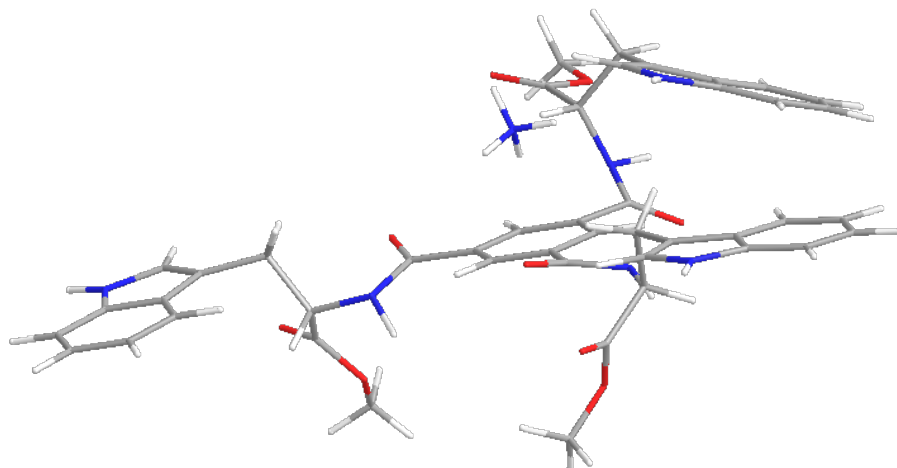


**Figure 50 – Proposed ammonium-BTA **5** interaction**

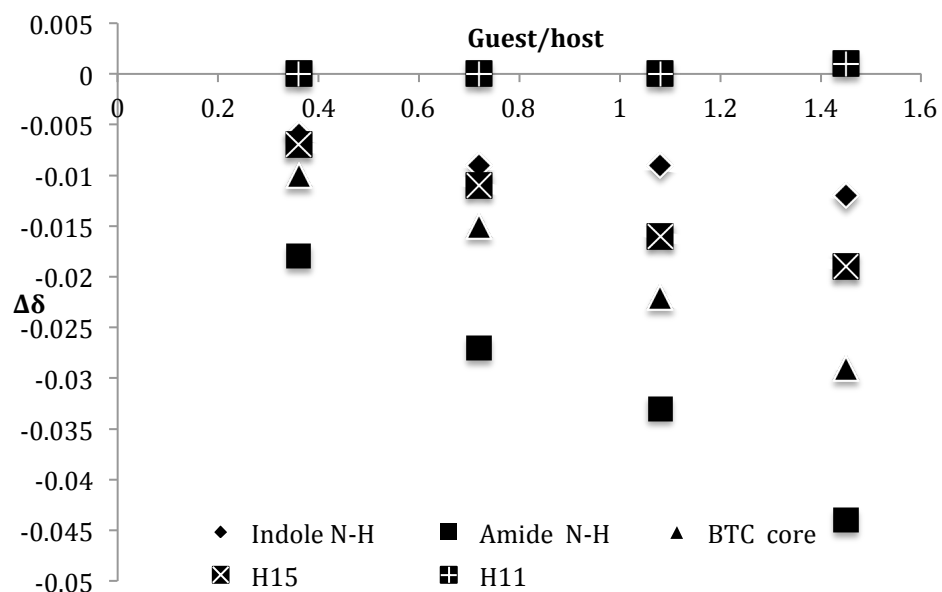


Figure 51 -  $\Delta\delta$  against guest/host proportion in the BTA 5 ammonium chloride titration experiment at 25 °C

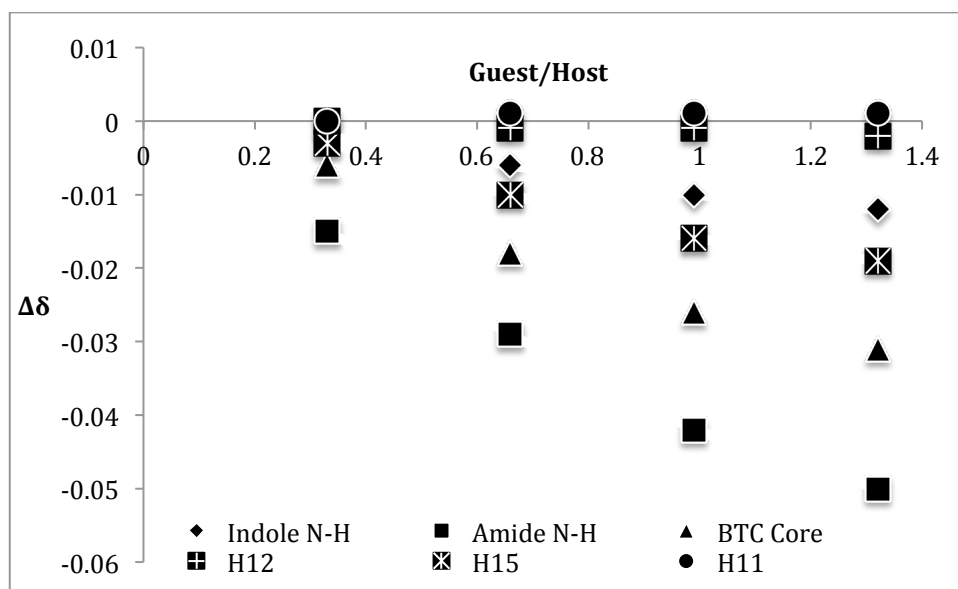
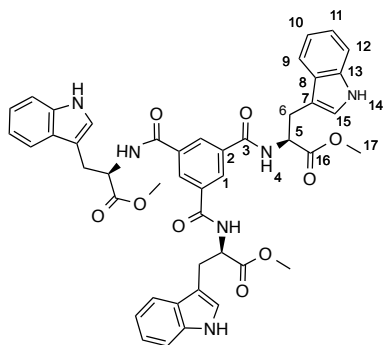


Figure 52 -  $\Delta\delta$  against guest/host proportion in the BTA 5 ammonium chloride titration experiment at 35 °C



**Table 6 -  $\Delta\delta$  in the BTAC 5 ammonium chloride titration experiment at 25 °C**

Guest/host	Indole N-H	Amide N-H	BTAC core	H12	H9	H15	H11	H10
*	0.000	0.000	0.000	0.000	0.000	0.000	0.000	0.000
<b>0.36</b>	-0.007	-0.017	-0.010	-0.001	0.000	-0.007	0.000	0.000
<b>0.72</b>	-0.009	-0.027	-0.015	-0.001	0.000	-0.011	0.000	-0.001
<b>1.08</b>	-0.009	-0.033	-0.022	-0.001	0.000	-0.016	0.000	0.000
<b>1.45</b>	-0.012	-0.044	-0.029	-0.002	0.000	-0.019	0.001	-0.001

**Note:** \* only the host molecule was present in the NMR tube

**Table 7 -  $\Delta\delta$  in the BTAC 5 ammonium chloride titration experiment at 35 °C**

Guest/host	Indole N-H	Amide N-H	BTAC core	H12	H9	H15	H11	H10
*	0.000	0.000	0.000	0.000	0.000	0.000	0.000	0.000
<b>0.33</b>	-0.002	-0.015	-0.007	0.000	0.000	-0.003	0.000	0.000
<b>0.66</b>	-0.006	-0.029	-0.018	-0.001	0.000	-0.010	0.001	0.000
<b>0.99</b>	-0.010	-0.042	-0.026	-0.002	-0.001	-0.017	0.001	-0.001
<b>1.32</b>	-0.012	-0.050	-0.031	-0.002	-0.001	-0.019	0.001	-0.001

**Note:** \* only the host molecule was present in the NMR tube



## 5. Conclusions and future perspectives

BTA **1** as reported had different behaviour regarding the solvent used, in THF in which it is reported to assemble into spheres a trend in chemical shift couldn't be obtained like in DMSO, in which fibre assemble occur. That implies a different molecular arrangement on each solvent, what results in different morphologies as reported<sup>53</sup>. That difference could be because of the each solvent dipolar moment and the difference in dipolar moment regarding water, which is needed for the assembly process.

Based on the concentration dependent experiments and NOESY to have aggregation into a stack with a large molecule behaviour it is needed to have a medium to large sized molecule like BTA **1**, **4** or **5**. The planarity of the system influences the assembly and in small molecules like BTA **2** or **3**, a more flexible monomer like the BTA **3** has a less favourable aggregation, that can be supported by the equilibrium constants calculated by the fitting to the isodesmic model. On the other hand, bigger compounds with more functional groups like BTA **4** and **5** despite their flexibility have a more uniform chemical shift change in the concentration dependent experiments. For BTA **1-3** only some of the signals had a chemical shift trend. That could be because of more favourable interaction between the functional groups such as H-bonding and  $\pi$  system interactions in the more structurally diverse BTA **4** and **5**. To describe the chemical equilibrium of these types of compounds it is needed to use a model more suited for these complex systems then the isodesmic model.

Because of the BTA **4** and **5** non-planar structure they could then be used to test for host-guest interactions, that was made for compound **5** and showed some chemical shift differences in the ammonium titration experiment.

In order to understand better the assembly of  $C_3$  symmetric molecules the synthesis of other possible BTA derivatives could be helpful. The introduction of a long alkyl chain that would favour hydrophobic binding forces for instance or to synthesize a similar molecule to BTA **1** which has been reported to assemble with 4-styrylaniline on the place of the azo benzene molecule.

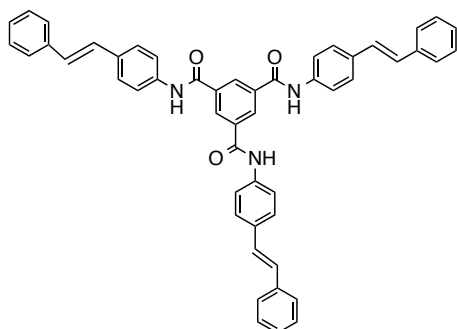


**Figure 53 – Possible BTA derived compound with 4-styrylaniline as a substituent**

That would keep the structural motif of the BTA **1** and be a good alternative to study for the same kind of proprieties and hopefully without the same handling issues.

The core structure could also be changed for something like melamine or cyanuric chloride, keeping some structural similarity and the molecular symmetry to the studied BTA.

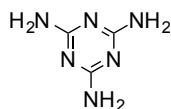


**Figure 54 – Melamine core**

On top of that the introduction of a NMR probe group into the structure like as fluorine, which has a good sensibility for NMR spectroscopy and a wide chemical shift range.

Regarding the NMR spectroscopy moving to a higher operating magnetic field could solve the problem of working at sub mM concentrations while looking into a critical concentration point that would force, aggregation and start the stacking assembly.

BTA **5** seemed to recognize the ammonium ion so further studies with that and other guest molecules should be made in order to understand the process and how the host molecules could be structurally modified to improve its ability for molecular recognition.

# Annexe

Table 8 - <sup>1</sup>H-NMR concentration dependent chemical shift of BTA 1

C (mM)	N-H	BTC Core	H7, H7'	H6, H6'	H10, H10'
<b>12.37</b>	11.062	8.833	8.133	7.995	7.899
<b>10.39</b>	11.074	8.827	8.129	7.994	7.898
<b>7.92</b>	11.053	8.825	8.126	7.995	7.898
<b>6.19</b>	11.046	8.829	8.128	7.995	7.898
<b>3.96</b>	11.042	8.824	8.125	7.995	7.898
<b>1.98</b>	11.020	8.825	8.123	7.996	7.897
<b>0.74</b>	10.994	8.822	8.119	8.046	7.946

C (mM)	N-H	BTC Core	H7, H7'	H6, H6'	H10, H10'
<b>12.37</b>	11.062	8.833	8.133	7.995	7.899
<b>10.39</b>	11.075	8.827	8.129	7.994	7.898
<b>7.92</b>	11.055	8.824	8.126	7.995	7.898
<b>6.19</b>	11.049	8.829	8.129	7.996	7.898
<b>3.96</b>	11.045	8.825	8.125	7.996	7.898
<b>1.98</b>	11.024	8.825	8.113	7.996	7.897
<b>0.74</b>	11.000	8.823	8.108	7.945	7.749

C (mM)	N-H	BTC Core	H7, H7'	H6, H6'	H10, H10'
<b>12.37</b>	11.062	8.833	8.133	7.995	7.898
<b>10.39</b>	11.075	8.827	8.130	7.994	7.898
<b>7.92</b>	11.054	8.824	8.126	7.995	7.898
<b>6.19</b>	11.048	8.829	8.129	8.051	7.946
<b>3.96</b>	11.048	8.825	8.126	7.997	7.899
<b>1.98</b>	11.024	8.825	8.113	7.998	7.997
<b>0.74</b>	10.998	8.822	8.109	7.898	7.895

Table 9 - <sup>1</sup>H-NMR concentration dependent chemical shift of BTA 2

<b>C (mM)</b>	<b>N-H</b>	<b>BTC Core</b>	<b>H6, H6'</b>	<b>H7, H7'</b>	<b>H8</b>
<b>20.90</b>	10.592	8.705	7.828	7.400	7.149
<b>15.05</b>	10.591	8.704	7.827	7.399	7.148
<b>11.70</b>	10.589	8.702	7.826	7.398	7.147
<b>10.03</b>	10.589	8.703	7.826	7.399	7.147
<b>7.52</b>	10.589	8.702	7.826	7.399	7.148
<b>5.02</b>	10.589	8.701	7.824	7.398	7.147
<b>2.51</b>	10.586	8.700	7.823	7.398	7.147
<b>0.84</b>	10.591	8.705	7.827	7.400	7.148

<b>C (mM)</b>	<b>N-H</b>	<b>BTC Core</b>	<b>H6, H6'</b>	<b>H7, H7'</b>	<b>H8</b>
<b>20.90</b>	10.590	8.705	7.827	7.400	7.148
<b>15.05</b>	10.589	8.704	7.826	7.399	7.147
<b>11.70</b>	10.589	8.703	7.826	7.399	7.147
<b>10.03</b>	10.588	8.702	7.825	7.399	7.147
<b>7.52</b>	10.588	8.702	7.825	7.399	7.147
<b>5.02</b>	10.588	8.701	7.824	7.399	7.147
<b>2.51</b>	10.586	8.700	7.823	7.398	7.147
<b>0.84</b>	10.587	8.700	7.823	7.397	7.147

<b>C (mM)</b>	<b>N-H</b>	<b>BTC Core</b>	<b>H6, H6'</b>	<b>H7, H7'</b>	<b>H8</b>
<b>20.90</b>	10.590	8.705	7.826	7.400	7.148
<b>15.05</b>	10.589	8.704	7.826	7.399	7.147
<b>11.70</b>	10.589	8.703	7.826	7.399	7.147
<b>10.03</b>	10.588	8.702	7.825	7.399	7.147
<b>7.52</b>	10.588	8.702	7.825	7.398	7.147
<b>5.02</b>	10.588	8.701	7.824	7.399	7.147
<b>2.51</b>	10.586	8.700	7.823	7.399	7.147
<b>0.84</b>	10.587	8.700	7.823	7.398	7.147

Table 10 - <sup>1</sup>H-NMR concentration dependent chemical shift of BTA 3

<b>C (mM)</b>	<b>N-H</b>	<b>BTC Core</b>	<b>H5</b>
<b>20.94</b>	9.287	8.517	4.506
<b>15.08</b>	9.284	8.515	4.505
<b>12.15</b>	9.279	8.513	4.505
<b>10.05</b>	9.281	8.512	4.504
<b>7.54</b>	9.278	8.511	4.504
<b>5.03</b>	9.272	8.509	4.504
<b>2.51</b>	9.272	8.508	4.504
<b>0.84</b>	9.267	8.506	4.504

<b>C (mM)</b>	<b>N-H</b>	<b>BTC Core</b>	<b>H5</b>
<b>20.94</b>	9.287	8.517	4.506
<b>15.08</b>	9.284	8.515	4.505
<b>12.15</b>	9.280	8.513	4.505
<b>10.05</b>	9.282	8.513	4.504
<b>7.54</b>	9.278	8.511	4.504
<b>5.03</b>	9.273	8.509	4.504
<b>2.51</b>	9.273	8.508	4.504
<b>0.84</b>	9.268	8.507	4.504

<b>C (mM)</b>	<b>N-H</b>	<b>BTC Core</b>	<b>H5</b>
<b>20.94</b>	9.289	8.519	4.506
<b>15.08</b>	9.288	8.516	4.506
<b>12.15</b>	9.281	8.513	4.505
<b>10.05</b>	9.285	8.514	4.505
<b>7.54</b>	9.283	8.513	4.504
<b>5.03</b>	9.275	8.509	4.504
<b>2.51</b>	9.277	8.509	4.504
<b>0.84</b>	9.273	8.508	4.503

Table 11 - <sup>1</sup>H-NMR concentration dependent chemical shift of compound 4

C (mM)	0.98	1.96	2.35	4.90	7.25	9.80
PhOH	9.206	9.206	9.205	9.212	9.212	9.212
NH	9.118	9.118	9.118	9.125	9.125	9.126
BTC core	8.383	8.383	8.383	8.387	8.388	8.388
H9, H9'	7.078	7.078	7.078	7.079	7.080	7.080
H8, H8'	6.659	6.659	6.659	6.660	6.660	6.660
H5	4.595	4.595	4.595	4.596	4.596	4.596
H13	3.629	3.629	3.629	3.629	3.629	3.629
H6	3.022	3.021	3.022	3.023	3.024	3.025

<b>C (mM)</b>	<b>0.98</b>	<b>1.96</b>	<b>2.35</b>	<b>4.90</b>	<b>7.25</b>	<b>9.80</b>
<b>PhOH</b>	9.206	9.207	9.207	9.209	9.211	9.214
<b>NH</b>	9.118	9.119	9.119	9.122	9.124	9.127
<b>BTC core</b>	8.383	8.383	8.383	8.385	8.386	8.388
<b>H9, H9'</b>	7.078	7.078	7.078	7.079	7.079	7.080
<b>H8, H8'</b>	6.659	6.659	6.659	6.660	6.660	6.660
<b>H5</b>	4.595	4.595	4.595	4.595	4.596	4.596
<b>H13</b>	3.629	3.629	3.629	3.629	3.629	3.629
<b>H6</b>	3.021	3.022	3.022	3.023	3.023	3.024

<b>C (mM)</b>	<b>0.98</b>	<b>1.96</b>	<b>2.35</b>	<b>4.90</b>	<b>7.25</b>	<b>9.80</b>
<b>PhOH</b>	9.206	9.207	9.207	9.208	9.211	9.214
<b>NH</b>	9.118	9.119	9.119	9.121	9.123	9.126
<b>BTC core</b>	8.383	8.383	8.383	8.385	8.386	8.387
<b>H9, H9'</b>	7.078	7.078	7.078	7.079	7.079	7.080
<b>H8, H8'</b>	6.659	6.659	6.659	6.660	6.660	6.660
<b>H5</b>	4.595	4.594	4.595	4.595	4.595	4.596
<b>H13</b>	3.629	3.629	3.629	3.629	3.629	3.629
<b>H6</b>	3.021	3.021	3.035	3.023	3.023	3.024



Table 12 - <sup>1</sup>H-NMR concentration dependent chemical shift of compound 5

C (mM)	0.86	2.59	5.18	7.77	9.50	11.22	15.97	21.58
Indole NH	10.815	10.815	10.817	10.819	10.819	10.829	10.830	10.832
Amide NH	9.142	9.143	9.147	9.151	9.152	9.164	9.165	9.169
BTC Core	8.426	8.427	8.432	8.434	8.436	8.447	8.448	8.451
H12	7.546	7.546	7.548	7.548	7.549	7.559	7.559	7.560
H9	7.312	7.312	7.313	7.314	7.314	7.324	7.324	7.325
H15	7.177	7.178	7.180	7.182	7.183	7.193	7.195	7.197
H11	7.045	7.045	7.046	7.047	7.047	7.057	7.057	7.058
H10	6.970	6.970	6.971	6.972	6.972	6.982	6.982	6.983
H5	4.716	4.716	4.718	4.719	4.719	4.729	4.730	4.731
H17	3.620	3.620	3.621	3.622	3.622	3.632	3.632	3.633

<b>C (mM)</b>	<b>0.86</b>	<b>2.59</b>	<b>5.18</b>	<b>7.77</b>	<b>9.50</b>	<b>11.22</b>	<b>15.97</b>	<b>21.58</b>
<b>Indole NH</b>	10.826	10.826	10.827	10.828	10.833	10.829	10.831	10.831
<b>Amide NH</b>	9.153	9.154	9.157	9.160	9.999	9.163	9.169	9.169
<b>BTC Core</b>	8.437	8.438	8.441	8.443	9.152	8.446	8.451	8.451
<b>H12</b>	7.557	7.557	7.558	7.558	8.006	7.559	7.560	7.560
<b>H9</b>	7.323	7.323	7.323	7.324	7.441	7.324	7.325	7.325
<b>H15</b>	7.188	7.189	7.190	7.192	7.254	7.134	7.197	7.197
<b>H11</b>	7.057	7.057	7.057	7.057	7.107	7.045	7.058	7.058
<b>H10</b>	6.982	6.982	6.982	6.982	7.007	6.982	6.983	6.983
<b>H5</b>	4.727	4.727	4.728	4.728	4.729	4.729	4.731	4.731
<b>H17</b>	3.630	3.631	3.631	3.631	3.632	3.632	3.633	3.633

<b>C (mM)</b>	<b>0.86</b>	<b>2.59</b>	<b>5.18</b>	<b>7.77</b>	<b>9.50</b>	<b>11.22</b>	<b>15.97</b>	<b>21.58</b>
<b>Indole NH</b>	10.825	10.826	10.829	10.828	10.830	10.829	10.832	10.831
<b>Amide NH</b>	9.153	9.154	9.157	9.160	9.161	9.163	9.166	9.169
<b>BTC Core</b>	8.437	8.438	8.441	8.443	8.444	8.446	8.448	8.451
<b>H12</b>	7.557	7.557	7.558	7.558	7.559	7.559	7.560	7.560
<b>H9</b>	7.323	7.323	7.323	7.324	7.324	7.324	7.325	7.325
<b>H15</b>	7.188	7.188	7.190	7.192	7.192	7.193	7.195	7.197
<b>H11</b>	7.057	7.057	7.057	7.057	7.057	7.057	7.059	7.058
<b>H10</b>	6.981	6.981	6.982	6.982	6.982	6.982	6.984	6.983
<b>H5</b>	4.727	4.727	4.728	4.728	4.729	4.729	4.730	4.731
<b>H17</b>	3.630	3.631	3.631	3.631	3.632	3.632	3.633	3.633

Table 13 - TMS corrected diffusion for BTA 1-5

BTA 1				BTA 2			
0.74 mM	D/D <sub>TMS</sub>	12.37 mM	D/D <sub>TMS</sub>	0.84 mM	D/D <sub>TMS</sub>	20.90 mM	D/D <sub>TMS</sub>
H11, H11', H12	0.24	H11, H11', H12	0.25	H8	0.37	H8	0.37
H10, H10'	0.25	H10, H10'	0.25	H7, H7'	0.37	H7, H7'	0.37
H6, H6'	0.25	H6, H6'	0.24	H6, H6'	0.37	H6, H6'	0.37
H7, H7'	0.23	H7, H7'	0.25	BTC Core	0.37	BTC Core	0.37
BTC core	0.21	BTC core	0.25	N-H	0.37	N-H	0.37

BTA 3				BTA 4			
0.84 mM	D/D <sub>TMS</sub>	20.94 mM	D/D <sub>TMS</sub>	0.98 mM	D/D <sub>TMS</sub>	9.80 mM	D/D <sub>TMS</sub>
H5	0.32	H5	0.29	H8, H8'	0.24	H13	0.28
BTC Core	0.35	BTC Core	0.31	H9, H9'	0.24	H5	0.27
		NH	0.31	BTC Core	0.25	H8, H8'	0.27
				phOH	0.26	H9, H9'	0.27
						BTC Core	0.28
						NH	0.27

Table 14 – TMS corrected diffusion at different concentration for BTA 5

C (mM)	H17	H5	H10	H11	H15	H9	H12	BTC Core	Amide NH	Indole NH
2.59	*	*	0.20	0.24	0.24	0.22	0.20	0.23	*	0.20
5.18	0.23	*	0.21	0.23	0.22	0.22	0.22	0.24	*	0.23
7.77	0.30	0.29	0.29	0.30	0.31	0.29	0.29	0.30	0.28	0.31
9.50	0.32	0.29	0.31	0.29	0.30	0.30	0.30	0.32	*	0.31
11.22	0.28	0.28	0.28	0.27	0.28	0.28	0.27	0.28	0.27	*
15.97	0.27	0.26	0.27	0.25	0.25	0.26	0.26	0.27	0.27	*
20.97	0.30	0.23	0.26	0.26	0.25	0.27	0.26	0.29	0.27	0.25

Note: \* signals couldn't be fitted

**Table 15 - Measured chemical shifts in the BTA 5 ammonium chloride titration experiment at 25 °C**

<b>Guest/host</b>	<b>Indol N-H</b>	<b>Amide N-H</b>	<b>BTC core</b>	<b>H12</b>	<b>H9</b>	<b>H15</b>	<b>H11</b>	<b>H10</b>
<b>*</b>	10.831	9.164	8.446	7.559	7.324	7.194	7.058	6.983
<b>0.36</b>	10.837	9.182	8.456	7.560	7.324	7.201	7.058	6.983
<b>0.72</b>	10.840	9.191	8.461	7.560	7.324	7.205	7.058	6.983
<b>1.08</b>	10.840	9.197	8.468	7.560	7.324	7.210	7.058	6.983
<b>1.45</b>	10.843	9.208	8.475	7.560	7.324	7.213	7.057	6.983

**Note: \* only the host molecule was present in the NMR tube**

**Table 16 - Measured chemical shifts in the BTA 5 ammonium chloride titration experiment at 35 °C**

<b>Guest/host</b>	<b>Indol N-H</b>	<b>Amide N-H</b>	<b>BTC core</b>	<b>H12</b>	<b>H9</b>	<b>H15</b>	<b>H11</b>	<b>H10</b>
<b>*</b>	10.790	9.102	8.438	7.558	7.323	7.188	7.055	6.980
<b>0.33</b>	10.792	9.117	8.444	7.558	7.323	7.191	7.055	6.980
<b>0.66</b>	10.796	9.131	8.456	7.559	7.323	7.198	7.054	6.980
<b>0.99</b>	10.800	9.144	8.464	7.559	7.323	7.204	7.054	6.980
<b>1.32</b>	10.802	9.152	8.469	7.560	7.323	7.207	7.054	6.980

**Note: \* only the host molecule was present in the NMR tube**

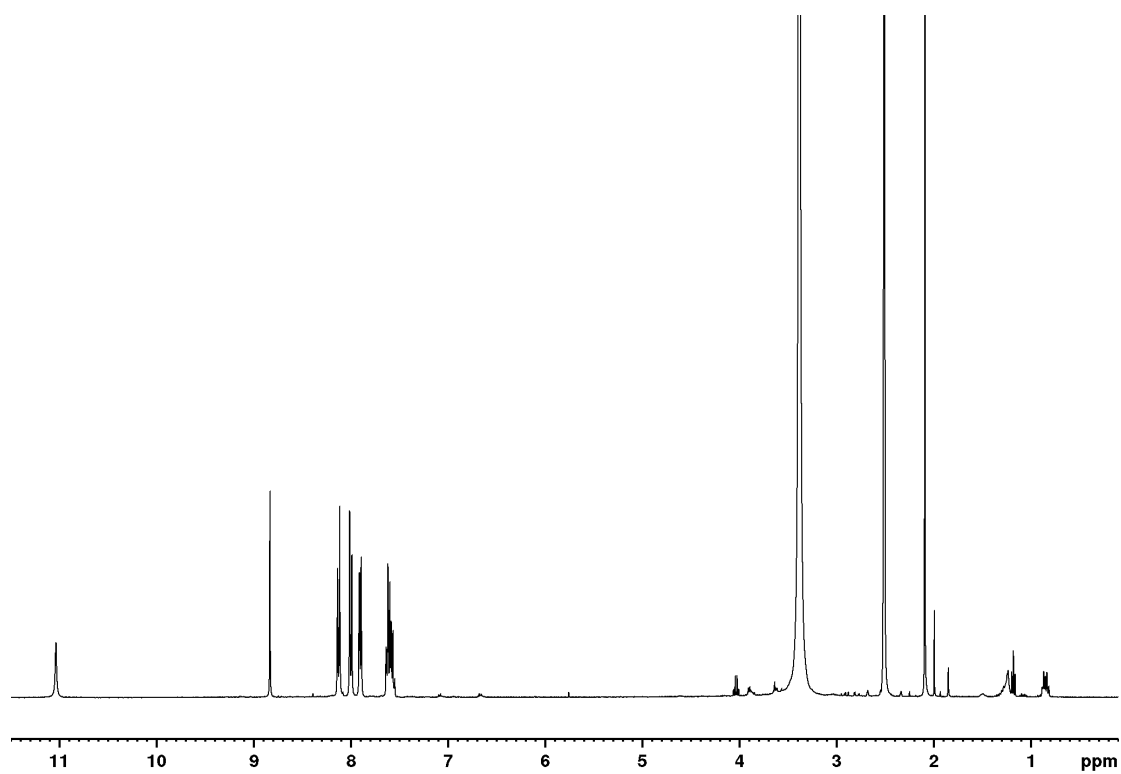


Figure 55 -  $^1\text{H}$  NMR spectrum of BTA 1 in  $\text{DMSO}-d_6$

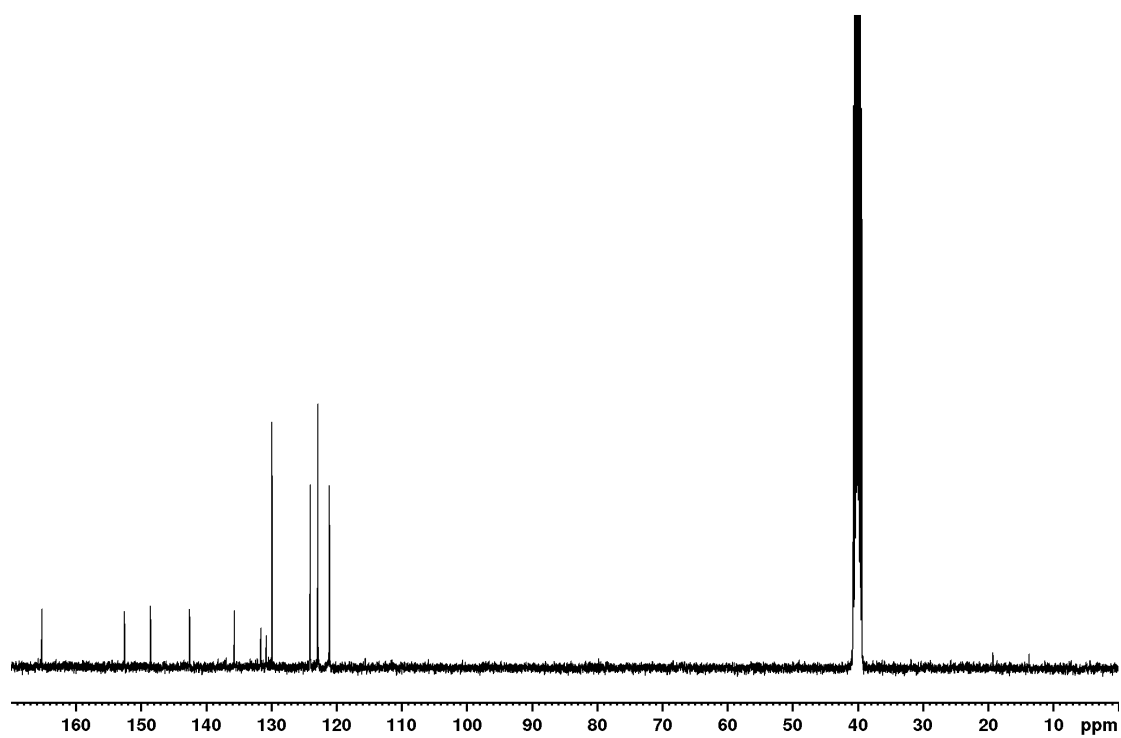


Figure 56 -  $^{13}\text{C}$  NMR spectrum of BTA 1 in  $\text{DMSO}-d_6$

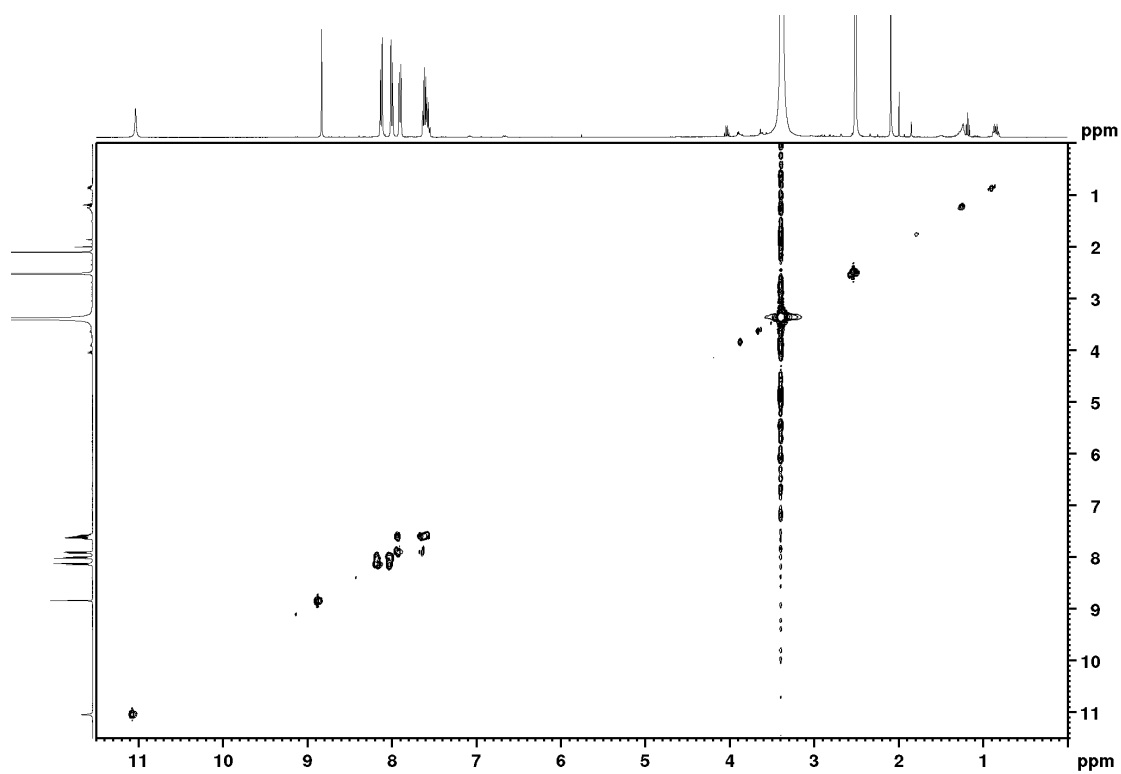


Figure 57 - COSY spectrum of BTA 1 in DMSO-*d*<sub>6</sub>

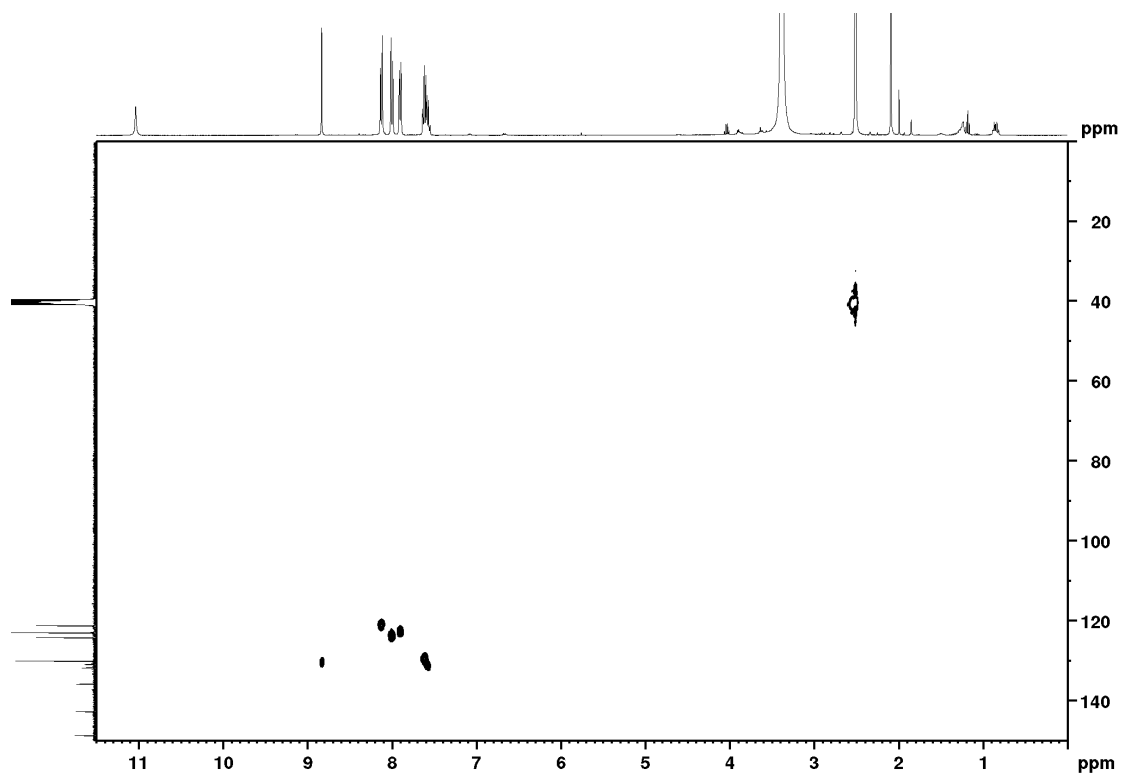


Figure 58 – HSQC spectrum of BTA 1 in DMSO-*d*<sub>6</sub>

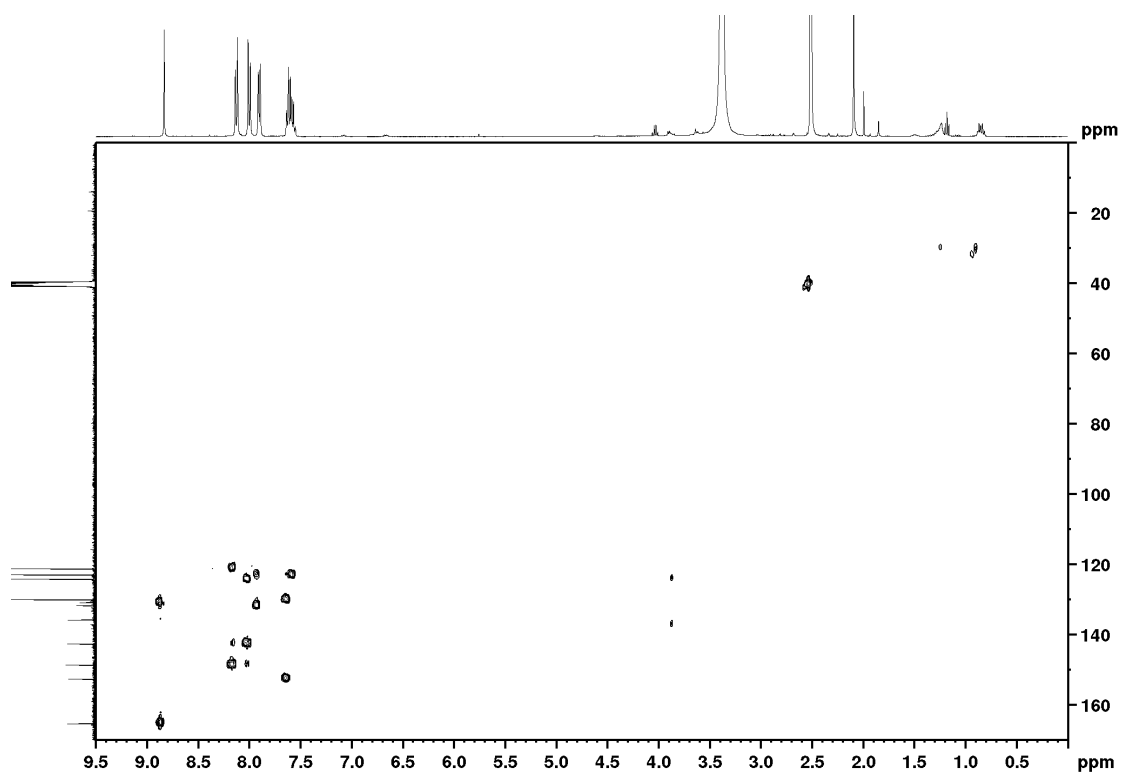


Figure 59 - HMBC spectrum of BTA 1 in DMSO-*d*<sub>6</sub>

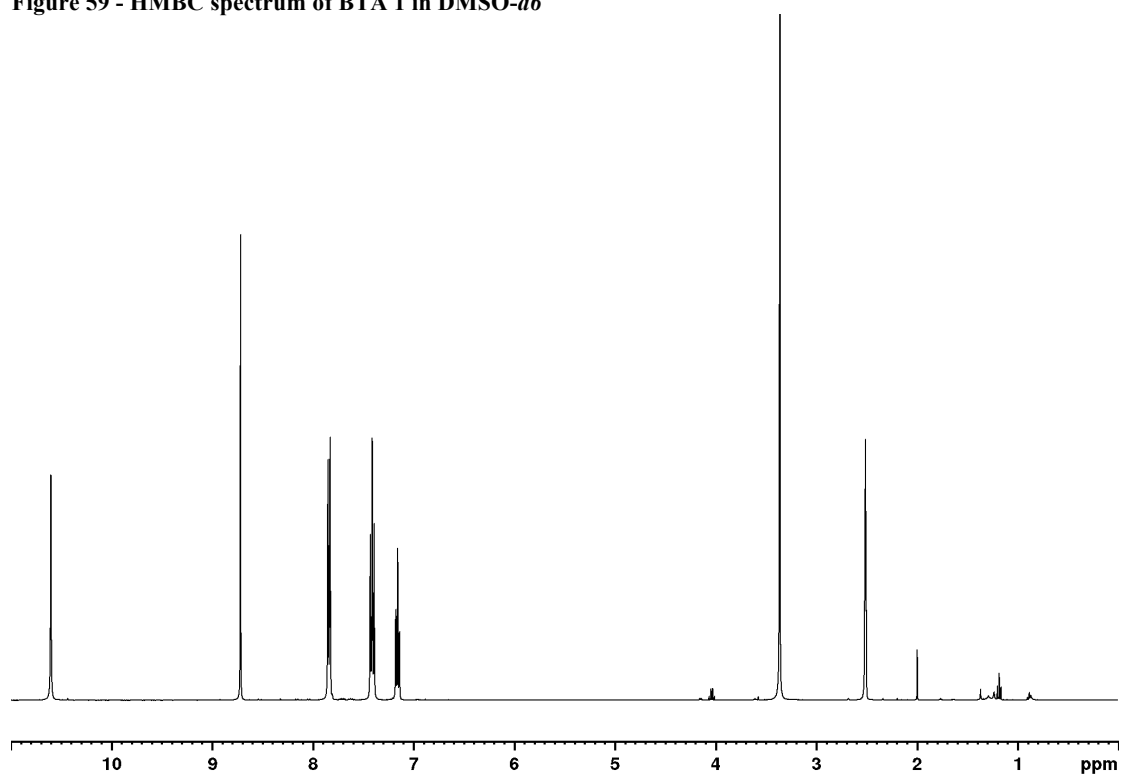


Figure 60 - <sup>1</sup>H NMR spectrum of BTA 2 in DMSO-*d*<sub>6</sub>



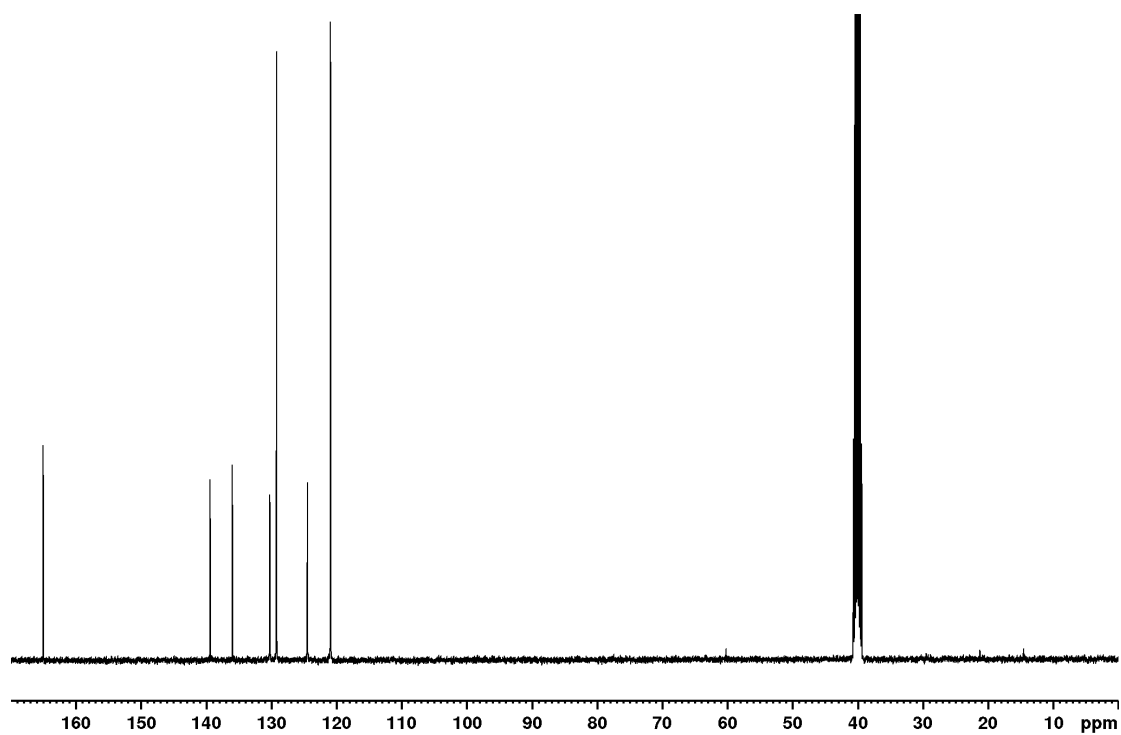


Figure 61 –  $^{13}\text{C}$  NMR spectrum of BTA 2 in  $\text{DMSO-}d_6$

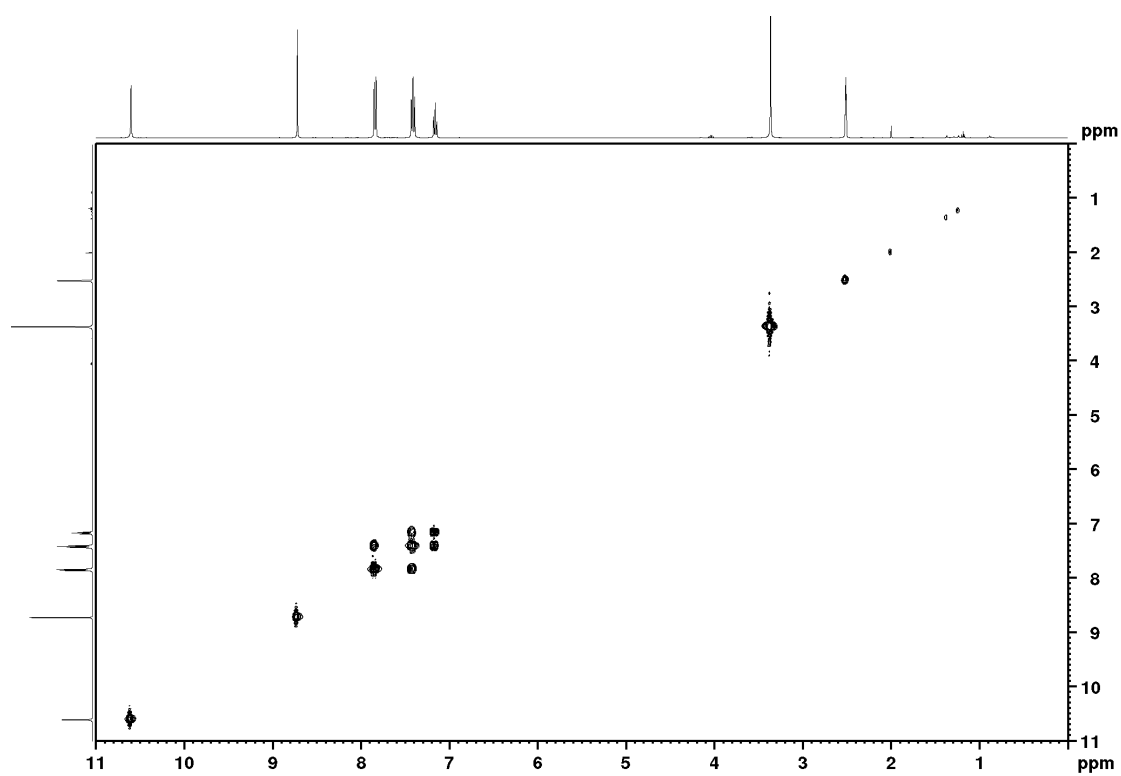


Figure 62 - COSY spectrum of BTA 2 in  $\text{DMSO-}d_6$

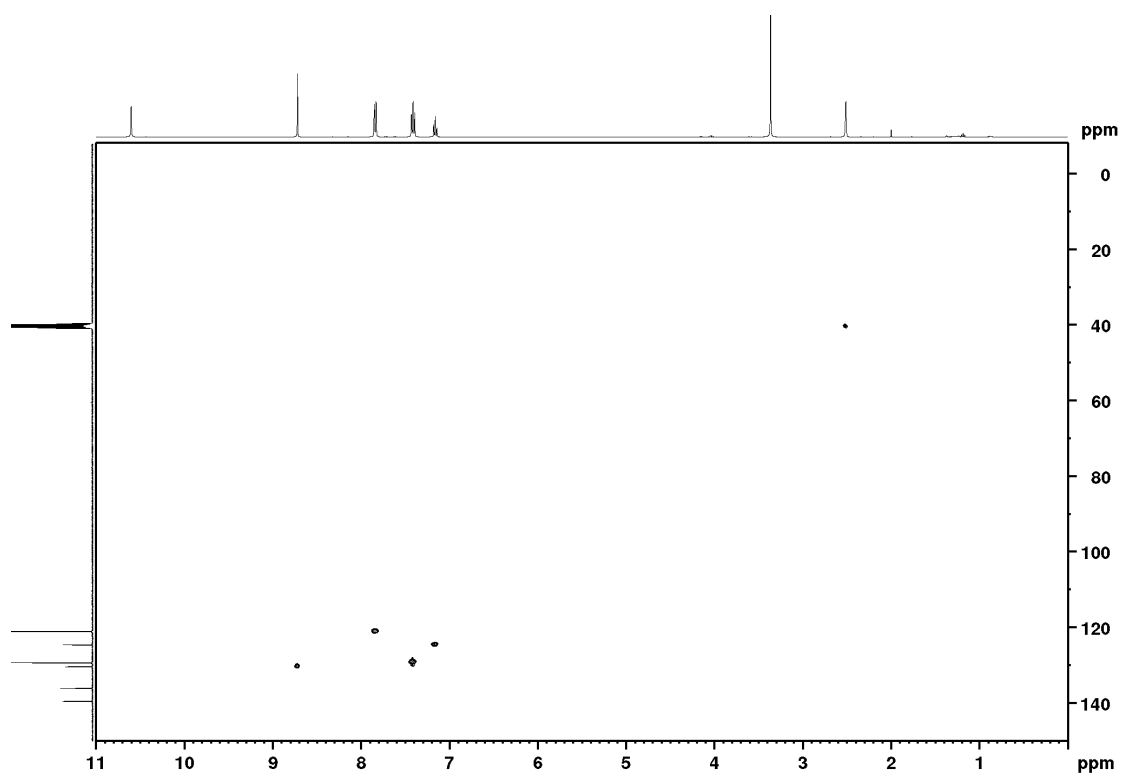


Figure 63 - HSQC spectrum of BTA 2 in DMSO-*d*6

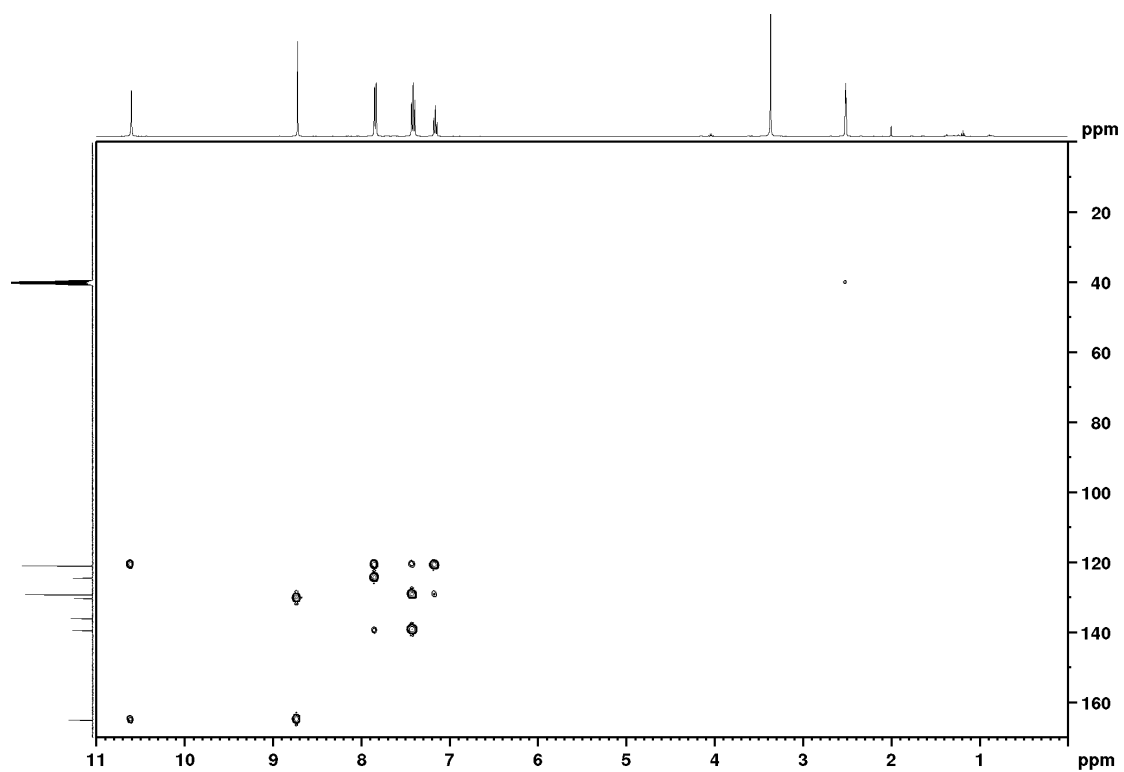


Figure 64 - HMBC spectrum of BTA 2 in DMSO-*d*6

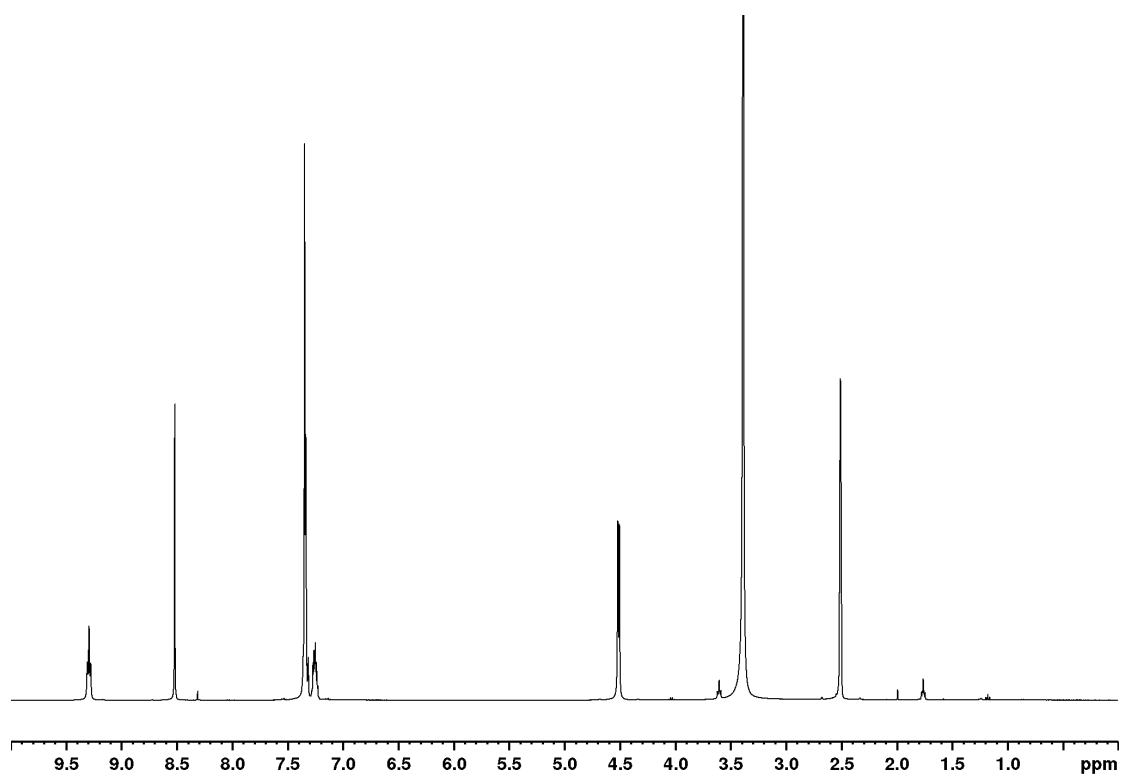


Figure 65 -  $^1\text{H}$  NMR spectrum of BTA 3 in  $\text{DMSO-}d_6$

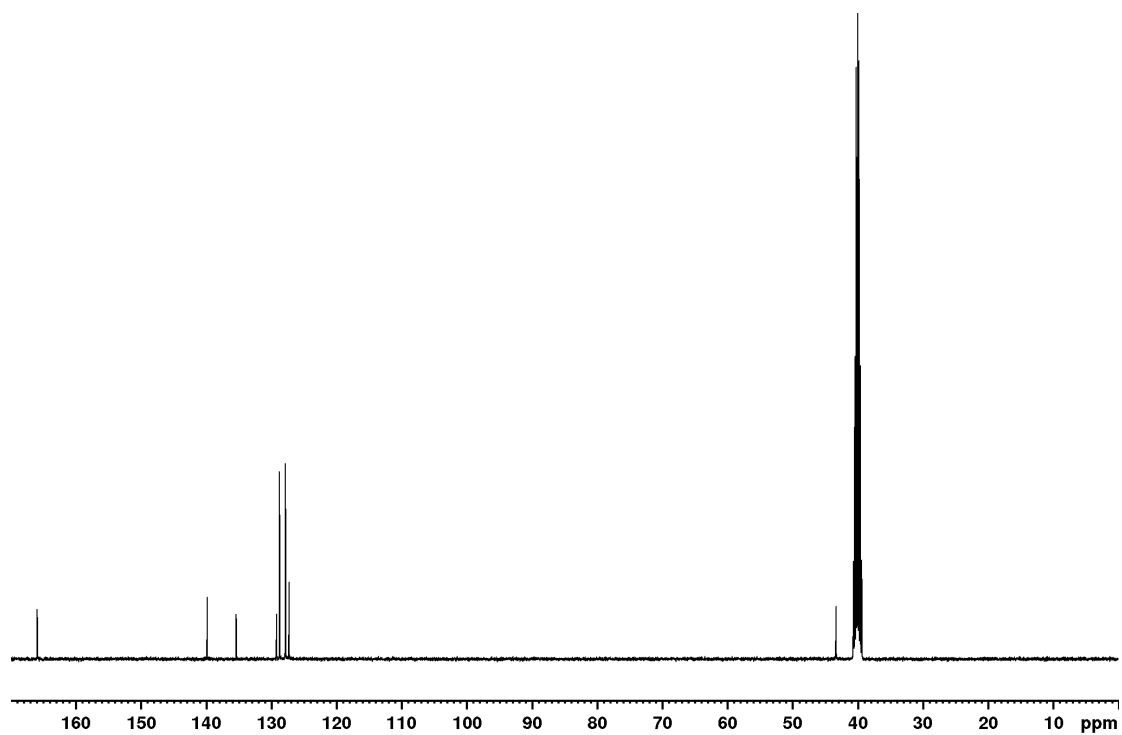


Figure 66 -  $^{13}\text{C}$  NMR spectrum of BTA 3 in  $\text{DMSO-}d_6$

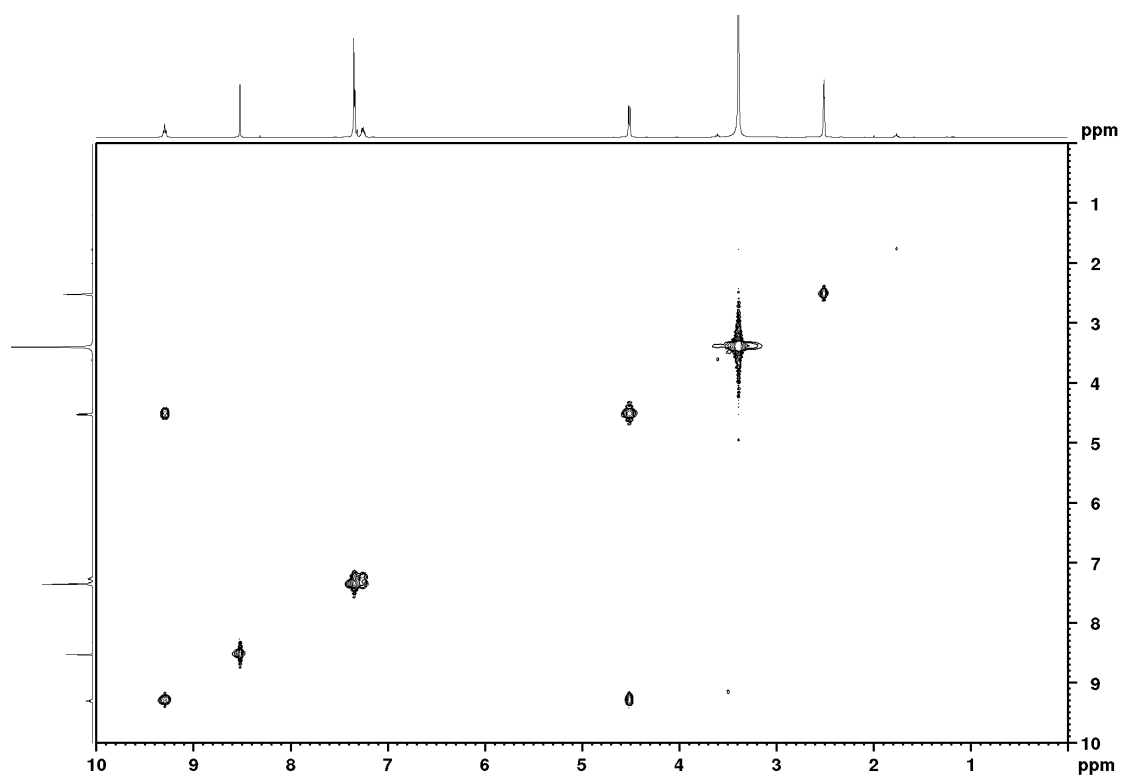


Figure 67 - COSY spectrum of BTA 3 in DMSO-*d*<sub>6</sub>

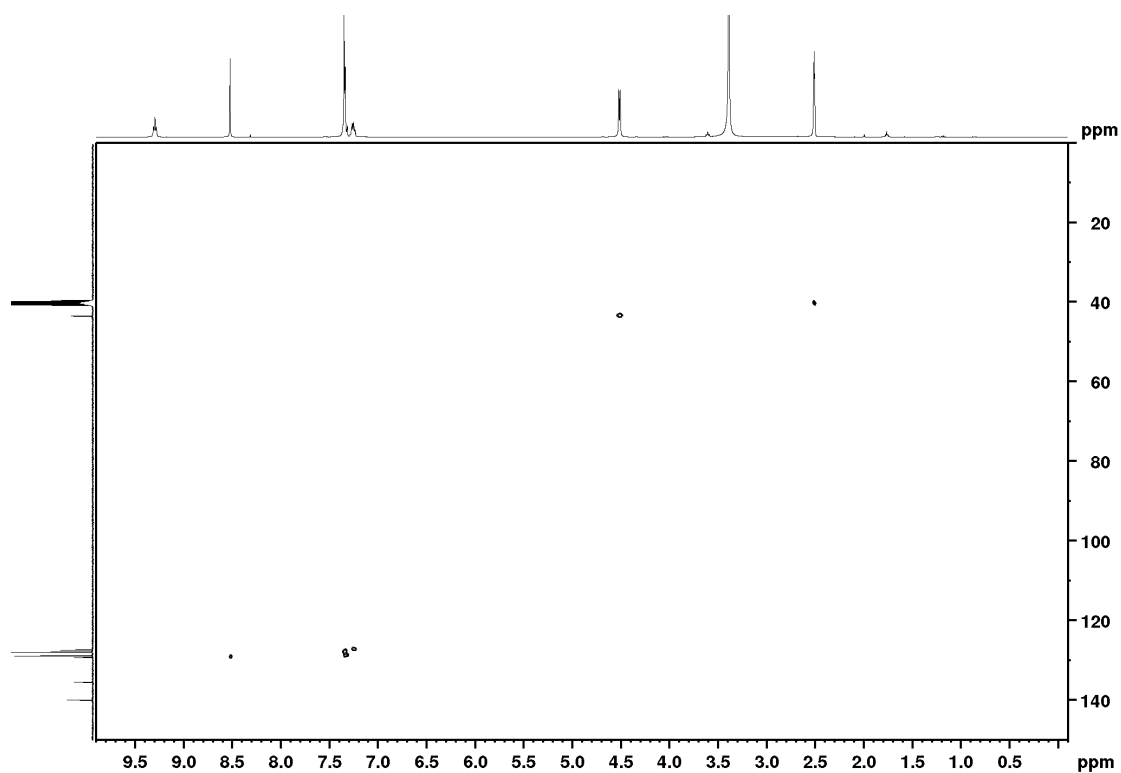


Figure 68 - HSQC spectrum of BTA 3 in DMSO-*d*<sub>6</sub>

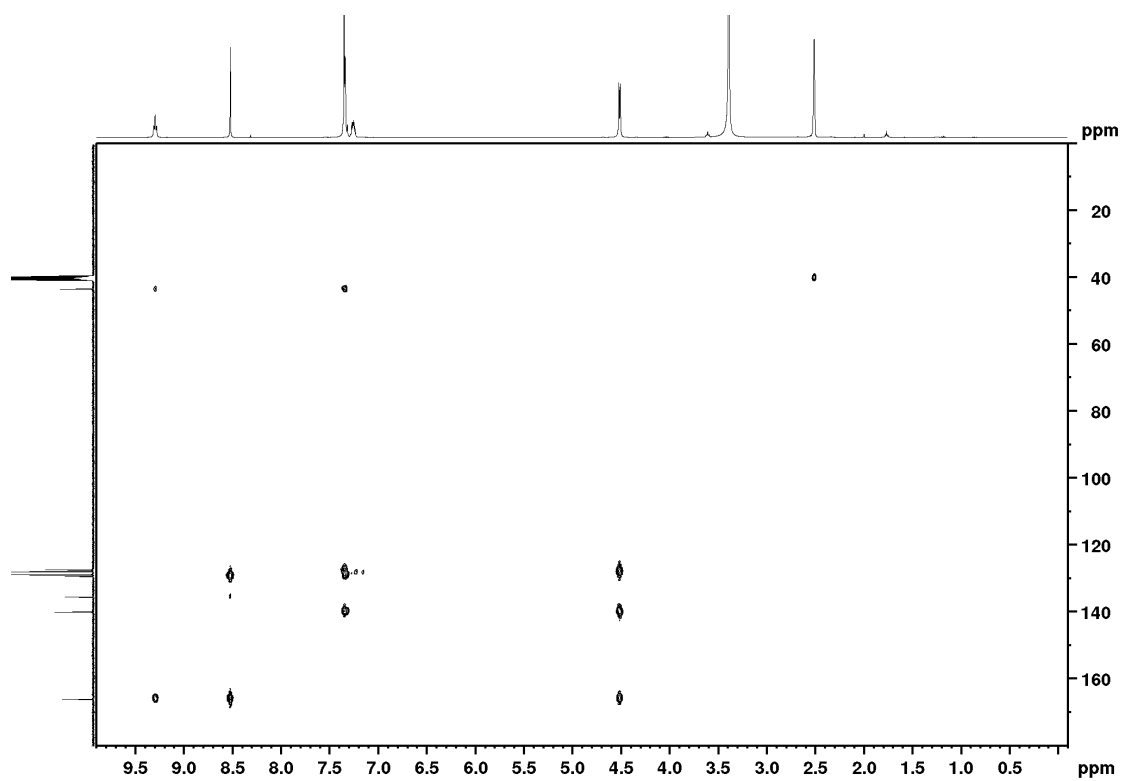


Figure 69 - HMBC spectrum of BTA 3 in DMSO-*d*<sub>6</sub>

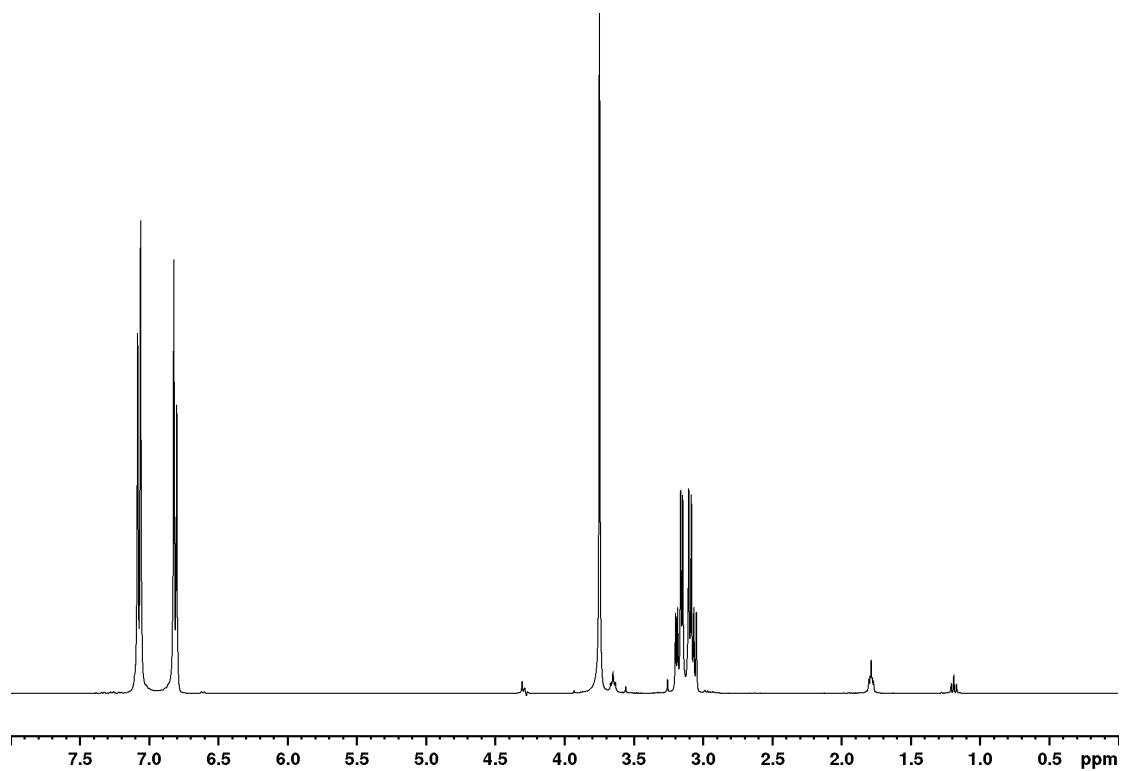


Figure 70 – Water suppressed <sup>1</sup>H NMR spectrum of tyrosine methyl ester hydrochloride in D<sub>2</sub>O

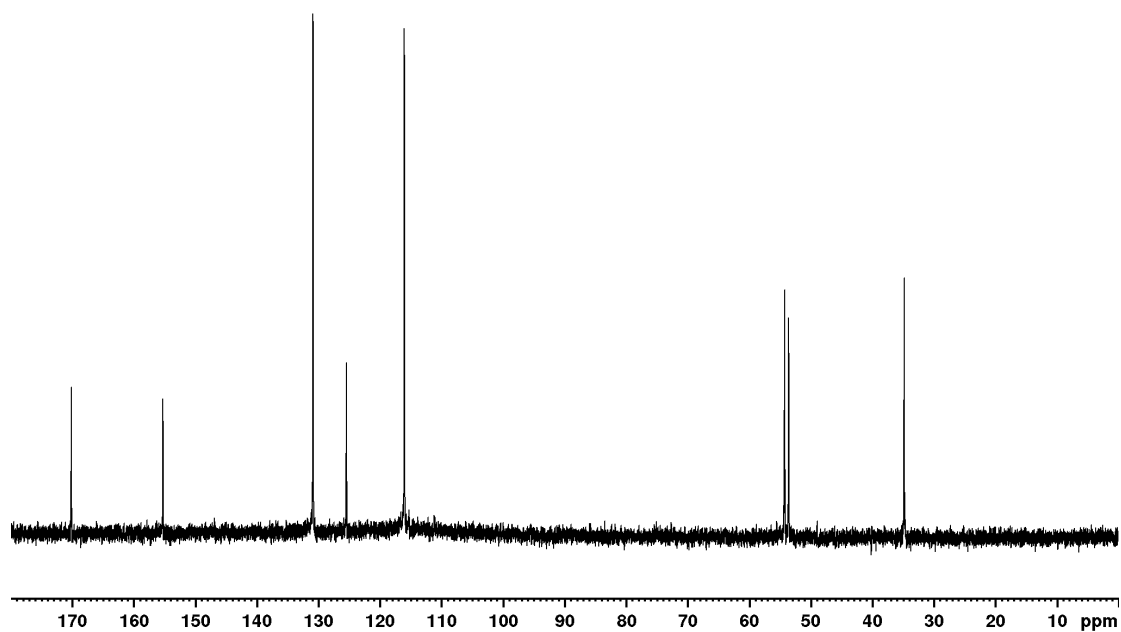


Figure 71 –  $^{13}\text{C}$  NMR spectrum of tyrosine methyl ester hydrochloride in  $\text{D}_2\text{O}$

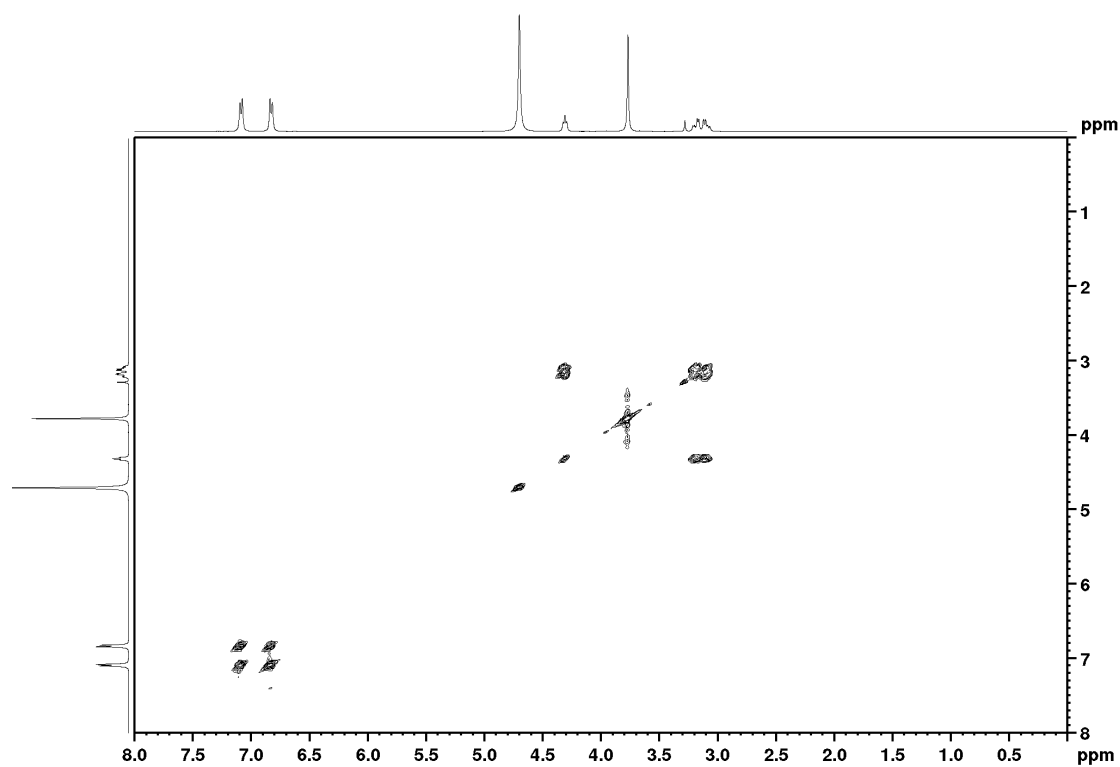


Figure 72 – COSY spectrum of tyrosine methyl ester hydrochloride in  $\text{D}_2\text{O}$

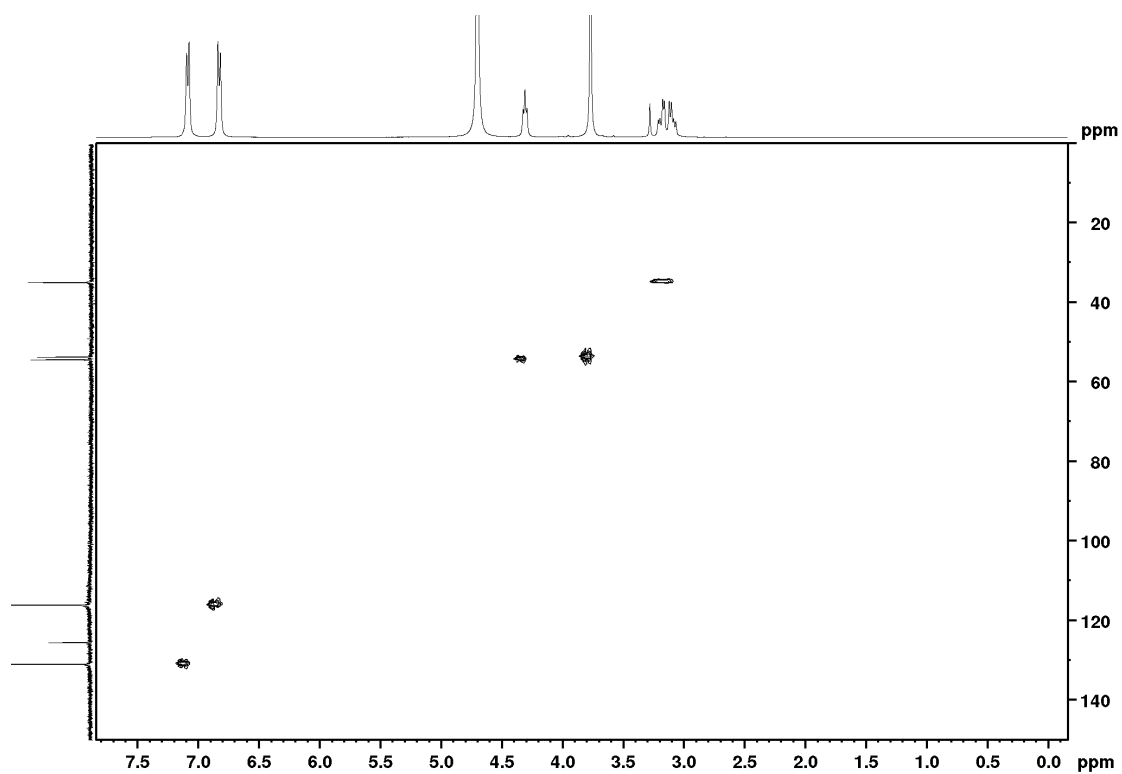


Figure 73 - HSQC spectrum of tyrosine methyl ester hydrochloride in D<sub>2</sub>O

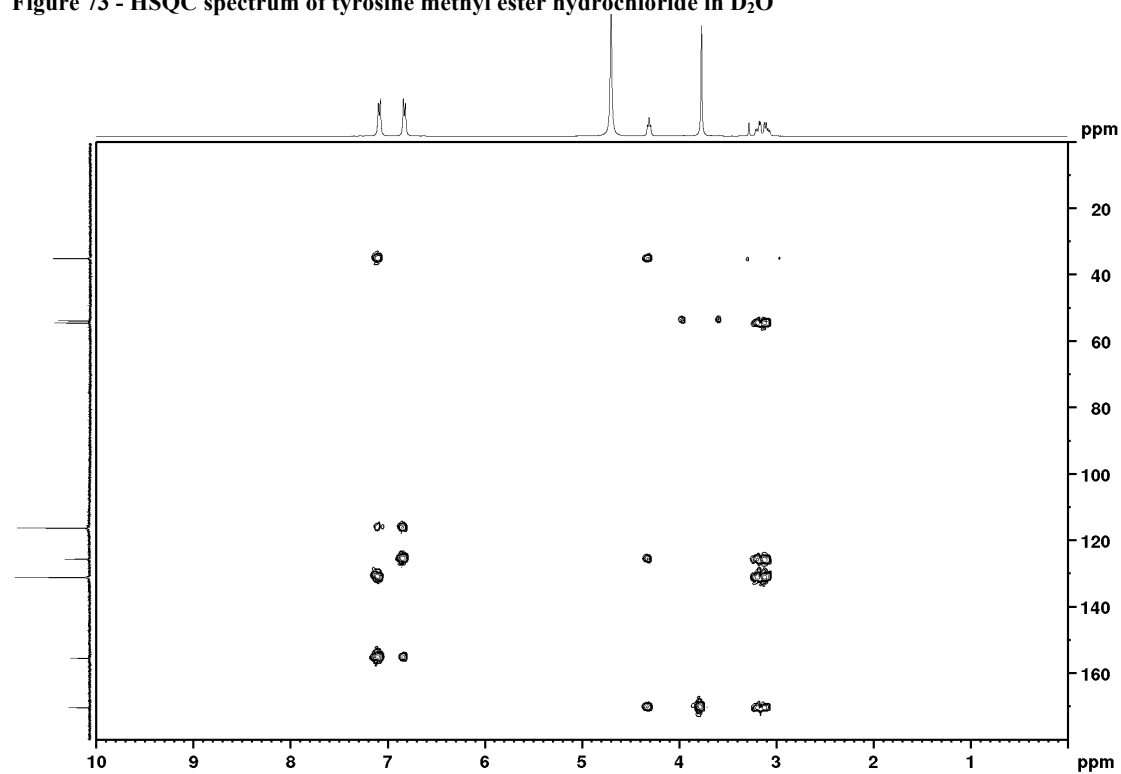


Figure 74 - HMBC spectrum of tyrosine methyl ester hydrochloride in D<sub>2</sub>O

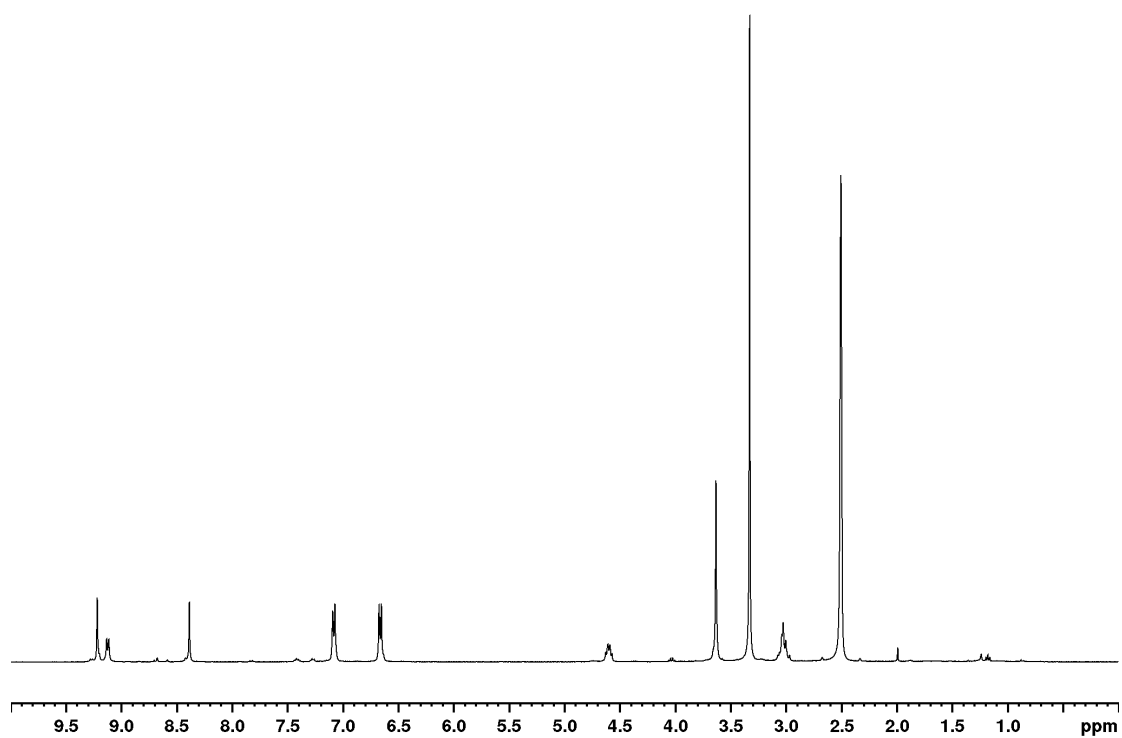


Figure 75 -  $^1\text{H}$  NMR spectrum of BTA 4 in  $\text{DMSO-}d_6$

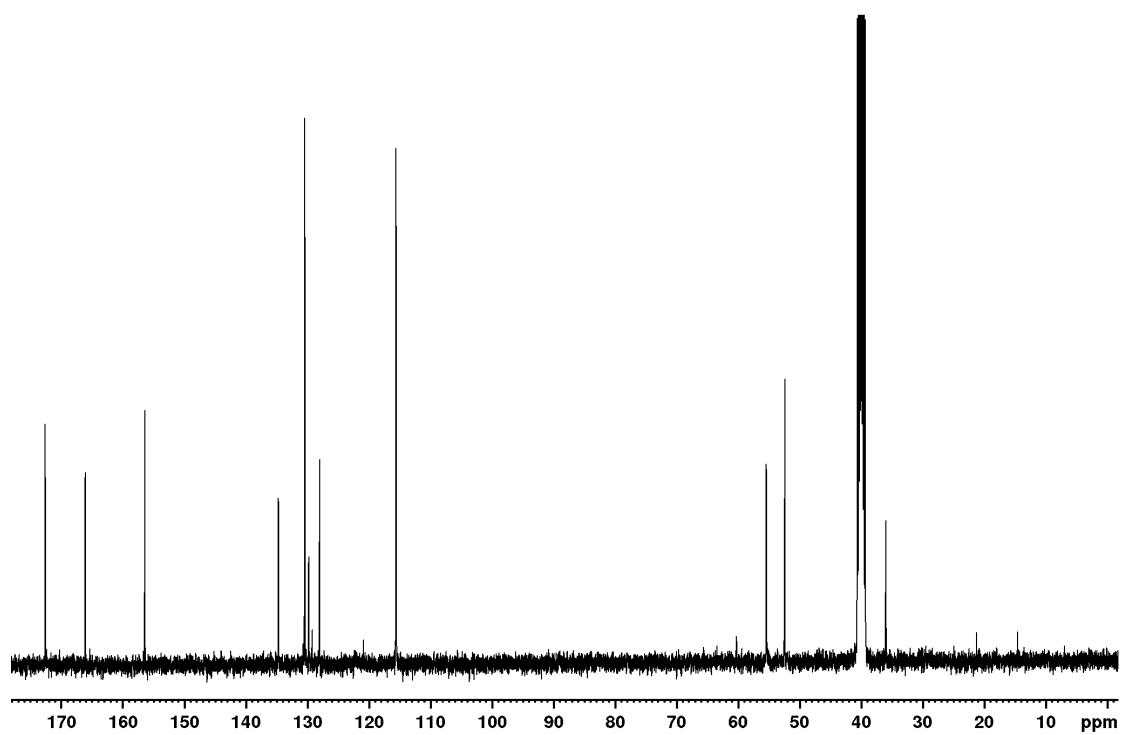


Figure 76 -  $^{13}\text{C}$  NMR spectrum of BTA 4 in  $\text{DMSO-}d_6$



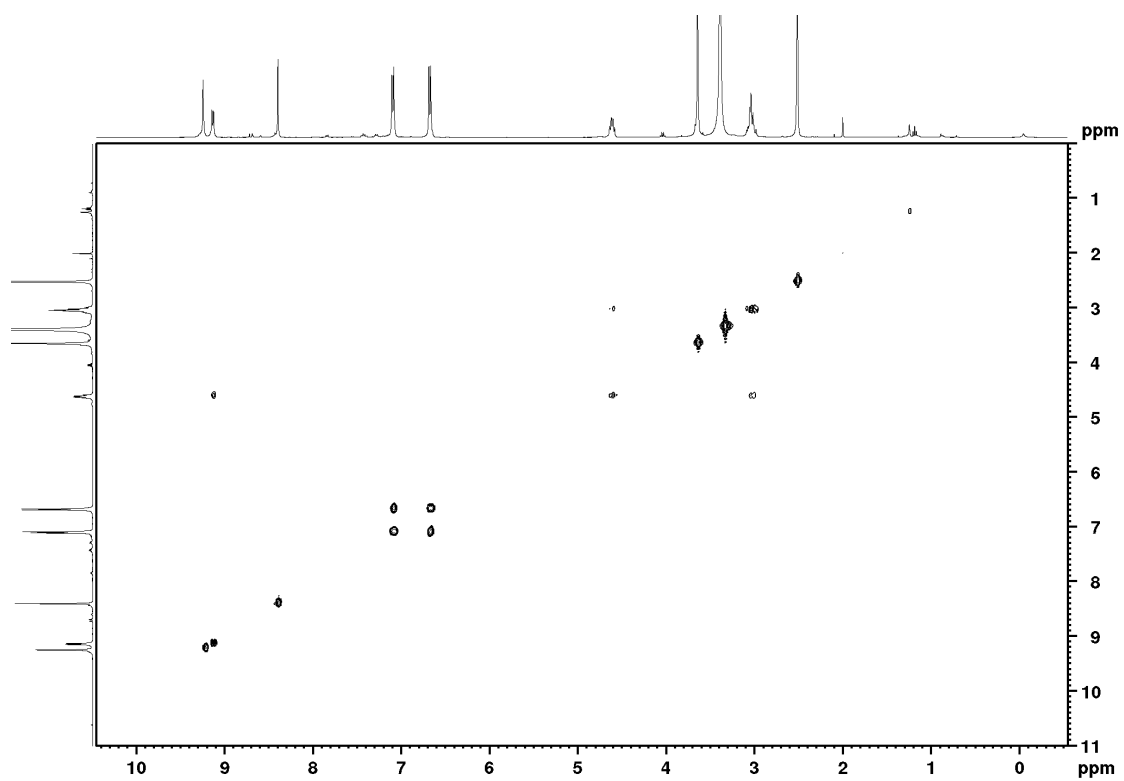


Figure 77 - COSY spectrum of BTA 4 in DMSO-*d*<sub>6</sub>

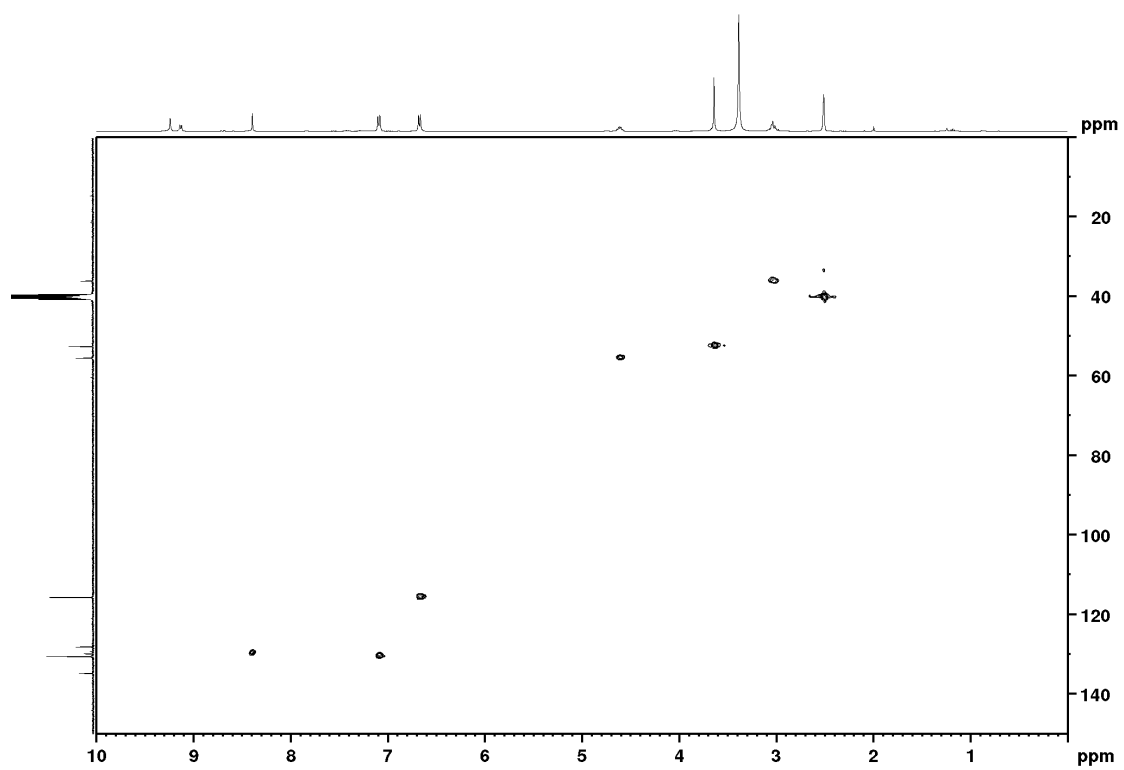


Figure 78 - HSQC spectrum of BTA 4 in DMSO-*d*<sub>6</sub>

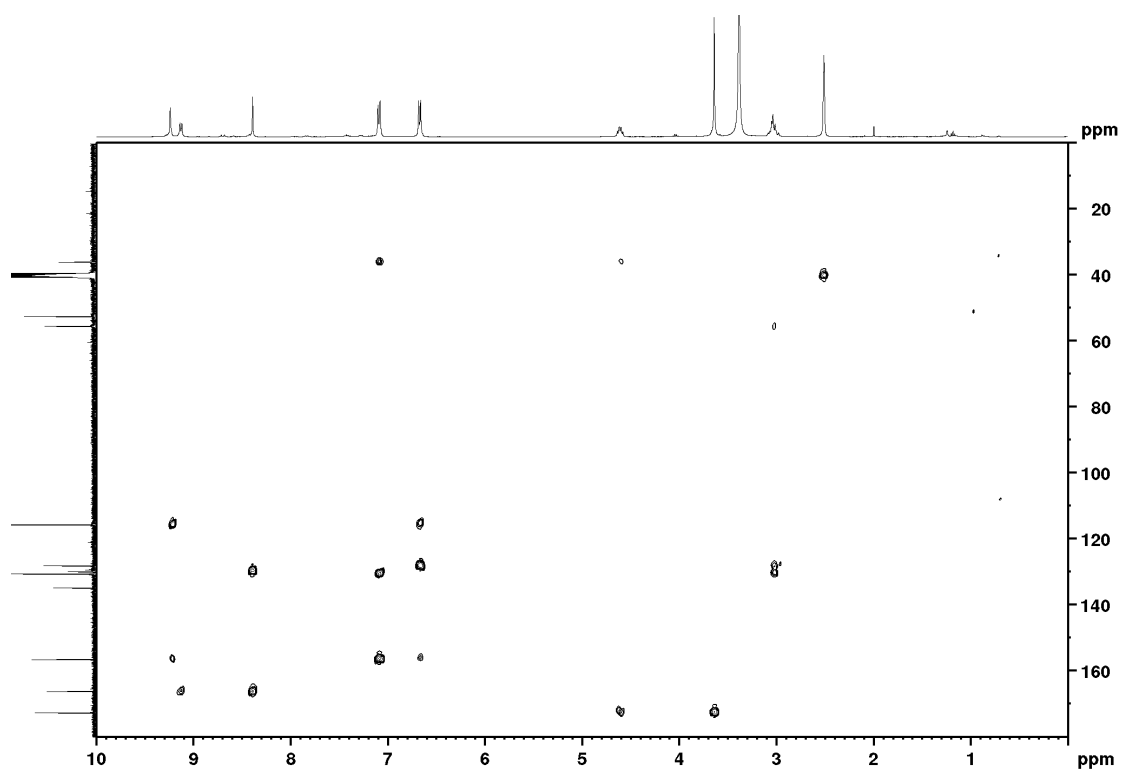


Figure 79 - HMBC spectrum of BTA 4 in DMSO-*d*<sub>6</sub>

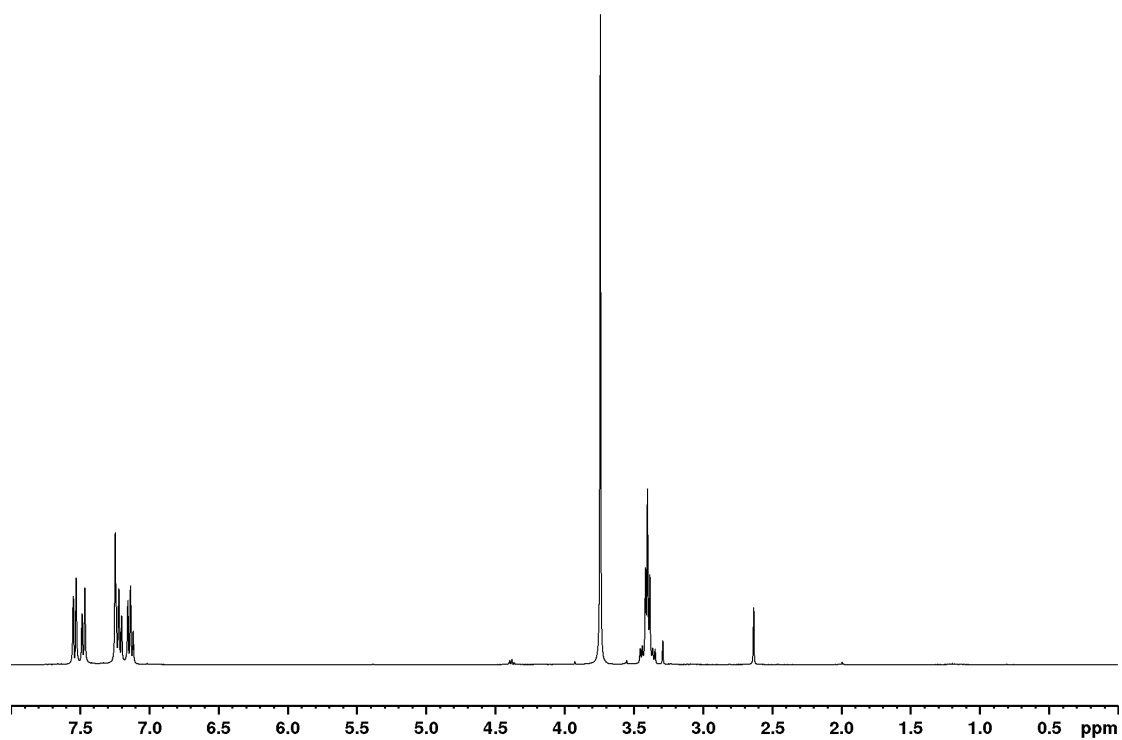


Figure 80 - Water suppressed <sup>1</sup>H NMR spectrum of tryptophan methyl ester hydrochloride in D<sub>2</sub>O

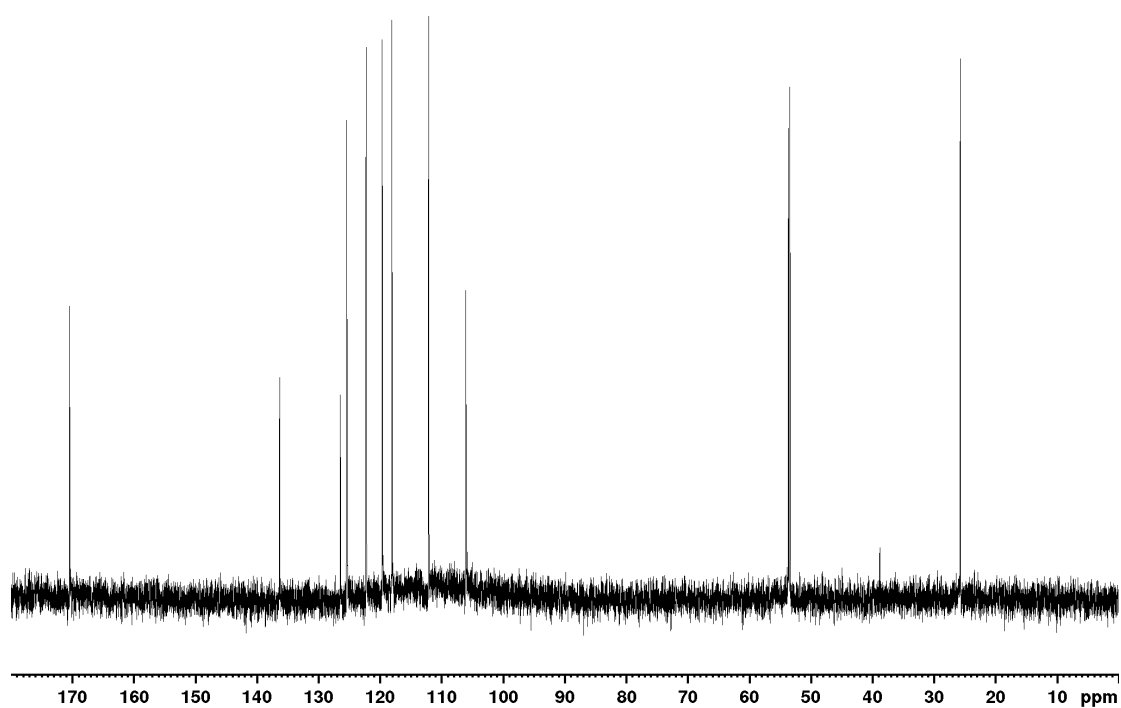


Figure 81 –  $^{13}\text{C}$  NMR spectrum of tryptophan methyl ester hydrochloride in  $\text{D}_2\text{O}$

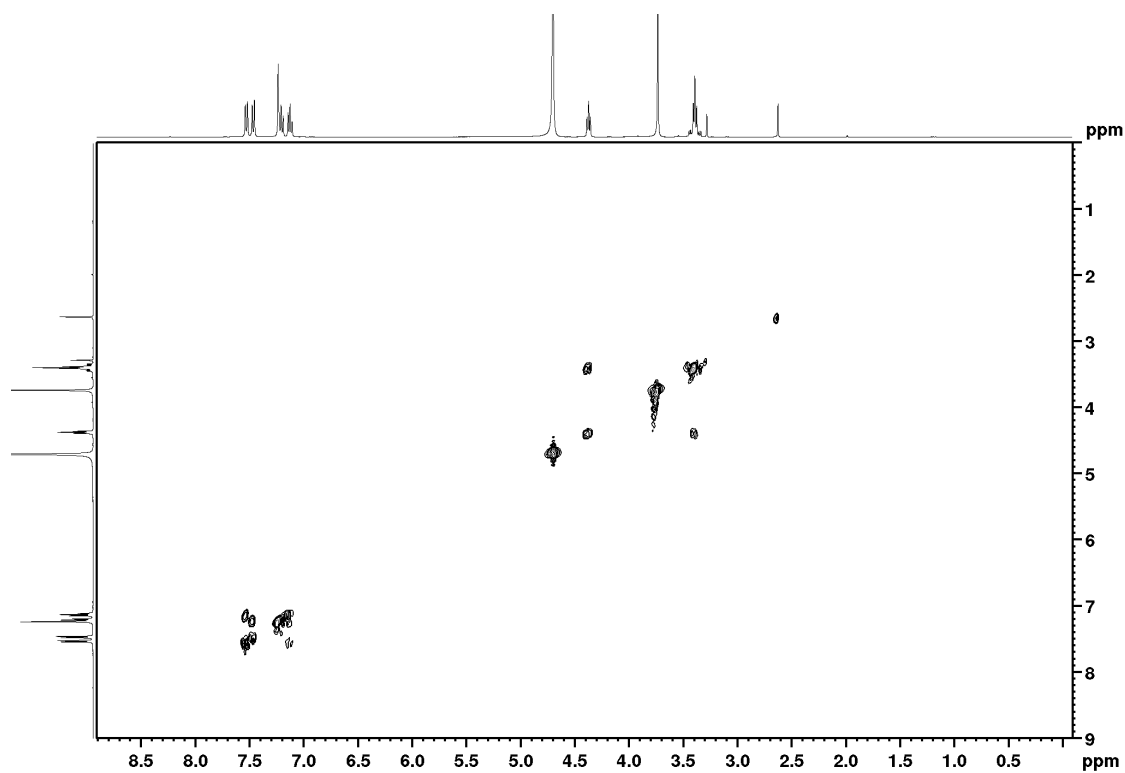


Figure 82 - COSY spectrum of tryptophan methyl ester hydrochloride in  $\text{D}_2\text{O}$

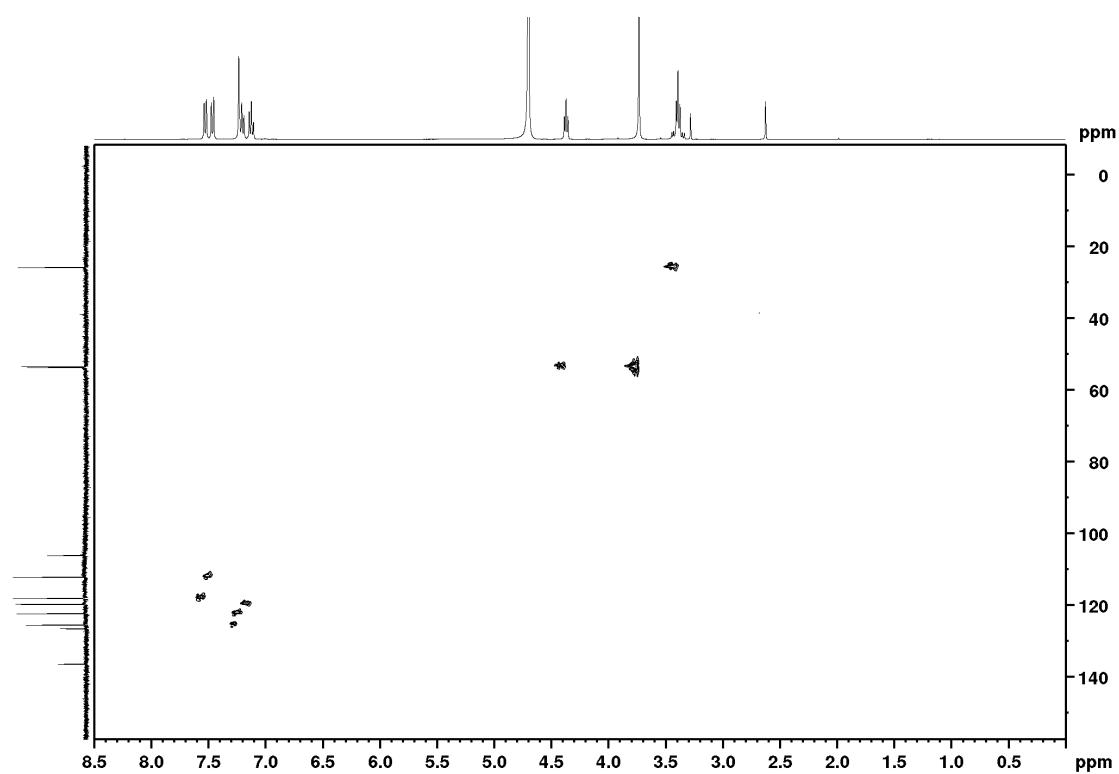


Figure 83 - HSQC spectrum of tryptophan methyl ester hydrochloride in D<sub>2</sub>O

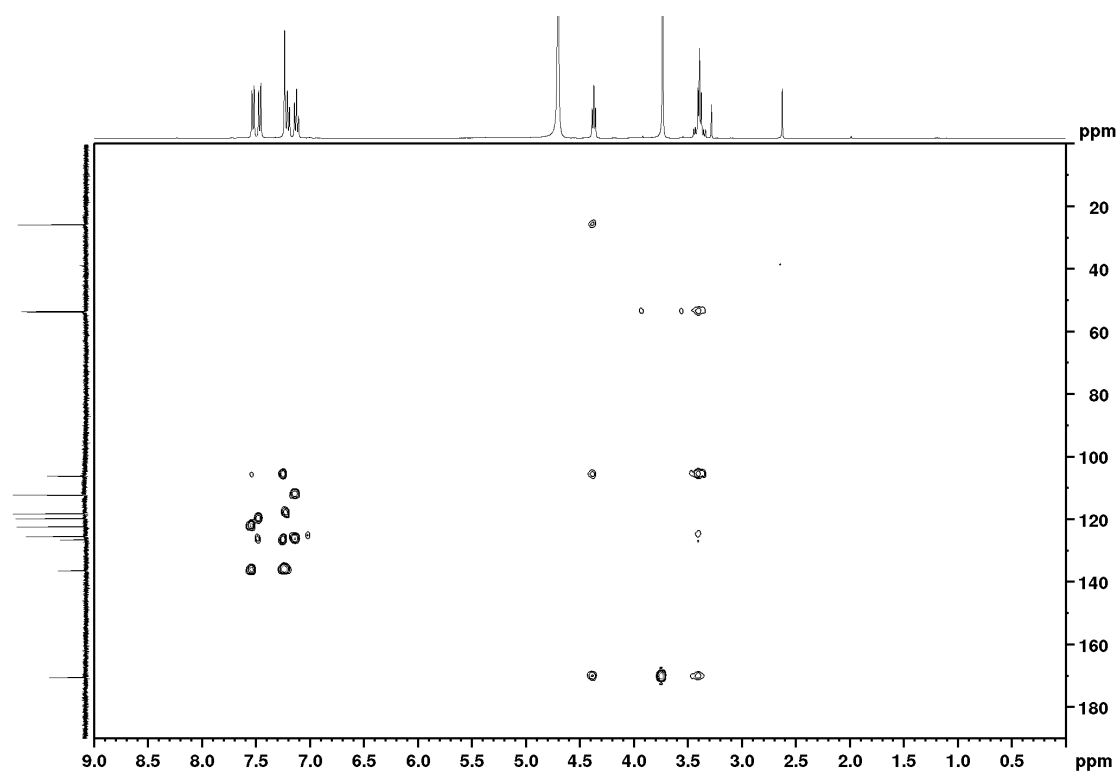


Figure 84 - HMBC spectrum of tryptophan methyl ester hydrochloride in D<sub>2</sub>O

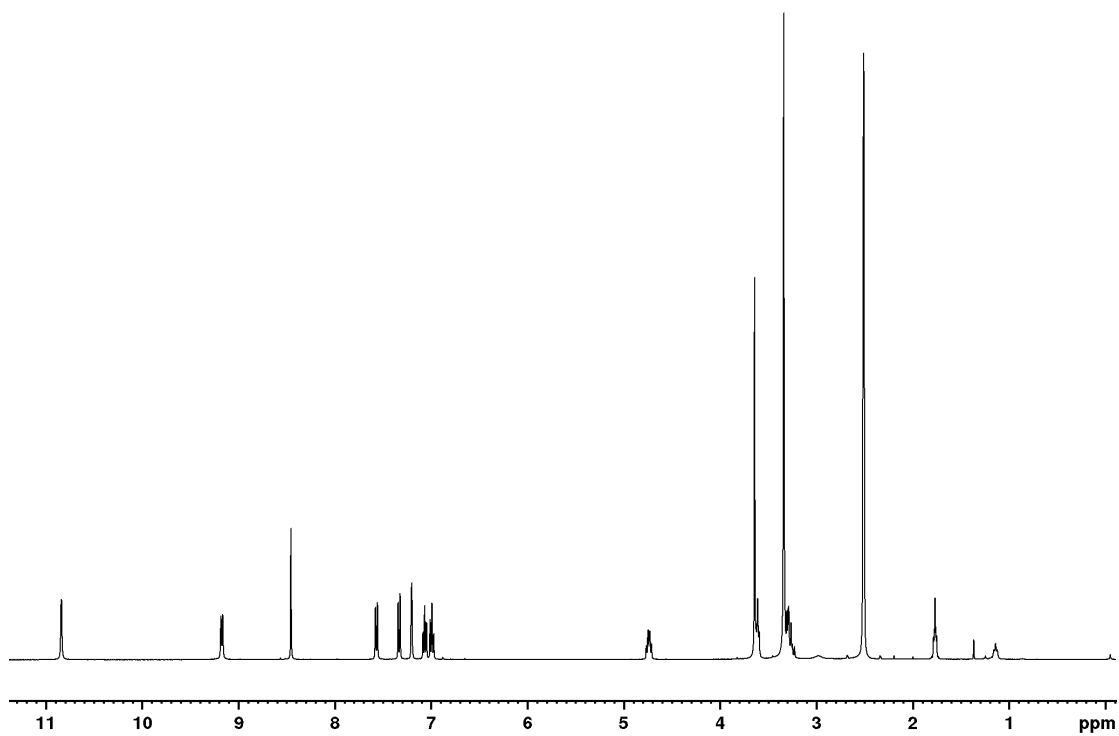


Figure 85 -  $^1\text{H}$  NMR spectrum of BTA 5 in  $\text{DMSO-}d_6$

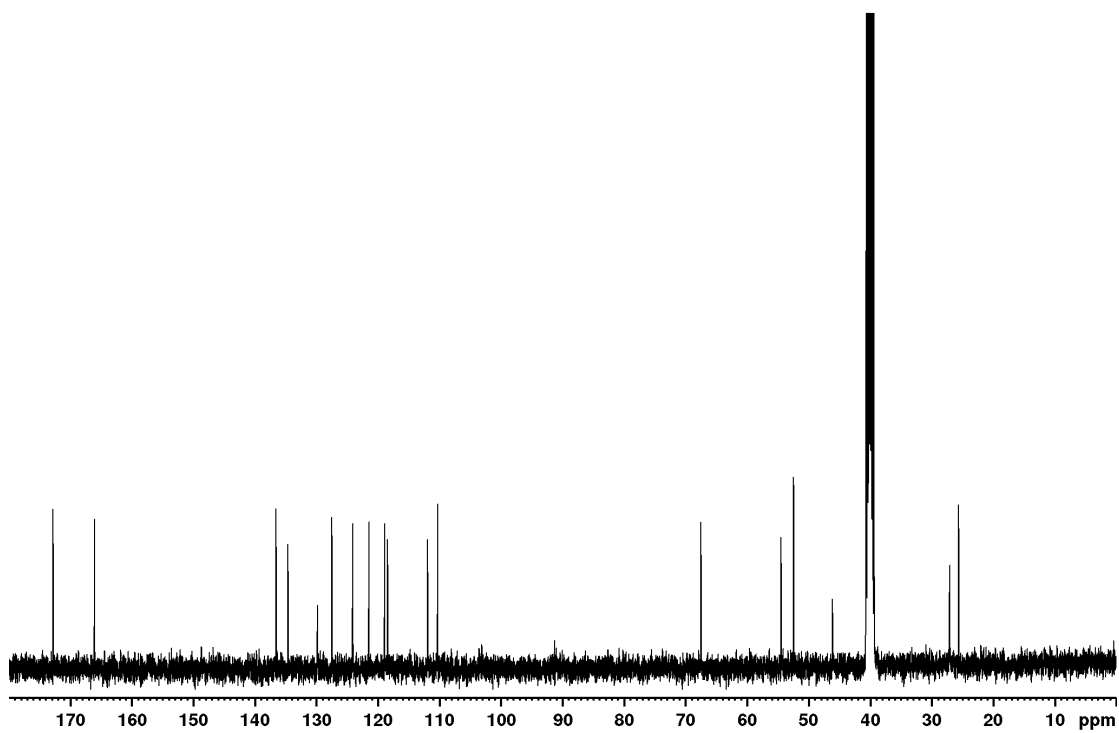


Figure 86 -  $^{13}\text{C}$  NMR spectrum of BTA 5 in  $\text{DMSO-}d_6$

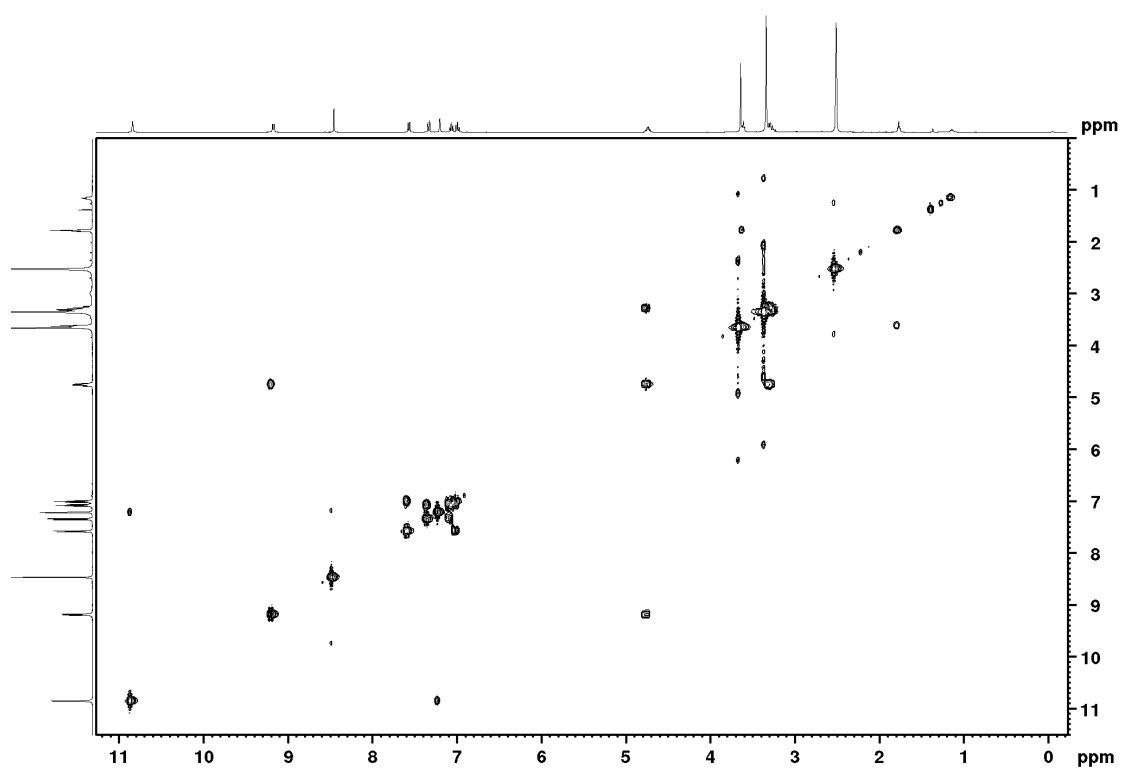


Figure 87 - COSY spectrum of BTA 5 in DMSO-*d*<sub>6</sub>

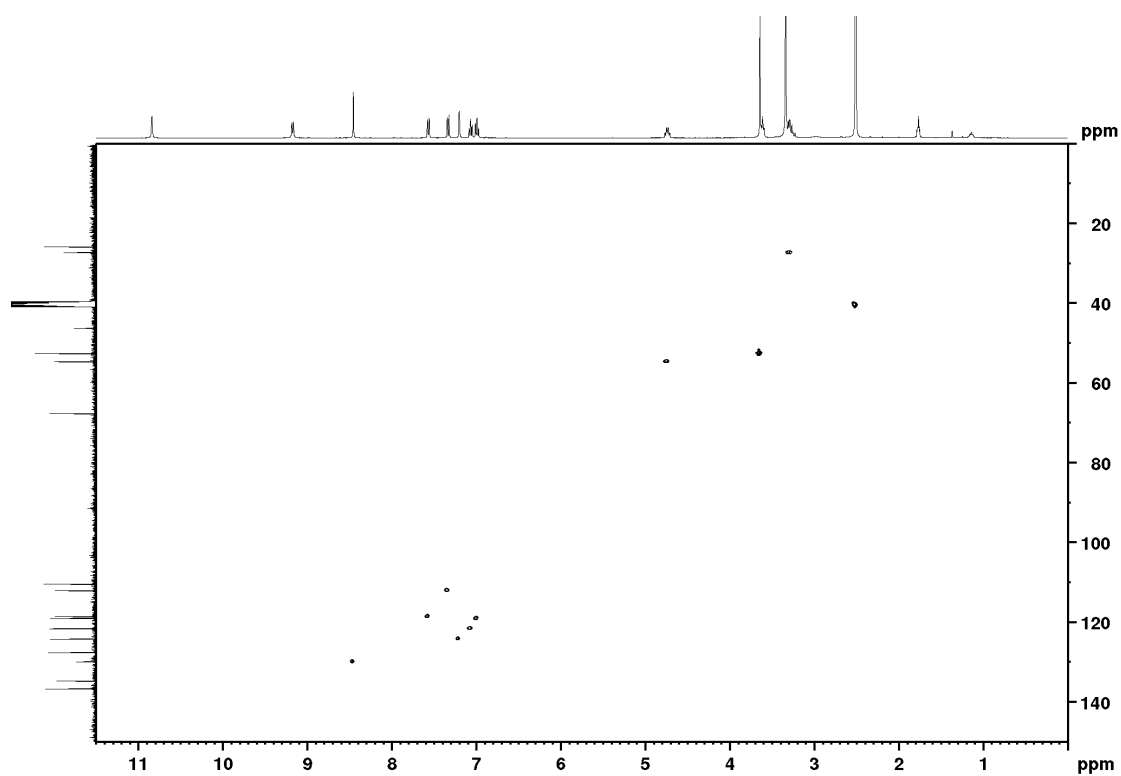


Figure 88 - HSQC spectrum of BTA 5 in DMSO-*d*<sub>6</sub>

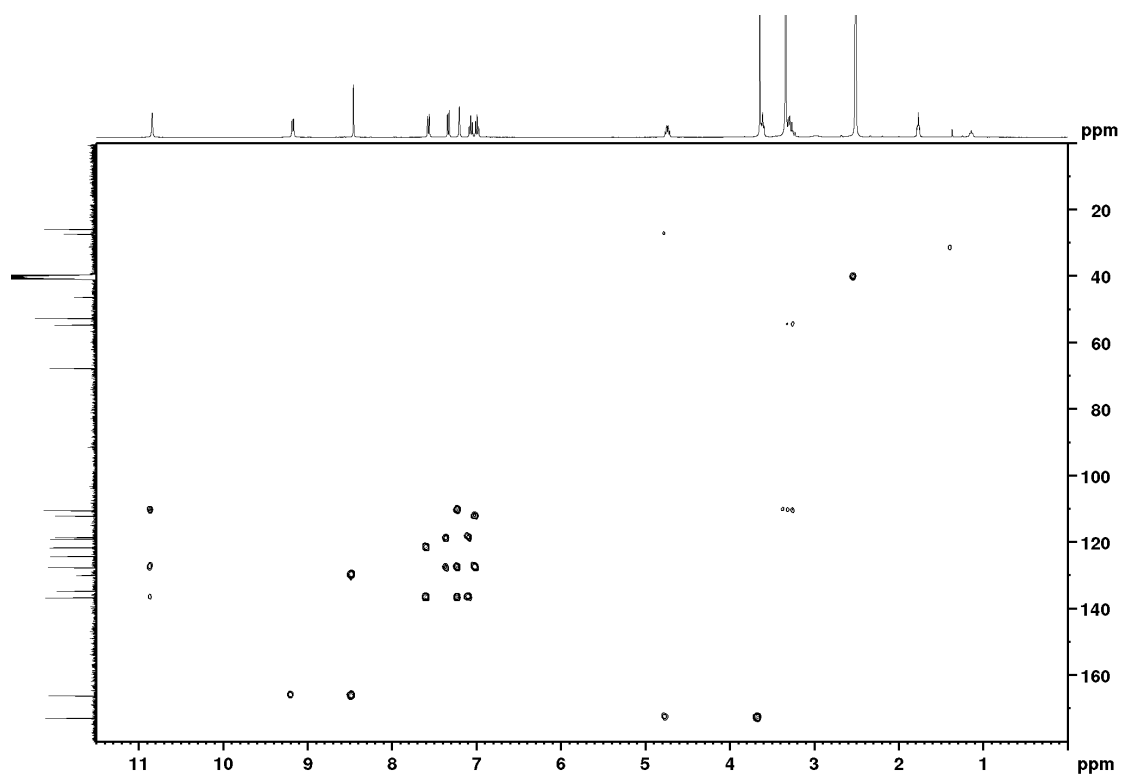


Figure 89 - HMBC spectrum of BTA 5 in DMSO-*d*<sub>6</sub>

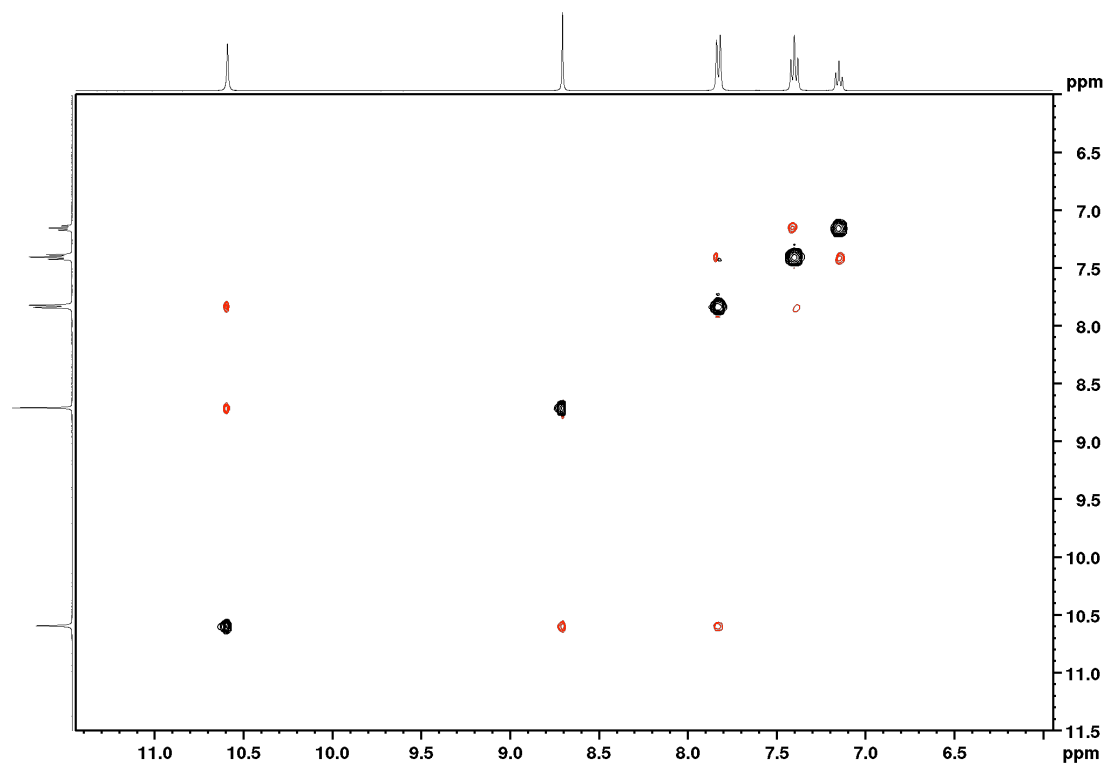


Figure 90 - NOESY spectrum of BTA 2 at 20.90 mM in DMSO-*d*<sub>6</sub>

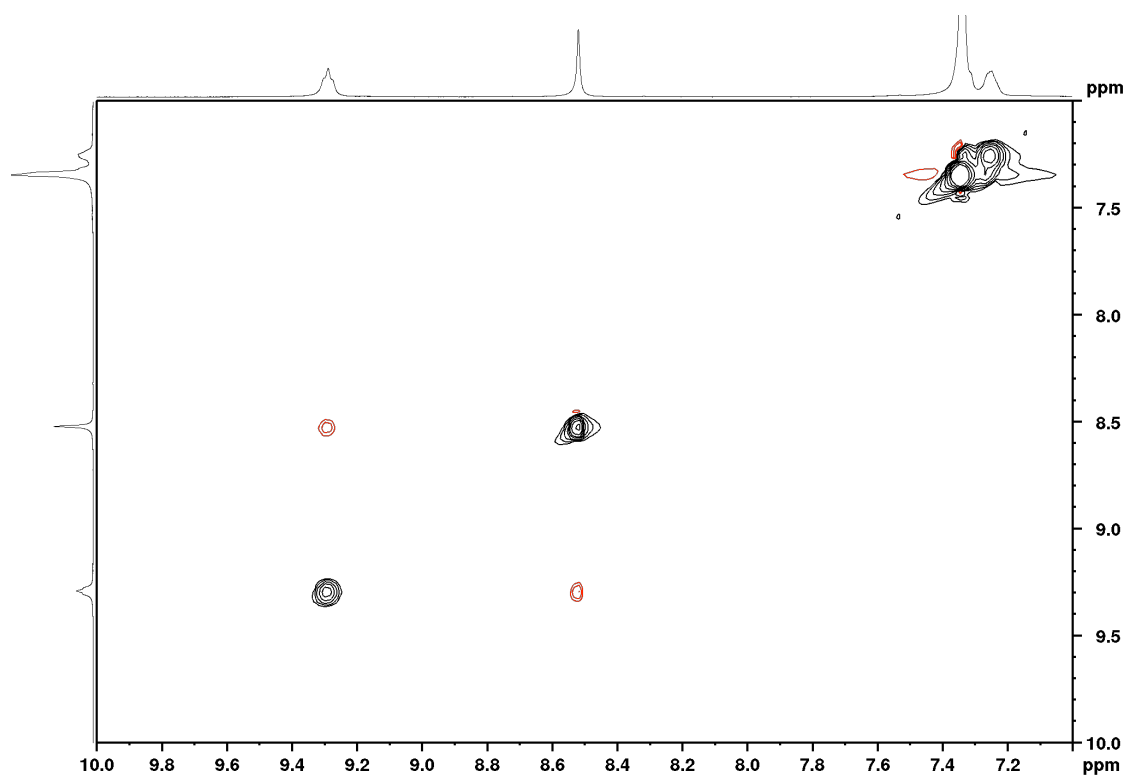


Figure 91 - NOESY spectrum of BTA 3 at 20.94 mM in DMSO-*d*<sub>6</sub>

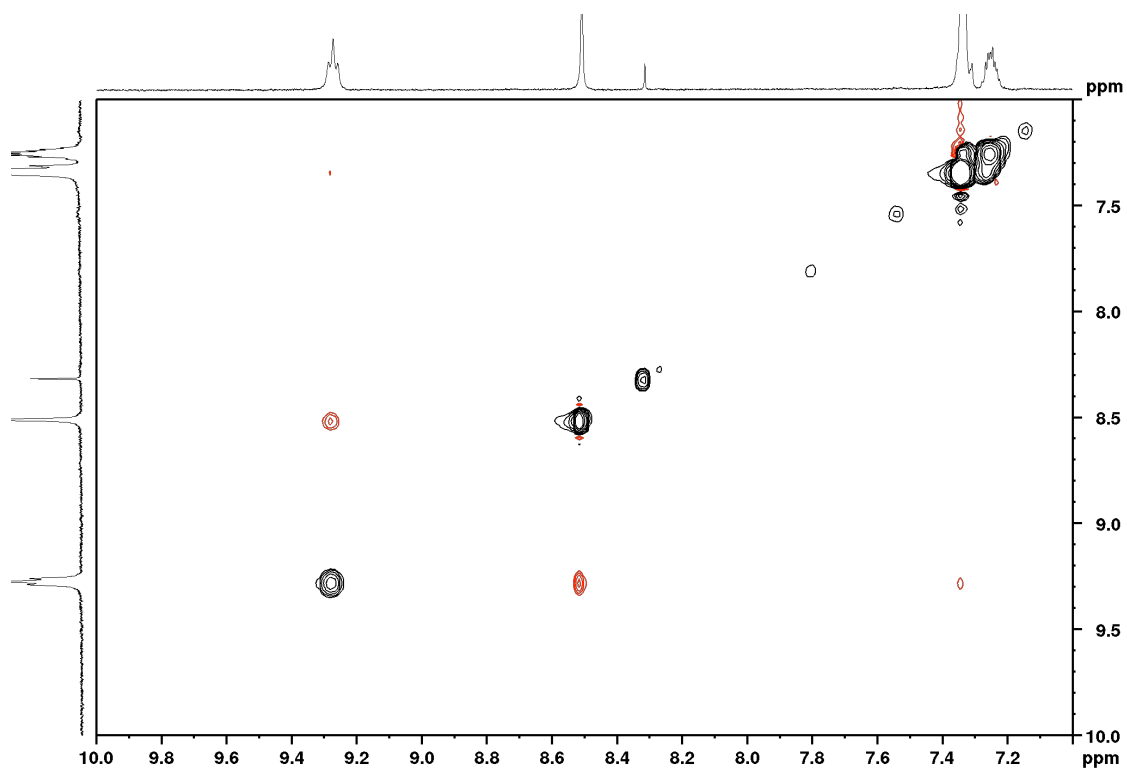


Figure 92 - NOESY spectrum of BTA 3 at 0.84 mM in DMSO-*d*<sub>6</sub>



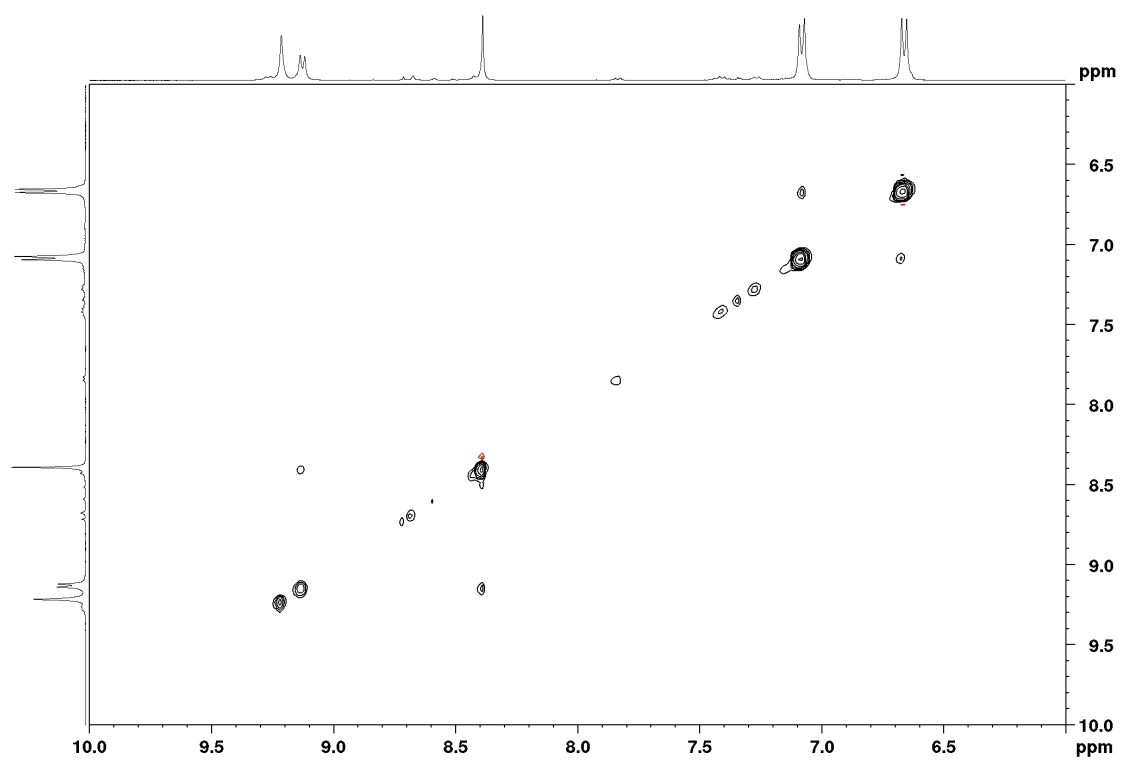


Figure 93 - NOESY spectrum of BTA 4 at 9.80 mM in DMSO-*d*<sub>6</sub>

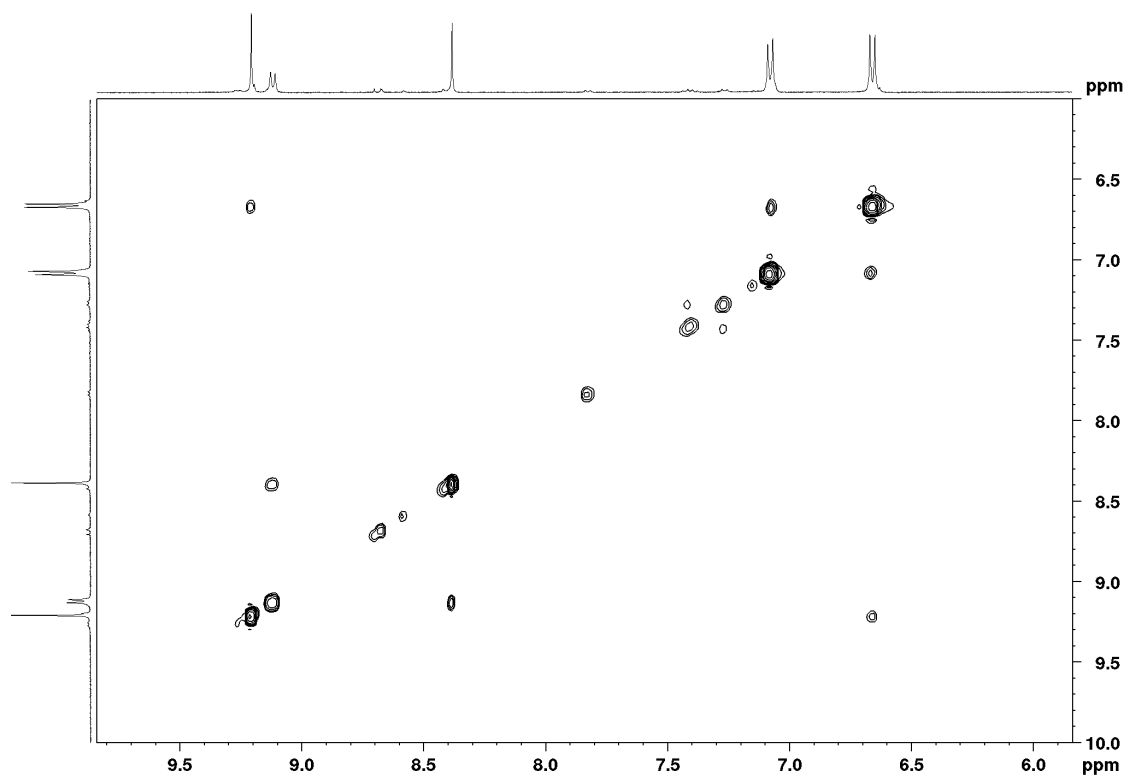
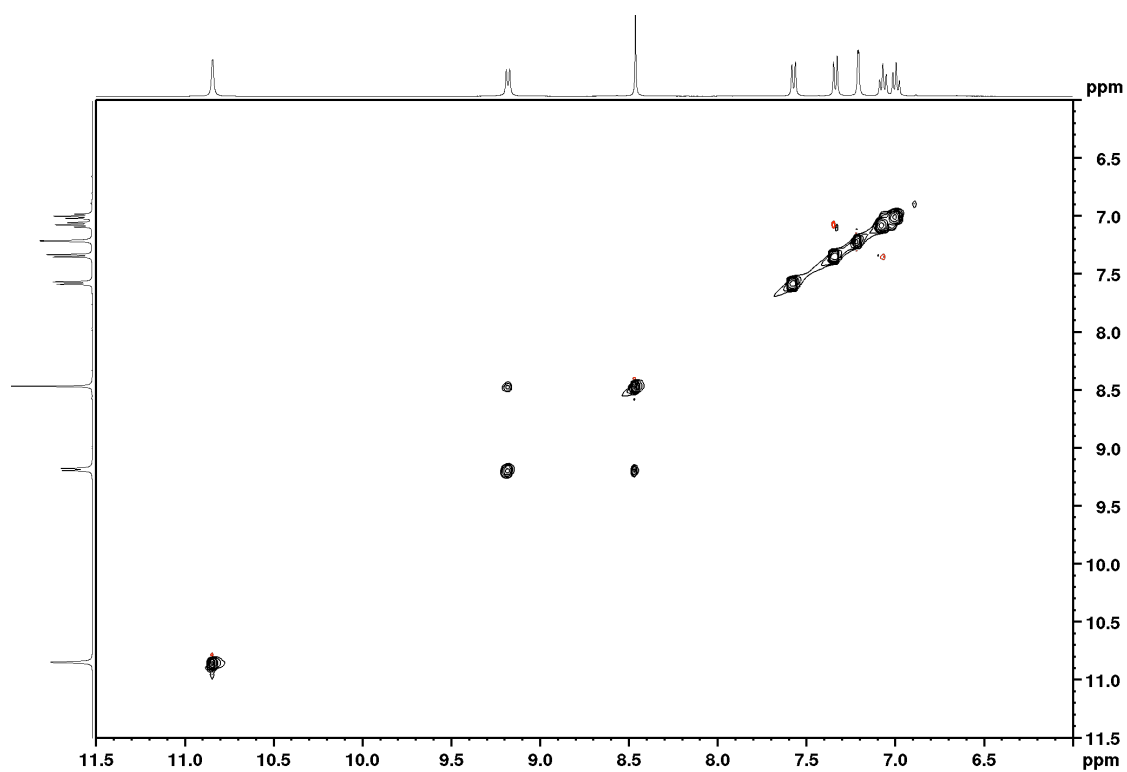
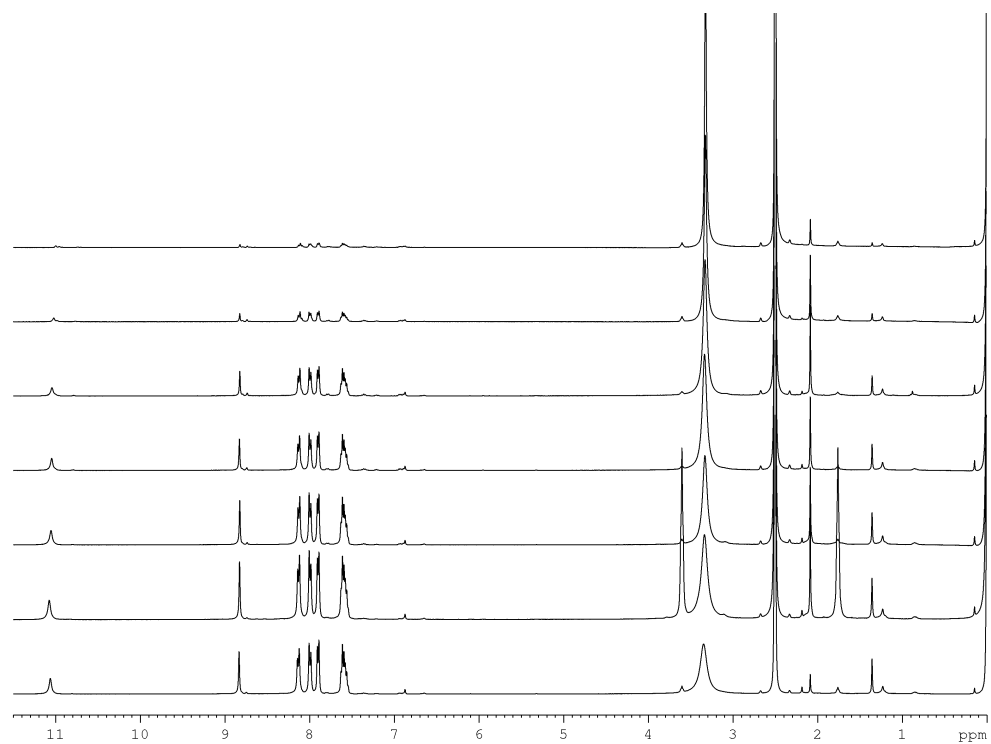


Figure 94 - NOESY spectrum of BTA 4 at 0.98 mM in DMSO-*d*<sub>6</sub>



**Figure 95 - NOESY spectrum of BTA 5 at 20.97 mM in DMSO-*d*6**



**Figure 96 - Full stack of BTA 1 concentration dependent spectra from 0.74 mM to 12.37 mM**

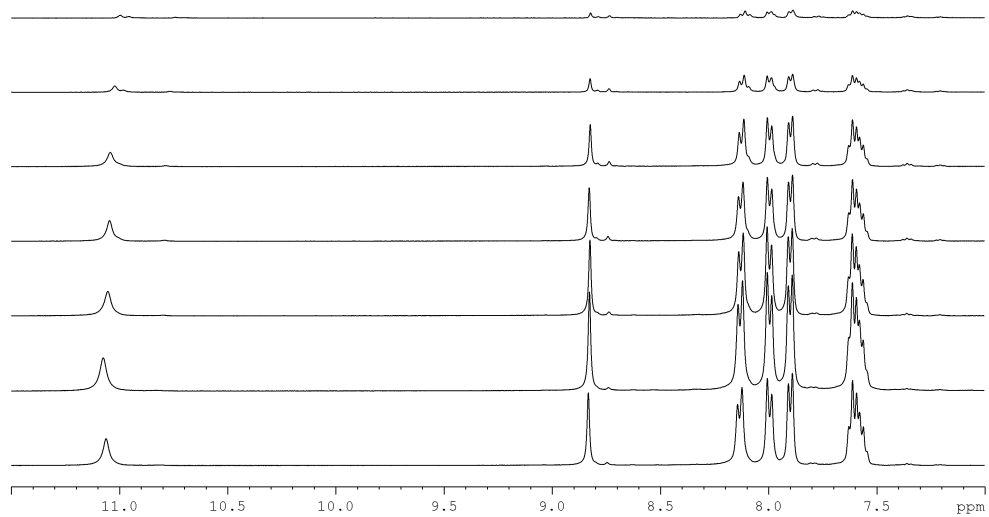


**Figure 97 - Aromatic region of BTA 1 concentration dependent spectra from 0.74 mM to 12.37 mM**

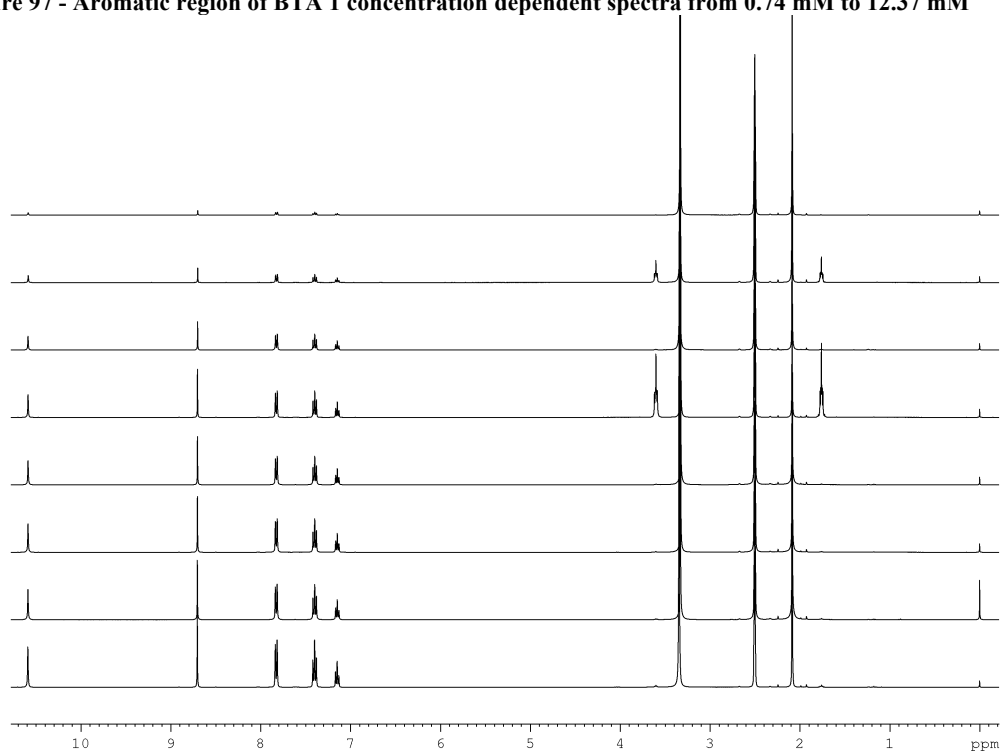


**Figure 98 - Full stack of BTA 2 concentration dependent spectra from 0.84 mM to 20.90 mM**

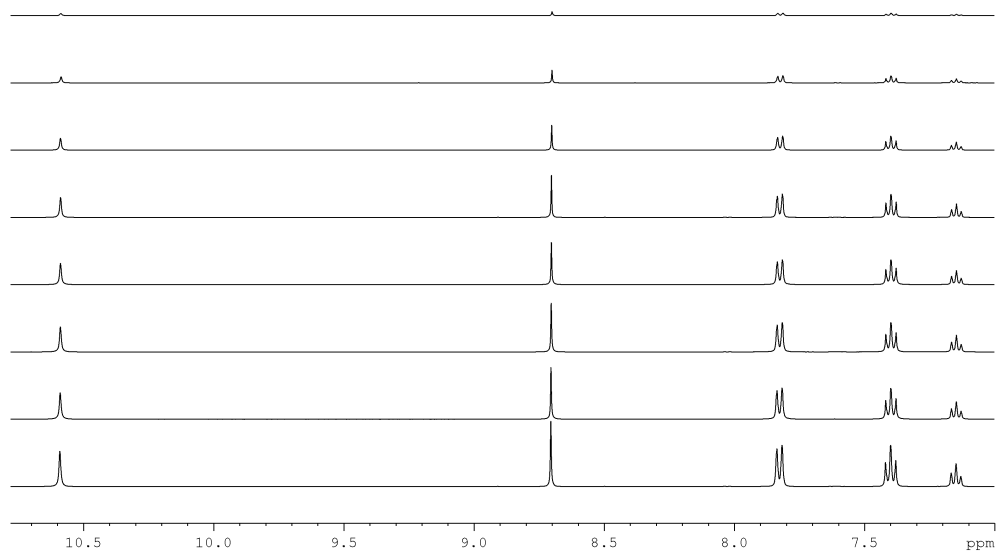


**Figure 99 - Aromatic region of BTA 2 concentration dependent spectra from 0.84 mM to 20.90 mM**

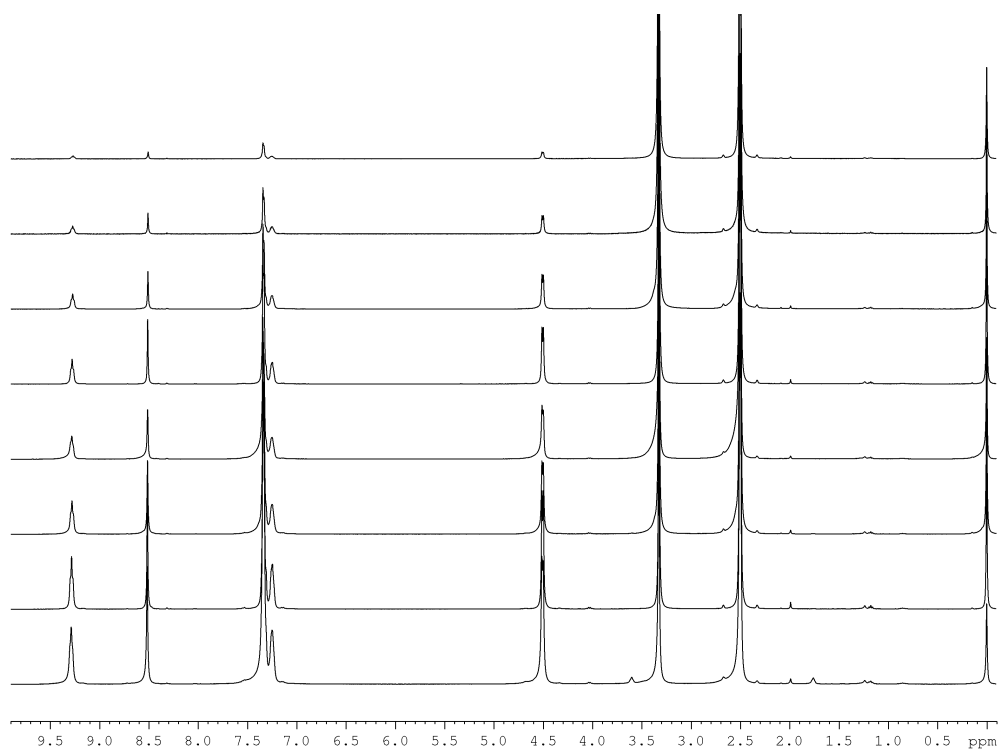


**Figure 100 - Full stack of BTA 3 concentration dependent spectra from 0.84 mM to 20.94 mM**

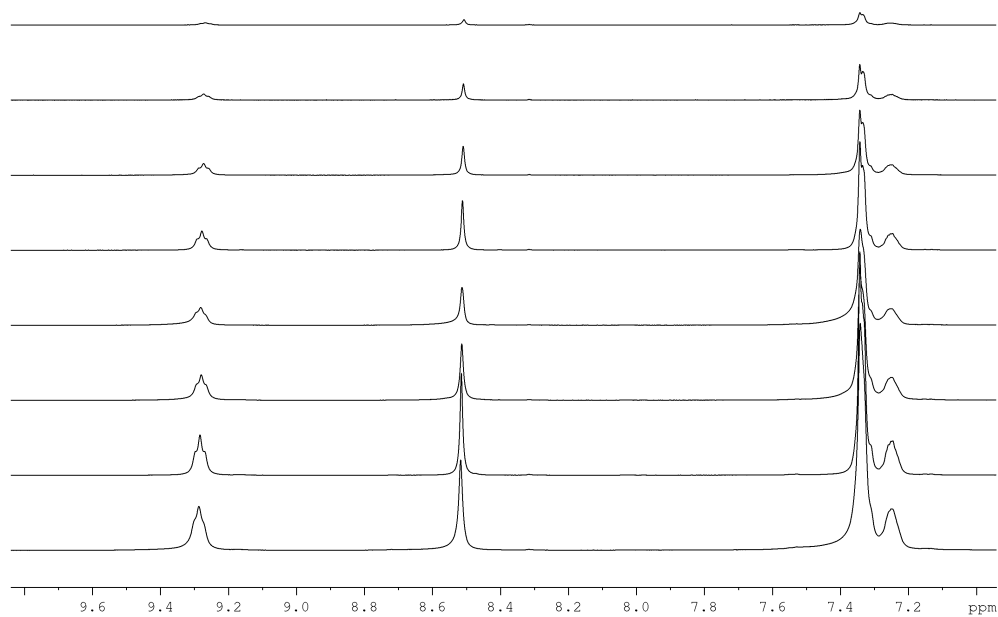


**Figure 101 - Aromatic region of BTA 3 concentration dependent spectra from 0.84 mM to 20.94 mM**

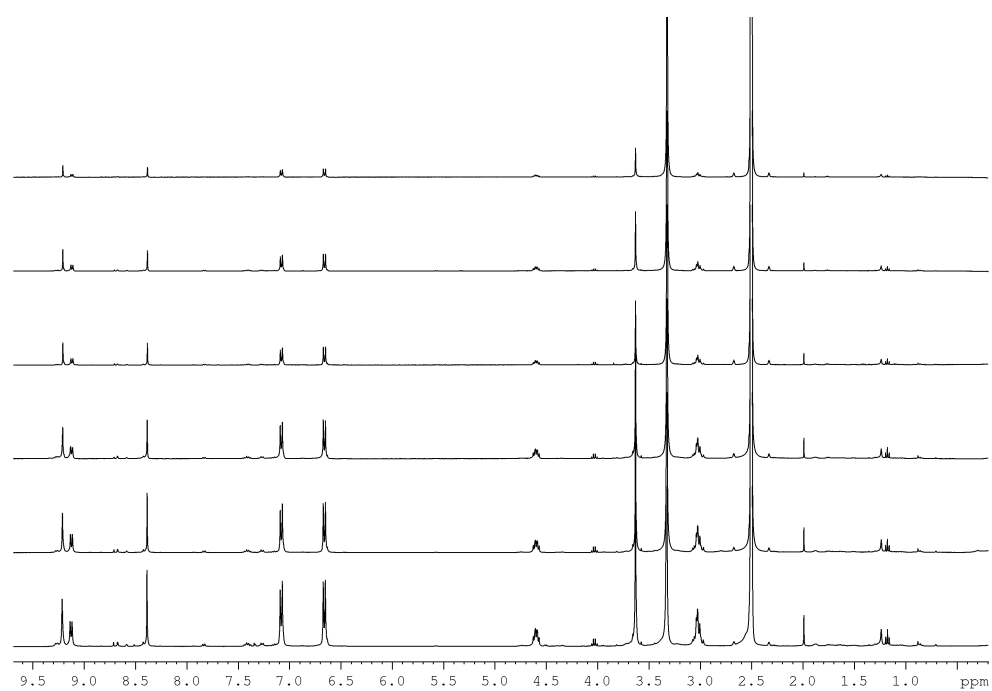


**Figure 102 - Full stack of BTA 4 concentration dependent spectra from 0.98 mM to 9.80 mM**

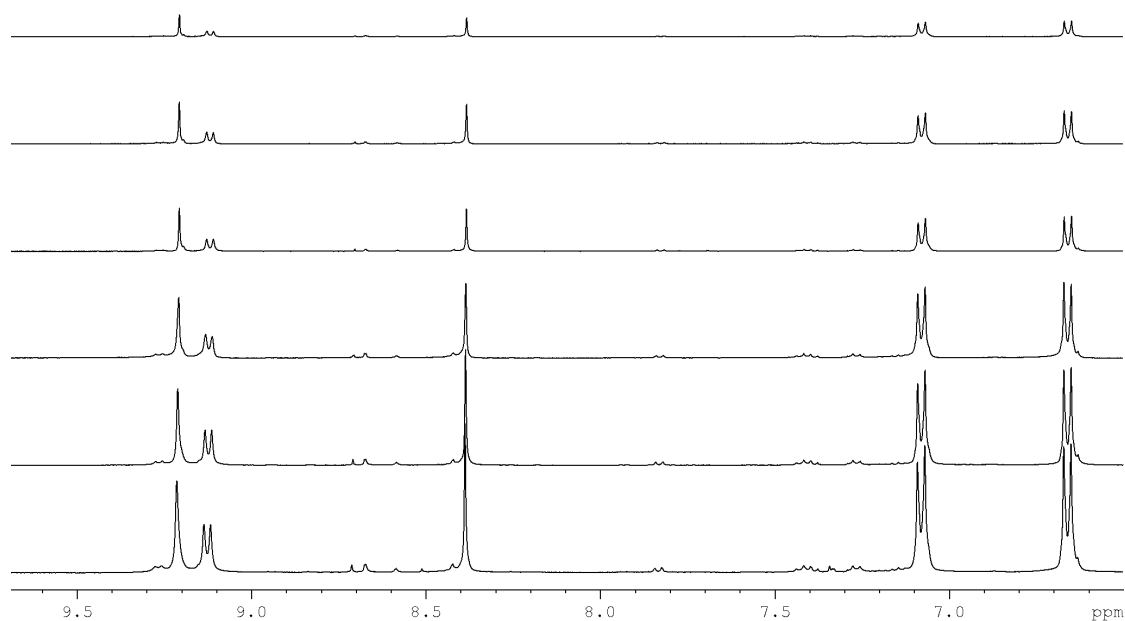


**Figure 103 - Aromatic region of BTA 4 concentration dependent spectra from 0.98 mM to 9.80 mM**

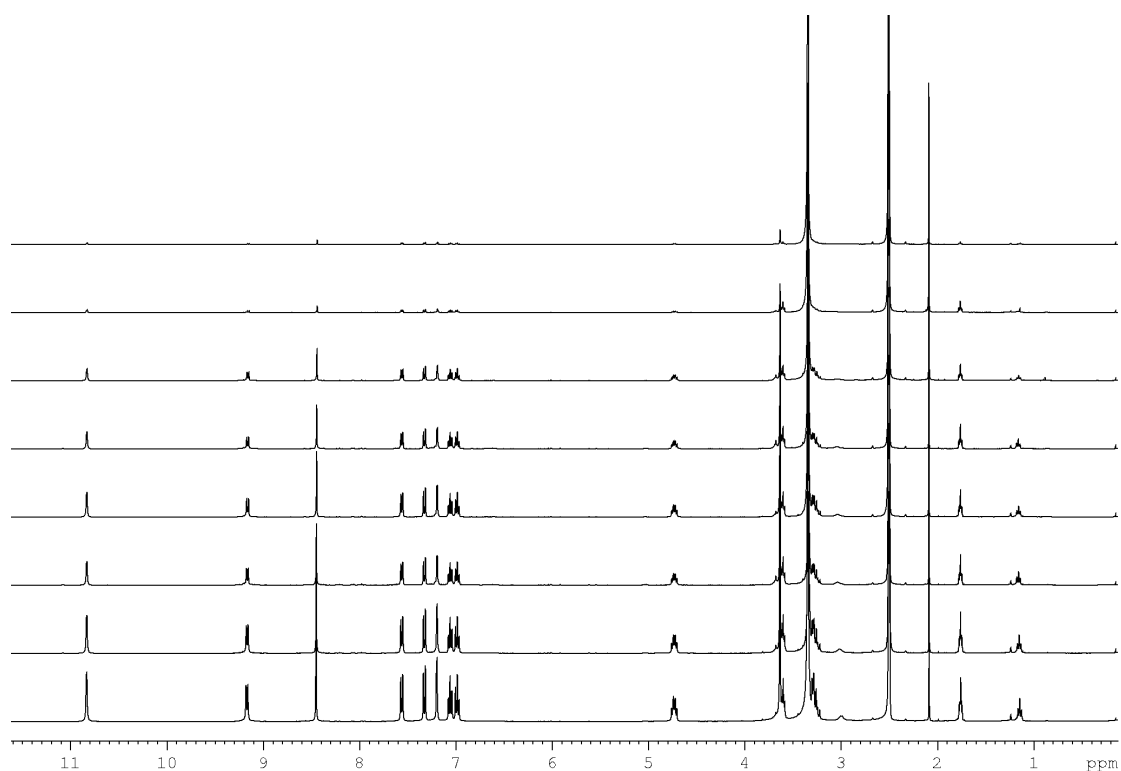


**Figure 104 - Full stack of BTA 5 concentration dependent spectra from 0.86 mM to 21.58 mM**

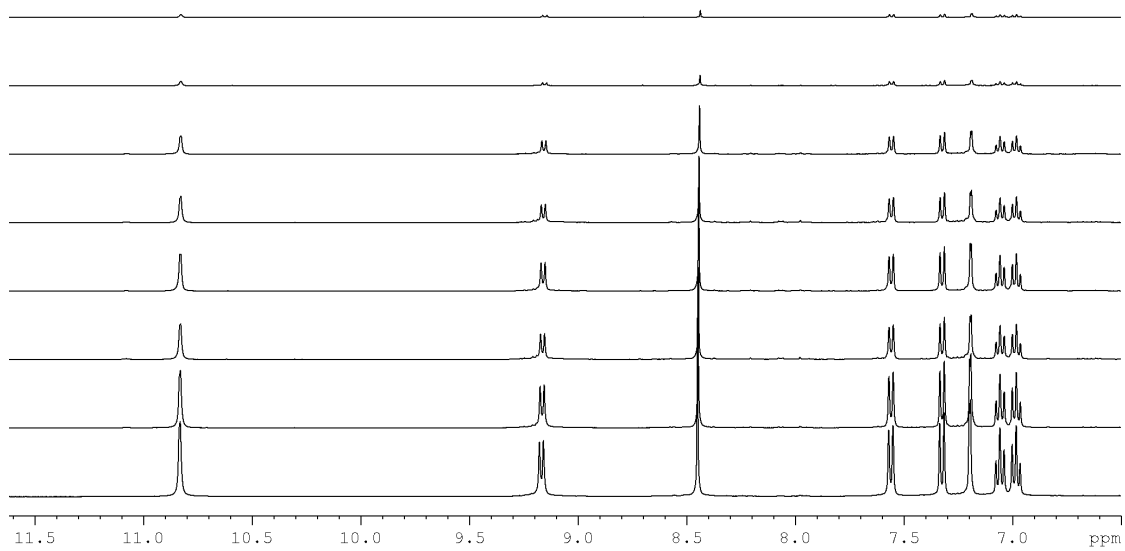


**Figure 105 - Aromatic region of BTA 5 concentration dependent spectra from 0.86 mM to 21.58 mM**

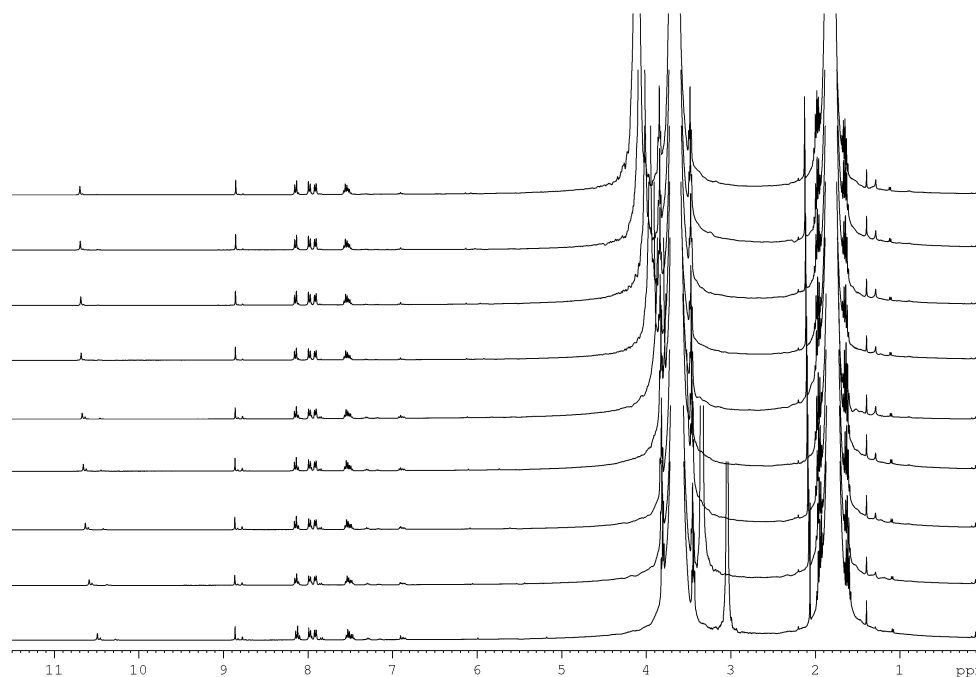


**Figure 106 – Full stack of <sup>1</sup>H-NMR spectra in the water titration experiments of BTA 1 in THF from 2.0% of added H<sub>2</sub>O to 15.3%**

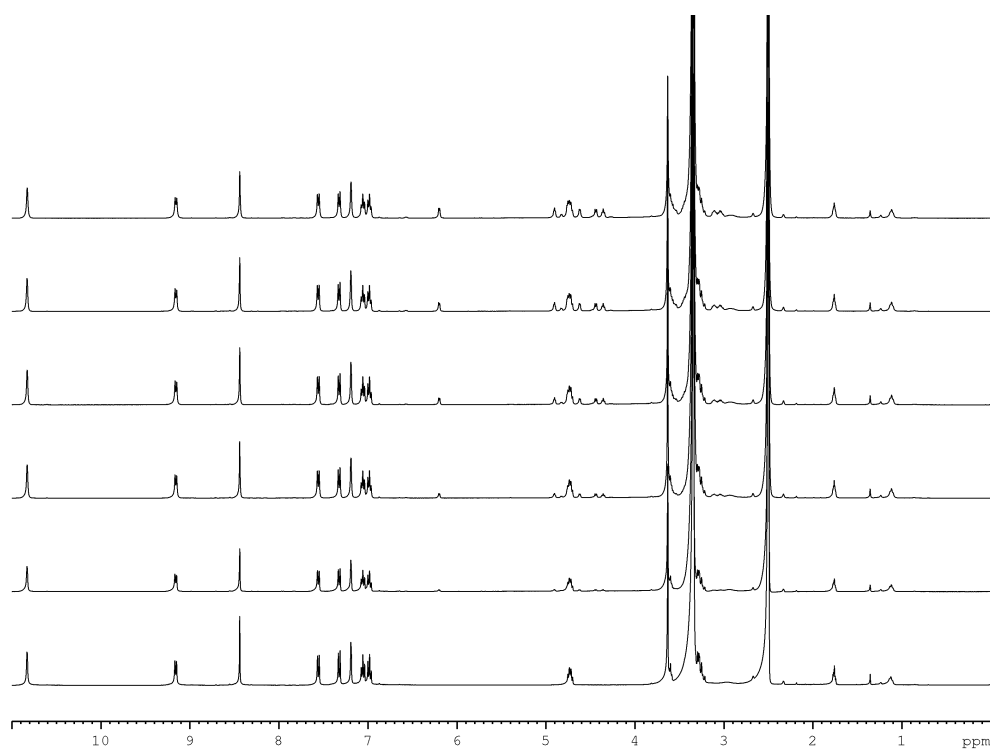


**Figure 107 - Full stack of  $^1\text{H}$ -NMR experiments in the glucose titration**

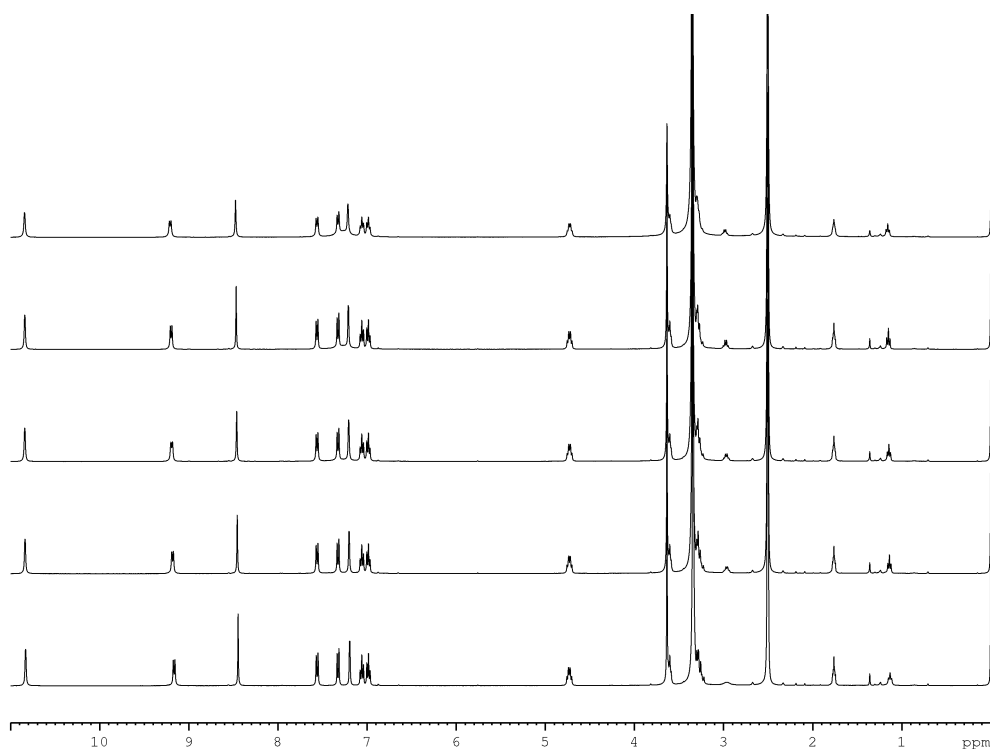


**Figure 108 - Full stack of  $^1\text{H}$ -NMR experiments in the ammonium chloride titration at 25 °C starting with only host present until a guest/host ratio of 1.45**



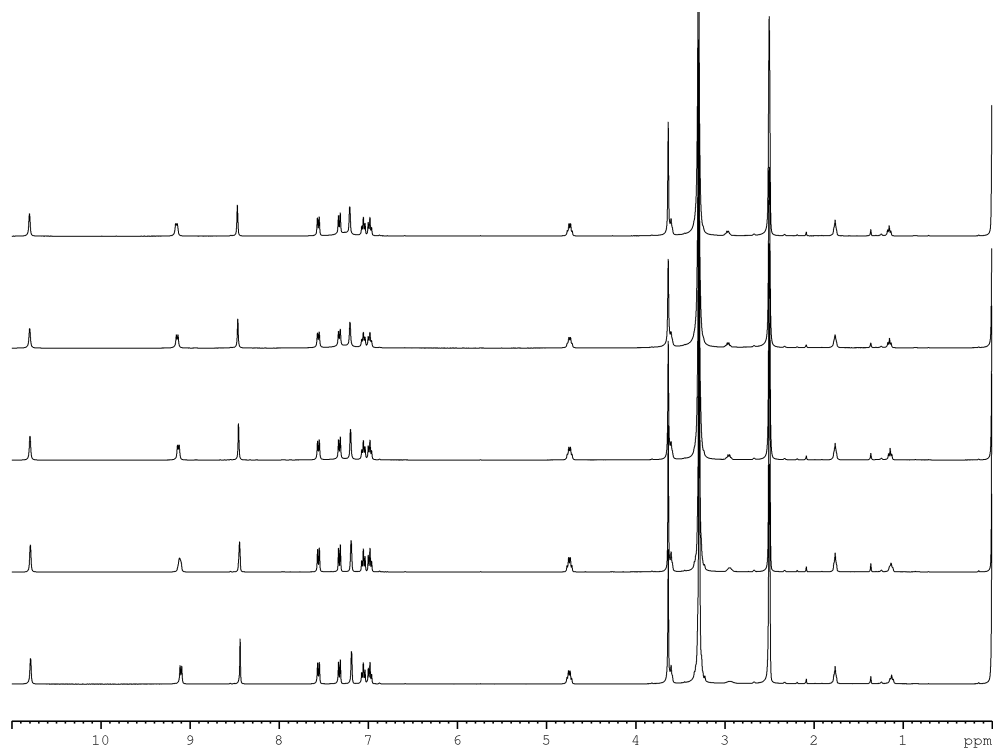


**Figure 109 - Full stack of  $^1\text{H}$ -NMR experiments in the ammonium chloride titration at 35 °C starting with only host present until a guest/host ratio of 1.32**

# References

- (1) Lehn, J. *Angew. Chemie Int. Ed. English* **1988**, *27*, 89–112.
- (2) Lawrence, D. S.; Jiang, T.; Levett, M. *Chem. Rev.* **1995**, *95*, 2229–2260.
- (3) Wolf, K. L.; Wolff, R. *Angew. Chemie* **1949**, *61*, 191–201.
- (4) Bosman, a. W.; Janssen, H. M.; Meijer, E. W. *Chem. Rev.* **1999**, *99*, 1665–1688.
- (5) Kambhampati, S. P.; Kannan, R. M. *J. Ocul. Pharmacol. Ther.* **2013**, *29*, 151–165.
- (6) Numata, M.; Kaneko, K.; Tamiaki, H.; Shinkai, S. *Chemistry* **2009**, *15*, 12338–12345.
- (7) Discher, D. E.; Eisenberg, A. *Science* **2002**, *297*, 967–973.
- (8) Tschierske, C. *Angew. Chem. Int. Ed. Engl.* **2013**, *52*, 8828–8878.
- (9) Lehn, J.-M. *Science* **2002**, *295*, 2400–2403.
- (10) Brunori, M. *Trends Biochem. Sci.* **1984**, *9*, 247.
- (11) York, N. *Functional tissue engineering*; 2004; Vol. 7.
- (12) Swiegers, G. F.; Malefetse, T. J. *Chem. Rev.* **2000**, *100*, 3483–3538.
- (13) Lv, K.; Zhang, L.; Liu, M. *Langmuir* **2014**, *30*, 9295–9302.
- (14) Canary, J. W. *Chem. Soc. Rev.* **2009**, *38*, 747.
- (15) Van Gorp, J. J.; Vekemans, J. a J. M.; Meijer, E. W. *J. Am. Chem. Soc.* **2002**, *124*, 14759–14769.
- (16) Lightfoot, M. P.; Mair, F. S.; Pritchard, R. G.; Warren, J. E. *Chem. Commun.* **1999**, 1945–1946.
- (17) Han, M.; Hara, M. *J. Am. Chem. Soc.* **2005**, *127*, 10951–10955.
- (18) Qiu, Y.; Chen, P.; Liu, M. *J. Am. Chem. Soc.* **2010**, *132*, 9644–9652.
- (19) Russew, M.-M.; Hecht, S. *Adv. Mater.* **2010**, *22*, 3348–3360.
- (20) Natansohn, A.; Rochon, P. *Chem. Rev.* **2002**, *102*, 4139–4176.
- (21) Mba, M.; Mazzier, D.; Silvestrini, S.; Toniolo, C.; Fatás, P.; Jiménez, A. I.; Cativiela, C.; Moretto, A. *Chemistry* **2013**, *19*, 15841–15846.
- (22) Busseron, E.; Ruff, Y.; Moulin, E.; Giuseppone, N. *Nanoscale* **2013**, *5*, 7098–7140.
- (23) Lim, Y.; Moon, K.-S.; Lee, M. *Chem. Soc. Rev.* **2009**, *38*, 925–934.
- (24) Matson, J. B.; Stupp, S. I. *Chem. Commun.* **2012**, *48*, 26.
- (25) Namiki, Y.; Fuchigami, T.; Tada, N.; Kawamura, R.; Matsunuma, S.; Kitamoto, Y.; Nakagawa, M. *Acc. Chem. Res.* **2011**, *44*, 1080–1093.
- (26) Zhou, Y.; Shimizu, T. *Chem. Mater.* **2008**, *20*, 625–633.
- (27) Antonietti, M.; Förster, S. *Adv. Mater.* **2003**, *15*, 1323–1333.
- (28) Reichardt, N. C.; Martín-Lomas, M.; Penadés, S. *Chem. Soc. Rev.* **2013**, *42*, 4358.

- (29) Lim, Y.; Lee, M. *Org. Biomol. Chem.* **2007**, *5*, 401–405.
- (30) Seeman, N. C. *Mol. Biotechnol.* **2007**, *37*, 246–257.
- (31) Kwak, M.; Herrmann, A. *Chem. Soc. Rev.* **2011**, *40*, 5745.
- (32) Kuzuya, A.; Komiyama, M. *Nanoscale* **2010**, *2*, 310–322.
- (33) Colson, Y. L.; Grinstaff, M. W. *Adv. Mater.* **2012**, *24*, 3878–3886.
- (34) Bamrungsap, S.; Zhao, Z.; Chen, T.; Wang, L.; Li, C.; Fu, T.; Tan, W. *Nanomedicine (Lond)*. **2012**, *7*, 1253–1271.
- (35) Baker, J. R. *Wiley Interdiscip. Rev. Nanomed. Nanobiotechnol.* **2013**, *5*, 423–429.
- (36) Lee, J.-H.; Kim, J.-W.; Cheon, J. *Mol. Cells* **2013**, *35*, 274–284.
- (37) Gibson, S. E.; Castaldi, M. P. *Angew. Chem. Int. Ed. Engl.* **2006**, *45*, 4718–4720.
- (38) Parkin, G. *Chem. Rev.* **2004**, *104*, 699–767.
- (39) Fournel, S.; Wieckowski, S.; Sun, W.; Trouche, N.; Dumortier, H.; Bianco, A.; Chaloin, O.; Habib, M.; Peter, J.-C.; Schneider, P.; Vray, B.; Toes, R. E.; Offringa, R.; Melief, C. J. M.; Hoebeke, J.; Guichard, G. *Nat. Chem. Biol.* **2005**, *1*, 377–382.
- (40) Dro, C.; Bellemin-Laponnaz, S.; Welter, R.; Gade, L. H. *Angew. Chemie - Int. Ed.* **2004**, *43*, 4479–4482.
- (41) Bellemin-Laponnaz, S.; Gade, L. H. *Angew. Chemie - Int. Ed.* **2002**, *41*, 3473–3475.
- (42) Bergueiro, J.; Freire, F.; Wendler, E. P.; Seco, J. M.; Quiñoá, E.; Riguera, R. *Chem. Sci.* **2014**, *5*, 2170.
- (43) Smulders, M. M. J.; Schenning, A. P. H. J.; Meijer, E. W. *J. Am. Chem. Soc.* **2008**, *130*, 606–611.
- (44) Palmans, A. R. A.; Vekemans, J. A. J. M.; Havinga, E. E.; Meijer, E. W. *Angew. Chemie Int. Ed. English* **1997**, *36*, 2648–2651.
- (45) Lehn, J. M. *Science* **1985**, *227*, 849–856.
- (46) Leung, D. K.; Atkins, J. H.; Breslow, R. *Tetrahedron Lett.* **2001**, *42*, 6255–6258.
- (47) Ruan, Y.; Taha, H. A.; Yoder, R. J.; Maslak, V.; Hadad, C. M.; Badjić, J. D. *J. Phys. Chem. B* **2013**, *117*, 3240–3249.
- (48) Ruan, Y.; Dalkılıç, E.; Peterson, P. W.; Pandit, A.; Dastan, A.; Brown, J. D.; Polen, S. M.; Hadad, C. M.; Badjić, J. D. *Chemistry* **2014**, *20*, 4251–4256.
- (49) Kim, S.; Kim, K.; Jung, J.; Shin, S. K.; Ahn, K. H. *Society* **2005**, *124*, 591–596.
- (50) Dougherty, D. a. *Science* **1996**, *271*, 163–168.
- (51) Ma, J. C.; Dougherty, D. A. **1997**.
- (52) Kim, S. G.; Kim, K. H.; Kim, Y. K.; Shin, S. K.; Ahn, K. H. *J. Am. Chem. Soc.* **2003**, *125*, 13819–13824.
- (53) Lee, S.; Oh, S.; Lee, J.; Malpani, Y.; Jung, Y.-S.; Kang, B.; Lee, J. Y.; Ozasa, K.; Isoshima, T.; Lee, S. Y.; Hara, M.; Hashizume, D.; Kim, J.-M. *Langmuir* **2013**, *29*, 5869–5877.

- (54) Curtius, T. *J. Prakt. Chemie* **1915**, *91*, 39–102.
- (55) Sidney, M. Monomeric compounds comprising a plurality of vinyl groups, 1956.
- (56) Ried, W.; Königstein, F.-J. *Chem. Ber.* **1959**, *92*, 2532–2542.
- (57) Cantekin, S.; de Greef, T. F. a; Palmans, A. R. a. *Chem. Soc. Rev.* **2012**, *41*, 6125–6137.
- (58) Rajput, L.; Banerjee, R. *Cryst. Growth Des.* **2014**, *14*, 2729–2732.
- (59) Patel, R. P.; Price, S. *J. Org. Chem.* **1965**, *30*, 3575–3576.
- (60) Jana, P.; Paikar, A.; Bera, S.; Maity, S. K.; Haldar, D. *Org. Lett.* **2014**, *16*, 38–41.
- (61) Pelta, M. D.; Morris, G. a.; Stchedroff, M. J.; Hammond, S. J. *Magn. Reson. Chem.* **2002**, *40*, 147–152.
- (62) Nilsson, M. *J. Magn. Reson.* **2009**, *200*, 296–302.
- (63) Hunter, C. a.; Anderson, H. L. *Angew. Chemie - Int. Ed.* **2009**, *48*, 7488–7499.
- (64) Smulders, M. M. J.; Nieuwenhuizen, M. M. L.; De Greef, T. F. a; Van Der Schoot, P.; Schenning, A. P. H. J.; Meijer, E. W. *Chem. - A Eur. J.* **2010**, *16*, 362–367.
- (65) Zhao, D.; Moore, J. S. *Org. Biomol. Chem.* **2003**, *1*, 3471–3491.
- (66) Nieuwenhuizen, M. M. L.; De Greef, T. F. a; Van Der Bruggen, R. L. J.; Paulusse, J. M. J.; Appel, W. P. J.; Smulders, M. M. J.; Sijbesma, R. P.; Meijer, E. W. *Chem. - A Eur. J.* **2010**, *16*, 1601–1612.
- (67) Pérez, A.; De Saá, D.; Ballesteros, A.; Serrano, J. L.; Sierra, T.; Romero, P. *Chem. - A Eur. J.* **2013**, *19*, 10271–10279.
- (68) Song, J.; Wang, H.; Li, M. *New J. Chem.* **2015**, *39*, 2711–2719.
- (69) Lohr, A.; Grüne, M.; Würthner, F. *Chem. - A Eur. J.* **2009**, *15*, 3691–3705.
- (70) Mayerhöffer, U.; Würthner, F. *Chem. Sci.* **2012**, *3*, 1215.
- (71) Martin, R. B. *Chem. Rev.* **1996**, *96*, 3043–3064.
- (72) Echue, G.; Lloyd-Jones, G. C.; Faul, C. F. J. *Chem. - A Eur. J.* **2015**, n/a – n/a.
- (73) Stals, P. J. M.; Smulders, M. M. J.; Martín-Rapún, R.; Palmans, A. R. a; Meijer, E. W. *Chemistry* **2009**, *15*, 2071–2080.
- (74) Gaussian 09, revision D.01, Frisch, M. J.; Trucks, G. W.; Schlegel, H. B.; Scuseria, G. E.; Robb, M. A.; Cheeseman, J. R.; Scalmani, G.; Barone, V.; Mennucci, B.; Petersson, G. A.; Nakatsuji, H.; Caricato, M.; Li, X.; Hratchian, H. P.; Izmaylov, A. F.; Bloino, J.; Zheng, G.; Sonnenberg, J. L.; Hada, M.; Ehara, M.; Toyota, K.; Fukuda, R.; Hasegawa, J.; Ishida, M.; Nakajima, T.; Honda, Y.; Kitao, O.; Nakai, H.; Vreven, T.; Montgomery, J. A., Jr.; Peralta, J. E.; Ogliaro, F.; Bearpark, M.; Heyd, J. J.; Brothers, E.; Kudin, K. N.; Staroverov, V. N.; Kobayashi, R.; Normand, J.; Raghavachari, K.; Rendell, A.; Burant, J. C.; Iyengar, S. S.; Tomasi, J.; Cossi, M.; Rega, N.; Millam, J. M.; Klene, M.; Knox, J. E.; Cross, J. B.; Bakken, V.; Adamo, C.; Jaramillo, J.; Gomperts, R.; Stratmann, R. E.; Yazyev, O.; Austin, A. J.; Cammi, R.; Pomelli, C.; Ochterski, J. W.; Martin, R. L.; Morokuma, K.; Zakrzewski, V. G.; Voth, G. A.; Salvador, P.; Dannenberg, J. J.; Dapprich, S.; Daniels, A. D.; Farkas, Ö.; Foresman, J. B.; Ortiz, J. V.; Cioslowski, J.; Fox, D. J. Gaussian, Inc., Wallingford CT, 2009.

- (75) Chen, S.; Ruan, Y.; Brown, J. D.; Gallucci, J.; Maslak, V.; Hadad, C. M.; Badjić, J. D. *J. Am. Chem. Soc.* **2013**, *135*, 14964–14967.
- (76) Cabrita, E. J.; Berger, S. *Magn. Reson. Chem.* **2001**, *39*, S142–S148.